

# **SANDIA REPORT**

SAND2008-6382

Unlimited Release

Printed September 2008

## **ASEDRA Evaluation Final Report**

Dr. Dean J. Mitchell, Dr. Rebecca Detwiler, and Dr. Glenn E. Sjoden

Prepared by  
Sandia National Laboratories  
Albuquerque, New Mexico 87185 and Livermore, California 94550

Sandia is a multi-program laboratory operated by Sandia Corporation, a Lockheed Martin Company, for the United States Department of Energy's National Nuclear Security Administration under Contract DE-AC04-94AL85000. This work was performed under the sponsorship of DOE/NNSA and DHS/DNDO.

Approved for public release; further dissemination unlimited.



**Sandia National Laboratories**

Issued by Sandia National Laboratories, operated for the United States Department of Energy by Sandia Corporation.

**NOTICE:** This report was prepared as an account of work sponsored by an agency of the United States Government. Neither the United States Government, nor any agency thereof, nor any of their employees, nor any of their contractors, subcontractors, or their employees, make any warranty, express or implied, or assume any legal liability or responsibility for the accuracy, completeness, or usefulness of any information, apparatus, product, or process disclosed, or represent that its use would not infringe privately owned rights. Reference herein to any specific commercial product, process, or service by trade name, trademark, manufacturer, or otherwise, does not necessarily constitute or imply its endorsement, recommendation, or favoring by the United States Government, any agency thereof, or any of their contractors or subcontractors. The views and opinions expressed herein do not necessarily state or reflect those of the United States Government, any agency thereof, or any of their contractors.

Printed in the United States of America. This report has been reproduced directly from the best available copy.

Available to DOE and DOE contractors from  
U.S. Department of Energy  
Office of Scientific and Technical Information  
P.O. Box 62  
Oak Ridge, TN 37831

Telephone: (865) 576-8401  
Facsimile: (865) 576-5728  
E-Mail: [reports@adonis.osti.gov](mailto:reports@adonis.osti.gov)  
Online ordering: <http://www.osti.gov/bridge>

Available to the public from  
U.S. Department of Commerce  
National Technical Information Service  
5285 Port Royal Rd.  
Springfield, VA 22161

Telephone: (800) 553-6847  
Facsimile: (703) 605-6900  
E-Mail: [orders@ntis.fedworld.gov](mailto:orders@ntis.fedworld.gov)  
Online order: <http://www.ntis.gov/help/ordermethods.asp?loc=7-4->

[0#online](#)



## **ASEDRA Evaluation Final Report**

Dr. Dean J. Mitchell  
Sandia National Laboratories  
P.O. Box 5800  
Albuquerque, NM 87185-0735

Dr. Rebecca Detwiler and Dr. Glenn E. Sjoden  
Nuclear and Radiological Engineering Department  
University of Florida

### **Abstract**

The performance of the Advanced Synthetically Enhanced Detector Resolution Algorithm (ASEDRA) was evaluated by performing a blind test of 29 sets of gamma-ray spectra that were provided by DNDO. ASEDRA is a post-processing algorithm developed at the Florida Institute of Nuclear Detection and Security at the University of Florida (UF/FINDS) that extracts characteristic peaks in gamma-ray spectra. The QuickID algorithm, also developed at UF/FINDS, was then used to identify nuclides based on the characteristic peaks generated by ASEDRA that are inferred from the spectra. The ASEDRA/QuickID analysis results were evaluated with respect to the performance of the DHSIsotopeID algorithm, which is a mature analysis tool that is part of the Gamma Detector Response and Analysis Software (GADRAS). Data that were used for the blind test were intended to be challenging, and the radiation sources included thick shields around the radioactive materials as well as cargo containing naturally occurring radioactive materials, which masked emission from special nuclear materials and industrial isotopes. Evaluation of the analysis results with respect to the ground truth information (which was provided after the analyses were finalized) showed that neither ASEDRA/QuickID nor GADRAS could identify all of the radiation sources correctly. Overall, the purpose of this effort was primarily to evaluate ASEDRA, and GADRAS was used as a standard against which ASEDRA was compared. Although GADRAS was somewhat more accurate on average, the performance of ASEDRA exceeded that of GADRAS for some of the unknowns. The fact that GADRAS also failed to identify many of the radiation sources attests to the difficulty of analyzing the blind-test data that were used as a basis for the evaluation. This evaluation identified strengths and weaknesses of the two analysis approaches. The importance of good calibration data was also clear because the performance of both analysis methods was impeded by the inability to define the energy calibration accurately.

## Acronyms

ACHIP	adaptive chi-processed
ASEDRA	Advanced Synthetically Enhanced Detector Resolution Algorithm
DNDO	Domestic Nuclear Detection Office
DRFs	Detector Response Functions
FINDS	Florida Institute of Nuclear Detection and Security
FWHM	full-width half-maximum
GADRAS	Gamma Detector Response Analysis Software
GUI	graphical user interface
HEU	highly enriched uranium
HPGe	high purity germanium
ID	identification
NaI	Sodium iodide
NNSA	National Nuclear Security Administration
NORM	Naturally Occurring Radioactive Materials
ppm	parts per million
SNL	Sandia National Laboratories
UF	University of Florida
WGpu	weapons-grade plutonium

# Contents

1. Introduction .....	9
1.1 AEDRA Description .....	9
1.2 User-controlled Parameters .....	10
1.3 GADRAS and DHSIsotopeID Description .....	12
1.4 Contrast between ASEDRA and DHSIsotopeID .....	13
2. Evaluation Procedure.....	13
2.1 Blind Testing .....	13
2.2 Calibration Issues and Approach .....	14
2.2.1 ASEDRA .....	14
2.2.2 GADRAS / DHSIsotopeID .....	15
2.3 Ground Truth and Evaluation Metrics.....	16
3. Analysis Results Summary .....	16
4. Conclusions .....	20
Appendix A: Analysis Details for ASEDRA with QuickID .....	23
Appendix B: Analysis Details for GADRAS/DHSIsotopeID .....	63

## Figures

Figures A-1-4. ASEDRA peaks rendered: U1 (top left), U2 (top right), U3 (bottom left), U4 (bottom right).....	24
Figure A-4a. ASEDRA peak extracted at high energy from spectrum U4. Although the calibration was only passable, ASEDRA was able to extract a photopeak aliased to a 2.22 MeV hydrogen H(n, $\gamma$ ) line from the denoised spectra, indicating the presence of neutrons in the sample.....	25
Figures A-5 and 5a, respectively. Analysis of U5 with unconservative (left) and conservative settings (right). This was later identified as a strontium beta source; assuming it was a heavily shielded gamma source, it was attributed by ASEDRA to be $^{235}\text{U}$ , or possibly $^{192}\text{Ir}$ , yet data correlation was poor. ....	26
Figure A-6. ASEDRA Analysis of U6, which was revealed to be $^{152}\text{Eu}$ behind a rotating lead “puzzle box” shield. ....	26
Figures A-7-10. ASEDRA peaks rendered: U7 (top left), U8 (top right), U9 (bottom left), U10 (bottom right).....	28
Figures A-11-14. ASEDRA peaks rendered: U11 (top left), U12 (top right), U13 (bottom left), U14 (bottom right). ....	29
Figure A-14a. High-energy region of U14 following post-analysis re-evaluation (denoised by ASEDRA). After it was revealed that U14 was a moderated $^{252}\text{Cf}$ source, we re-analyzed the spectrum with ASEDRA, lowering the threshold for the number of minimum detectable counts from 5 counts to 1 count (above background). Subsequently, ASEDRA extracted a peak (on the right) at 2188 keV, which falls within the search window for the 2224 keV hydrogen H(n, $\gamma$ ) line based on the evident calibration. Also extracted was a line at 2077 keV, attributed to a 2111 keV Fe(n, $\gamma$ ) line. ....	30
Figure A-15. ASEDRA Analysis of Unknown U15. ....	30
Figures A-16 – 20. ASEDRA peaks rendered: U16 (top left), U17 (top right), U18 (middle left), U19 (middle right), and U20 (bottom).....	31

Figures A-21 – 22. ASEDRA peaks rendered: U21 (left) and U22 (right).....	33
Figures A-23 – 24. ASEDRA peaks rendered: U23 (left) and U24 (right).....	33
Figures A-25 - 26. ASEDRA analysis of Unknowns 25 (U25) and 26 (U26). The figures are remarkably similar. ....	34
Figures A-27a - 27b. ASEDRA Analysis of Unknown 27; Figure 27a (left), the figure shows the lower energy region; Figure 27b (right) shows the higher energy regions and 2223 H(n, $\gamma$ ) peak. The other peak just below this is likely the 2111 keV Fe(n,y) peak—a definite indicator of SNM neutrons. Note that denoising of the spectra in ASEDRA makes attribution of (n,y) peaks possible. ....	35
Figures A-28 - 29. ASEDRA Analysis of Unknowns 28 (U28) and 29 (U29). ....	36
Figure B-1. The plot on the left compares the background-subtracted, measured spectrum for Event 1 (black $\pm$ 1-sigma error bars) with the best fit obtained with the DHSIsotopeID algorithm. The plot on the right shows the best fit using only shielded $^{137}\text{Cs}$ . ....	65
Figure B2. Comparison of the measured spectrum for Event 2 (black $\pm$ 1-sigma error bars) and several components associated with shielded isotopes that collectively represent the best fit to the data. ....	66
Figure B3. This plot gives a graphic representation of the DHSIsotopeID analysis result for Event 3.....	67
Figure B-4. The plot on the left side compares the measured data (black) with spectral components associated with $^{133}\text{Ba}$ (blue) and $^{137}\text{Cs}$ (red). Neutron emission is associated with the green continuum component that extends across the entire energy range and also gives rise to the hydrogen capture peak at 2223 keV. ....	68
Figure B-5. This plot compares the spectrum that was measured for Event 5 (black) with the computed spectrum for $^{90}\text{Sr}$ (blue). ....	69
Figure B-6. This figure compares spectra that were measured for Events 6 through 9 with the single-isotope solutions that DHSIsotopeID concluded were consistent with the observations. ....	70
Figure B-7. This figure compares spectra that were measured for Event 10 with the best fit, which is obtained using a combination of shielded $^{40}\text{K}$ and $^{239}\text{Pu}$ . ....	71
Figure B-8. The measured spectrum for Event 11 (black) is compared with the best fit that is obtained with a combination of $^{226}\text{Ra}$ (blue) and $^{232}\text{Th}$ (red). ....	72
Figure B-9. The measured spectrum for Event 13 (black) is compared with the best fit that is obtained with shielded $^{54}\text{Mn}$ (blue region). ....	73
Figure B-10. The measured spectrum for Event 14 (black) is compared with the best fit that is obtained with a combination of $^{239}\text{Pu}$ (red) and gamma rays associated with neutron emission (blue). ....	74
Figure B-11. This figure compares spectra that were measured for Events 15 through 17 and 29 with analysis results that were obtained with DHSIsotopeID. Each of these events was produced by $^{235}\text{U}$ in combination with a “masking” source. ....	75
Figure B-12. The only isotope that DHSIsotopeID identified from analysis of Event 18 was $^{40}\text{K}$ . ....	76
Figure B-13. Analysis of Event 21 revealed the presence of $^{238}\text{U}$ with high confidence. Plutonium may also have been present, but the confidence in this conclusion is much less certain because of uncertainty in the energy calibration offset parameters. ....	77
Figure B-22. Analysis of Event 22 revealed the presence of a positron emitter, which was identified as $^{18}\text{F}$ because this is a common positron emitter. ....	78
Figure B-16. Analysis of Event 23 revealed the presence of $^{239}\text{Pu}$ with high confidence and $^{235}\text{U}$ with fair confidence. ....	79

Figure B-17.	The measured spectrum for Event 24 (black) is compared with the best fit that is obtained with a combination of $^{131}\text{I}$ (blue) and $^{252}\text{Cf}$ (red).....	80
Figure B-18.	The original spectrum for Event 25 without background subtraction shows that counts in the range 70 to 190 keV were truncated to a maximum of 64k channels.....	81
Figure B19.	Analysis of Event 25 (left) and Event 26 (right).....	82
Figure B-20.	Analysis of Event 27 shows that $^{133}\text{Ba}$ (blue) and $^{239}\text{Pu}$ (red) were both present with high confidence. ....	82
Figure B-21.	Analysis of Event 28 shows that $^{239}\text{Pu}$ (blue) and $^{226}\text{Ra}$ (red) were both present with high confidence. ....	83

## Tables

Table 1.	Summary ground truth and analysis results using ASEDRA and DHSIsotopeID <sup>+</sup> .....	18
Table A-1.	Analysis of Unknown 6 .....	27
Table A-2.	ASEDRA/QuickID Blind Test Analysis Results .....	37
Table B-1.	Summary of Analysis Results using GADRAS .....	64

## **Acknowledgements**

This work was performed in support of DOE/NA-22. This evaluation could not have been performed without the assistance of John Blackadar of DHS/DNDO, who provided the blind test data upon which the evaluation was based.

# 1. Introduction

Due to the potential threat from nuclear terrorism, the detection of rogue nuclear materials before they enter the United States is absolutely essential. Scintillation radiation detectors, including inorganic crystals such as sodium iodide [1], have proven quite useful, but they have poor spectral resolution. Consequently, detecting the presence of special nuclear material (SNM) hidden in routine shipments of Naturally Occurring Radioactive Materials (NORM) or medical isotopes is challenging with scintillation detectors. One approach to providing positive identifications of radioactive isotopes is to use high-purity germanium (HPGe) detectors, which have high resolution but are considerably more expensive and less portable than scintillation detectors. Extensive research efforts have also focused on improving analysis algorithms and room-temperature detector resolution using different detector materials [2].

Researchers at the University of Florida/Florida Institute of Nuclear Detection and Security (UF/FINDS) have focused on post-processing algorithms to improve detection of radiation signatures derived from scintillator detectors. The ASEDRA (Advanced Synthetically Enhanced Detector Resolution Algorithm) algorithm was developed to post-process scintillator detector spectra in a differential approach, called synthetic spectrum enhancement, to render photopeaks with high accuracy. ASEDRA, which is currently in an advanced development stage, yields photopeaks with sufficient resolution to identify SNM-bearing materials [3,4]. The post-processed spectrum is rendered in a few seconds on a standard laptop computer. To test this approach and compare it with a standard identification tool (Gamma Detector Response Analysis Software (GADRAS) developed by Sandia National Laboratories [5]), the National Nuclear Security Administration (NNSA) funded a study to evaluate the accuracy of analysis results that are obtained with the two codes. The comparison was made by performing a blind test using gamma-ray spectra that were supplied by the Department of Homeland Security. The identities of the radiation sources that were present when the spectra were collected were not revealed to the researchers until reports were submitted to the Department of Homeland Security, Domestic Nuclear Detection Office (DNDO), to document analysis results obtained with the two analysis applications. This final report compares the analysis results with the ground truth, and discusses how the analysis results were obtained.

## 1.1 ASEDRA Description

ASEDRA incorporates a multi-step sweep to extract photopeaks; it begins with an initial novel denoising algorithm based on an adaptive chi-square metric called "ACHIP" to remove stochastic noise from low-count spectra, yet preserve fine detail. Then, sweeping initially from the high-energy end of the spectrum, a novel detector response algorithm is applied using Detector Response Functions (DRFs) derived from a database of high-resolution, pre-computed Monte Carlo transport computations. DRFs are applied through scaling to sequentially strip and de-convolve the complete spectrum attributed to identified photopeaks, revealing new features in the detector spectrum. This process is repeated until the residual spectrum no longer contains peaks that meet

the criteria in ASEDRA for DRF attribution. This analysis uses ASEDRA to analyze and identify peaks in unknown spectra, and then identifies nuclides with the QuickID program, which correlates nuclides for each peak present. The ASEDRA analysis was conducted independently by the two UF/FINDS researchers, Dr. Detwiler and Dr. Sjoden, and final results were compiled by consolidating information that was obtained by the two analysts.

## 1.2 User-controlled Parameters

The following describes the available settings in a “process.txt” file, which the analyst provides to direct the operation of ASEDRA.

- **Low energy tailing.** Applied only at low energies, this setting compensates for low-energy tailing with two additional parameters, *Rtail* and *FWHMtail*, which control the prominence and length of the low-energy tail. The idea is that the low-energy side of a photopeak can be modeled as a weighted average of two peaks: one with the same full-width, half-max (FWHM) as the right side, and one with a larger full-width, half-max to represent the longer tail on the low-energy side. *Rtail* is the weight of the Gaussian with the larger full-width, half-max. *FWHMtail* is that larger full-width, half-max, measured in keV. The value of *Rtail* should be in the range of [0.0, 1.0] and typically is 0.25. The value of *FWHMtail* is typically 25 keV or less.
- **Peak aliasing factor.** This factor enables a sweeping of the entire synthetic peak output, aliasing peaks that are too close to dominant peaks, so that minor incidental peaks are eliminated and attributed through summation into an adjacent “locally dominant” peak. If set to a positive real value, the aliasing factor defines the number of FWHM widths (at a particular energy) considered surrounding above or below prominent peaks. A nominal value recommended for this parameter is ~0.5. Note: This peak aliasing factor is disabled if using a “-1” setting. This feature can be used to prevent “false echoes” of synthetic peaks extracted surrounding a true peak feature. In developmental tests, this feature adds significant robustness to ASEDRA, since it makes the peaks identified more accurate and less dependent on a “precisely tuned” DRF.
- **Denoising settings.** The chi-squared threshold should usually be set to -1, indicating that the new adaptive chi-processed (ACHIP) denoising should be used. A chi-squared threshold of 0 turns off denoising completely. Positive values of the chi-squared threshold turn on an obsolete version of denoising, which is not recommended. When the chi-squared threshold is set to -1, as recommended, the alpha setting controls the behavior of adaptive ACHIP denoising. Alpha should be in the range of [0.005, 0.995]. Smaller values of alpha lead to more denoising, but also increase the risk of removing real features. ACHIP adaptively smoothes spectra to remove stochastic noise, and chi-squared analysis ensures that statistically significant features are not removed.

- **Shielding materials** (from Detector Response Functions (DRFs)). A container can shield a sample, preventing its radiation from reaching the detector and changing the shape of DRFs. The "shielding material" parameter in process.txt indicates the material of a scattering shield placed between the source and the detector, and determines which set of detector response functions will be used. So far, ASEDRA includes precomputed, Monte-Carlo-generated detector response functions range from 0 to 5 according to the list below.

Type	Description
0	2x2" NaI, point source, no shield
1	2x2" NaI, point source, thin iron shield
2	4x4x16" NaI portal, small source, lower (bottom), no shield
3	4x4x16" NaI portal, small source, upper (top), no shield
4	4x4x16" NaI portal, small source, lower (bottom), steel shield (shielded)
5	4x4x16" NaI portal, small source, upper (top), steel shield (shielded)

NOTE: For DRF Type 1, the "thin iron shield" is a full density, 0.5-cm iron scatter shield in front of the point source, 10 cm from the detector. The 4 × 4 × 16 in. NaI Portal DRFs (DRF Types 2 – 5) assume large, dual-opposing NaI systems summed from interactions from a spherical 5-cm radius source located 140 cm off the ground, 140 cm from the steel portal monitor box. For the shielded Portal DRFs (Type 4 or 5), a 1-cm spherical shell of 40% full density stainless steel surrounds the source. The "lower" (bottom) portal monitor box, also containing dual-opposing NaI detectors, spans up to ~2 m in height adjacent to the ground, while the "upper" DRFs are based on portal monitor boxes that span from ~2 m to 4 m (just above the lower box portal assemblies). Note the list of DRFs is maintained for the graphical user interface (GUI) in a file list "environments.txt".

- **Peak rejection threshold.** If small peaks are considered uninteresting, they can be rejected by setting the peak rejection threshold. A photopeak whose height in counts is less than or equal to the peak rejection threshold will not be identified. Generally, ASEDRA analyses using "Settings 2" in this study used a threshold setting below those in "Settings 1".
- **Relative channel threshold.** Each time ASEDRA finds a peak, it tries to remove the effects of that peak and the spectrum associated with it. To prevent "leftover" subtracted counts from leading to "false" peaks, the "relative channel threshold" indicates that each synthetic peak must represent some minimum percentage of the original spectrum at that point.
- **Scattered counts scale factor.** Actual operating conditions (e.g., geometry, Compton effects, solid angle, etc.) will not precisely match the Monte-Carlo-simulated geometry originally used for deriving detector response functions.

Additional objects, such as a floor or table, may significantly increase the scattered counts associated with a full energy photopeak. The “scattered counts scale factor” indicates the degree to which scattered counts in the Monte-Carlo-generated detector response functions should be “scaled up” to account for relative changes in the scattering environment. A value of 2.0, for example, would double the amount of scattered counts, while 1.0 would have no impact. One can set this value to -1 for adaptive scaling, but adaptive scaling has not been adequately tested. Used in conjunction with peak aliasing, the scattered counts scale factor is an effective parameter.

The large uncertainties in energy calibrations that are noted in the spectra for the unknowns are addressed by applying two different sets of ASEDRA settings; “Settings 1” are typically more conservative, yielding fewer, stronger peaks, and to complete the study, in some cases, the calibration was adjusted. The “Settings 2” ASEDRA parameters typically employed lower thresholds to render weaker peaks present in the spectra with a wider search window without recalibration. For both cases, nuclide identification was performed using the separate, developmental QuickID package. Based on compilation of the results from the two sets of ASEDRA settings used, a final recommendation for nuclide identification (ID) based on the peaks found by ASEDRA attributed by QuickID was made. As noted below, the poor calibration and drifting gain evident in all of the data posed a significant challenge, which would occur for any nuclide peak identification and ID algorithm. In any event, the ASEDRA results were processed using the most appropriate method that seemed reasonable; the details are presented in this report.

### ***1.3 GADRAS and DHSIsotopeID Description***

GADRAS is a comprehensive application that incorporates several radiation analysis algorithms, detector response functions for gamma-ray and neutron detectors, a radiation transport interface, and various plotting tools. This evaluation focuses on the performance of the DHSIsotopeID algorithm, which is a component of GADRAS that is most suitable for automatic isotope identification. The DHSIsotopeID algorithm fits spectra with combinations of templates for shielded and unshielded isotopes. The reduced chi-square difference ( $\chi_r^2$ ) is used to quantitatively describe the quality of the fit. The value of  $\chi_r^2$  is equal to 1.0 if the difference between the measured and computed spectrum exactly equals the estimated variance. However, obtaining a value of  $\chi_r^2$  approximately equal to 1.0 does not necessarily indicate high confidence that an isotope is present because it may be able to obtain low values of  $\chi_r^2$  with more than one combination of isotopes if the data are of poor statistical quality. The problem of establishing the confidence in the isotope assessment is addressed by fitting the spectra with several combinations of isotopes. High confidence for the presence of an isotope is only established if the quality of the fit is good and it is not possible to obtain satisfactory agreement with combinations that do not include the isotope.

One solution set compares the foreground spectrum with the background spectrum if a background spectrum is available. The only degree of freedom in this solution is the

magnitude of the background, which can vary due to background suppression effects. Each of the other solution sets includes combinations of the measured background (if available) and the natural isotopes  $^{40}\text{K}$ ,  $^{226}\text{Ra}$  and  $^{232}\text{Th}$ . The following source combinations are explored:

- Natural only
- Natural + SNM
- Natural + Industrial
- Natural + Medical
- Natural + Beta
- All isotopes

Weighting factors, which are based on the inverse of  $\chi_r^2$ , are assigned to each solution set. Confidence estimates are then estimated for each isotope by summing the product of the weighting factors and the uncertainty estimates derived from multiple linear regression. Spectral templates for a given isotope are mixed as dictated by coefficients that are derived from the linear regression solutions, which provides the ability to interpolate among various shielding configurations. Sources that are selected for inclusion in a final solution set are obtained by selecting all of the isotopes that have significant confidence levels. The confidence estimates are then recomputed by including the final solution with all of the other solution sets.

#### ***1.4 Contrast between ASEDRA and DHSIsotopeID***

The ASEDRA algorithm and DHSIsotopeID obtain isotope identifications by approaching the problem from opposite extremes; in effect, ASEDRA applies a differential analysis approach, while DHSIsotopeID applies an integral analysis approach. ASEDRA begins by decomposing the spectrum into a series of peaks without reference to specific isotopes or gamma-ray energies. Isotopes are then identified by using the QuickID algorithm to infer which isotopes might have produced the peaks within estimated energy uncertainties. In contrast, DHSIsotopeID starts with templates for a variety of isotopes in various shielding configurations, and it proceeds to fit the entire spectra using combinations of these templates without explicitly identifying peaks. This process is referred to as a full-spectrum analysis.

## **2. Evaluation Procedure**

### ***2.1 Blind Testing***

The main element of the evaluation involved blind testing of the data using the two algorithms. The blind test data were provided by Dr. John Blackadar of DNDO. Researchers at SNL and UF/FINDS team did not know the actual source identities at the time of the testing or during the tabular test results submittal phase of reporting. A set of 20 radiation measurements were delivered on 6/27/2008, and an additional 9 data

sets were delivered on 7/7/2008. Each data set consisted of a measurement of an unknown radiation source, plus associated background and calibration spectra.

The initial concept for this evaluation was for ASEDRA and GADRAS to be compared in an automated way to minimize the influence imposed by skills of the analysts. However, the quality of the energy calibration spectra was found to be unsatisfactory for the following reasons:

- No radiation sources were present in several of the calibration spectra.
- None of the calibration sources were suitable for determination of both gain and offset parameters because the sources either emitted only low-energy gamma rays ( $^{57}\text{Co}$  and  $^{153}\text{Sm}$ ) or medium-energy gamma rays ( $^{137}\text{Cs}$ ). Although files that are produced by the GR-135 detectors that produced the blind test data include quadratic energy calibration terms, these terms only provide crude compensation for detector nonlinearities.
- The energy calibration parameters drifted, in some cases rather severely, between the time the calibration measurements were performed and when the spectra were recorded for the unknown radiation sources.

## **2.2 Calibration Issues and Approach**

### **2.2.1 ASEDRA**

Accurate and detailed energy calibration is required for ASEDRA to perform optimally; based on the available data, this was not the case. For these spectra, achieving a suitable energy calibration presented a considerable challenge for ASEDRA analysis using the data sets that were provided. Based on background peaks (1460-keV and 2614-keV peaks) in background and source spectra, the calibration was observed to drift from one spectrum to the next, and sometimes from background to spectrum measurement, by 25 keV or more. In addition, the calibration data provided with each run were often inadequate to generate an energy calibration spanning 30 keV to 3 MeV. In addition, the calibration sources for spectra 1, 2, and 4 through 7 spanned only the lower energy regions, up to approximately 100 – 122 keV; calibration files 8 through 12 contained only one strong energy point (662 keV), and calibration files 14 through 20 proved to be background radiation. Many of the calibration files for data sets 21 through 29 resembled duplicate data, and so it was uncertain if several of the files supplied truly correlated to their intended spectra.

The following methods were used in processing ASEDRA results to address these problems:

- For spectra U1 – U20, when possible, an overall calibration was generated from the cumulative calibration spectra, and was adjusted for detector drift based on positions of background peaks.

- For spectra U21 – U29, however, only a cumulative calibration was used, as background peaks were less prominent.

In addition, a wider-than-normal energy attribution window (2.5% – 3.75%) was used in the “QuickID” nuclide identification software for both data sets to account for uncertainty in the energy calibration. Also, ASEDRA requires a FWHM calibration table as a function of energy that should be as accurate as possible for the detector supplied to ensure accurate processing of peak energy and magnitude. However, a FWHM calibration dataset was not provided. To address this issue, a calibration file was therefore generated for use using a standard FWHM calibration file for a 2 in. × 2 in. NaI detector, then scaled based on the available FWHMs measured from representative peaks in the available calibration data. The computational time for execution of ASEDRA averaged 3 seconds (spanning 0 to 6 seconds) per set of unknown spectra using a standard duo-core computer at 2 GHz running Windows Vista. Uncertainties in the isotope identification results were biased by subjective judgment associated with the energy calibration process. The provision of more suitable calibration spectra would have eliminated this uncertainty bias and it would have also improved the accuracy of the isotope identifications.

### **2.2.2 GADRAS / DHSIsotopeID**

Due to deficiencies in the quality and applicability of the calibration spectra, energy calibration was performed by the following interactive process. Analysis was first performed using a set of energy calibration parameters that were defined in the data files. These preliminary results were used to identify multi-line sources that are suitable for characterizing the detector nonlinearities. This assessment selected Unknown 3, which was obviously produced by either  $^{232}\text{U}$  or a  $^{228}\text{Th}$ , as the basis for energy calibration for the first 20 unknowns. Unknowns 21 through 29 appear to have been recorded with a different instrument because of differences in detector resolution energy calibration parameters that were recorded in the data files. Therefore, Unknown 29, which exhibits several gamma rays associated with the  $^{226}\text{Ra}$  decay chain, was used as a basis for evaluating detector nonlinearities that are applicable to Unknowns 21 through 29. After determining the nonlinearity terms, the gain and/or offset parameters were adjusted for each data set based on features in the spectra. Since calibration measurements were often inapplicable, calibration spectra were not always chosen for refinement of the calibration parameters. Analysis was then performed using small adjustments of the gain and/or offset in order to select parameters that produced the best fit.

The interactive process of evaluating energy calibration parameters was necessitated because of the poor quality of the energy calibration spectra. However, analysis results that are reported in this paper were obtained by automatic execution of DHSIsotopeID after the energy calibration parameters had been established. The computational time for execution of DHSIsotopeID was less than 0.1 seconds per set of unknown spectra. Uncertainties in the isotope identification results were biased by subjective judgment associated with the energy calibration process. The provision of more suitable

calibration spectra would have eliminated this uncertainty bias and it would have also improved the accuracy of the isotope identifications.

### **2.3 Ground Truth and Evaluation Metrics**

Analysis results spreadsheets for the 29 unknowns were prepared independently by the UF/FINDS and Sandia analysts, who were not aware of results of the other organization or the source identities while data were being analyzed. The two analysis groups did not exchange their reports until after analysis results spreadsheets had been documented independently and submitted to DNDO. DNDO provided ground truth information shortly thereafter. Since the results were prepared independently, it's not surprising that methods of reporting were not directly comparable. In order to reconcile the results, the UF/FINDS team adopted the reporting formalism that is used by GADRAS but they did not alter the significance of results that were reported. The reporting formalism follows reported isotopes by (H), (F) or (L) to signify high, fair, or low confidence, respectively. A semicolon is used to separate isotopes when more than one isotope is identified. Reporting multiple isotopes does not necessarily imply that more than one isotope was present when the spectrum was measured, although this would normally be the case if multiple isotopes were reported with high confidence. Multiple isotopes might also be reported if the identification is uncertain.

## **3. Analysis Results Summary**

Section 3 summarizes the analysis results and compares the isotope identifications with ground truth information in a single table (Table 1). Isotopes that are reported correctly are highlighted in **bold type**. The accuracy of the analysis results is represented by color codes, as follows:

- **Green – Entirely correct result:**  
The principal isotopes were identified and the type of source (i.e., NORM, SNM, medical, or industrial) was inferred correctly based on the isotope identification.
- **Yellow – Generally correct result:**  
The principal isotope was identified correctly and any additional isotopes that were reported were either assigned lower confidence or they were of the same type as isotopes that were identified.
- **Red – Incorrect result:**  
The analysis result is incorrect if the principal isotope was not identified or the significance of the result was incorrect because important isotopes were not identified. For example, an analysis result would be viewed as incorrect if the algorithm did not detect that something else was present when a weak radiation source was masked by NORM even if most of the emission is attributable to NORM and the NORM isotopes were identified correctly.

Table 1 compares ground truth information with analysis results that were obtained with ASEDRA/QuickID and the GADRAS analysis algorithm DHSIsotopeID. Most of the ground truth information is self-explanatory. However, shielding configurations that are described as “rotating puzzle boxes” require additional descriptions. The rotating puzzle boxes were devised by DNDO to enable measurements with a variety of detectors that were placed around the test objects in a circular arrangement. Shielding materials in the puzzle configuration were rotated during the measurements to ensure that all detectors viewed radiation source through the same average shielding. The puzzle box was arranged in way that was intended to avoid streaming paths, and the intention was not to produce radiation signatures that could not have been produced by static shields. Nevertheless, inspection of the spectra reveals that some of the data could not have been produced by static shields. For example, the spectrum for Unknown 2, which the ground truth states is a  $^{133}\text{Ba}$  source behind a rotating lead puzzle box, exhibits a peak near 81 keV, which would not have been observed if the source were always shielded by the average thickness of lead, which was sufficient to attenuate even the high-energy gamma rays (see Fig. B2). Table 1 also includes several footnotes to denote important caveats to some of the results noted in Table 1. The *Test Plan* assembled prior to the analysis specified that the isotopes should be those listed in ANSI standards for radioactive isotope identifiers; this was not the case, and caused isotopes that were correctly attributed initially using ASEDRA/ QuickID, such as  $^{166\text{m}}\text{Ho}$  (used in unknowns U7, U8, and U17). Based on the test plan, these isotopes were subsequently ruled out by UF/FINDS researchers, who then selected the “next-best” fit for probable identification, deemed plausible given the large drift in calibration.

In any case, the objective of this report is to compare ASEDRA against analysis results that were obtained with GADRAS rather than to evaluate the performance of ASEDRA in absolute terms. Overall, this was a very difficult test suite for a variety of reasons, and the shielding implemented in many of the unknowns is only one of several factors that rendered the spectra difficult to analyze.

**Table 1. Summary ground truth and analysis results using ASEDRA and DHSIsotopeID\***

Unknown	Ground Truth	Analysis Results	
		ASEDRA**	GADRAS / DHSIsotopeID
1	Cs137 + AmBe (soil density gauge)	* Cs137(H)	Cs137(H);Pu239(H)
2	Ba133 (behind rotating lead puzzle box)	Tl201(H);Ba133(H);Co57(H); W-Shielding(F); Ce141(L)	In111(H);U235(H);U237(H); Ba133(H);I131(H)
3	U232 (behind rotating lead puzzle box)	U232(H); Irrad Th232(H); Th228(F); Am241(F); Ra226(F)	U232(H);U235(F)
4	Ba133 + Cs137 + Cf252	Ba133(H);Cs137(H); WGPu(F)	Ba133(H);Cs137(H)
5	Sr89 (beta source)	** U235(H); Ir192(F)	Sr90(H) (beta source)
6	Eu152 (behind rotating lead puzzle box)	Shielded Eu152(H); U235(F); Ba133(F)	Eu152(H)
7	Ho166m (behind rotating steel puzzle box)	*** Shielded Enriched U(H); Mn54(F), Th-232(L)	Ho166m(H)
8	Ho166m	*** Enriched U(H); Mn54(F)	Ho166m(H)
9	Ba133	U235(H); Ba133(H); Co57(F); Eu- 155(L)	Ba133(H)
10	Mo99 + potash fertilizer (22% K <sub>2</sub> O)	K40(H); Irrad Th(F); Eu-155(L)	K40(H);Pu239(H)
11	U232 + terra-cotta roofing tile	K40(H); U238(F); Irrad Th(F); U233(L)	Th232(H);Ra226(H)
12	I131 + kitty litter	I131(H); Ba133(F); U-238(L); Xe133(L)	Th232(H);Ra226(H)
13	Mn54 (behind rotating steel puzzle box)	Mn54(H); Mn56(F); Shielded Irrad Th(L); U233(L)	Mn54(H)
14	Cf252 inside 15 cm of polyethylene	**** BKG(F); Xe133(F)	Pu239(H);Neutron(H)
15	HEU + Ra226	Ra226(H); U235(F); Ga67(L)	Ra226(H);U235(H)
16	HEU + Ga67	Ga67(H); U235(F); BKG(F); Ba133(L); Co57(L)	Ga67(H);U235(H);Th232(H)
17	HEU + Ho166m	*** Enriched U(H); Np237(F)	Ho166m(H);U235(H);Th232(H)
18	HEU + potash fertilizer (22% K <sub>2</sub> O)	*** K40(H)	K40(H)
19	Np237 + terra cotta roofing tile	Shielded WGPu(H); K40(F); Np237(F)	In111(H);Ba133(H);Ga67(H); K40(H);U235(F)
20	Np237 + (behind rotating lead puzzle box)	Shielded Ga67(H); Pu239(F), Ir192(L)	In111(H);Ga67(H);Lu177m(H); Cf252(H);U237(H);U235(F); U232(F)
21	Cf252 + DU	Shielded Enriched U(H); U238(F); U235(F), Co57(F); K40(F)	U238(H);Pu239(F)
22	F18	**** Irradiated U(L)	F18(H)
23	Pu239	WGPu(H); Ba-133(F); Cs-137(F); Ga67(F); Shielded U-238(F); Mn-54(L)	Pu239(H);U235(F)
24	Pu239 + I131	I131(H); WGPu(H); Irrad U(F); Ba133(F); Cs137(F); Mn-54(L)	I131(H); Cf252
25	Np237	Shielded Ga67(H); Ba133(F); Enriched U(F)	Np237(H)
26	Np237 + Ga67	Shielded Ga67(H); Ba133(F); Enriched U(F)	Np237(H)
27	Pu239 + Ba133	WGPu(H); Ba133(F); Ga67(F), Cs137(F); Np237(L); Irrad Th(L)	Ba133 (H);Pu239(H)
28	Pu239 + Ra226	Shielded WGPu(H); Ga-67(F); DU(F)	Pu239(H);Ra226(H)
29	HEU + Ra226	Ra226(H); K40(F); I131(F); Co57(L)	Ra226(H);U235(H)

Table 1 footnotes:

- + (H) = High; (F) = Fair; (L) = Low, each is expressed as a relative confidence.
- \*\* Due to the poor detector energy calibration data and uncertain FWHM data versus energy behavior associated with the spectra, the QuickID software was employed as an independent package with a peak aliasing window as large as 3.75% to attribute photopeaks found by ASEDRA, which often resulted in multiple possible nuclide identifications; the results indicating nuclides in the Table 1, reported in a detailed spreadsheet submitted in the blind, are flagged with a relative confidence using (H), (F) or (L), and reflect a combination of the two settings used in ASEDRA analysis --one that incorporated data recalibration, and one less conservative without data recalibration. A comment of "Shielded" was added if it appeared evident that one or more low-energy gammas that should be present was/were suppressed in the analysis. A comment of "Irrad" meaning "irradiated" was given if nuclides consistent with irradiated isotopes were indicated in the analysis.
- \*\*\* In addition to K-40, two significant gamma lines extracted by ASEDRA using "Settings 2" reported in the blind spreadsheet data at 190 and 139 keV could have been attributed to the two prominent U-235 peaks at energies of 186 keV and 143.8 keV, respectively, with the observed drift in the energy calibration; for some reason, these two lines were simply not labeled as "U-235" by the analysts in reporting the blind data.
- \* Other faint gamma lines that appeared to be consistent with WGPu were extracted with ASEDRA using less conservative settings; however, given the large variation in the calibration data, these were not attributed, although the spectrum was regarded as suspicious
- \*\* Strontium beta emitters were not attributed by QuickID. ASEDRA is designed to synthetically render photopeaks as a result of gamma emission only, without accounting for beta emission.
- \*\*\* Ho166m was in fact attributed by ASEDRA using QuickID in these spectra, but was dismissed since this nuclide was not an approved source material as noted in the Test Plan published for this effort. Further, given the large drifts in energy calibration, "next-best" attributions were therefore made by the analysts.
- \*\*\*\* During post-evaluation assessment, lowering the minimum detectable threshold for detected peaks in ASEDRA from 5 counts to 1 count in the less conservative settings revealed a 2.4 count neutron peak within the search window for 2.22 MeV gammas, indicating a hydrogen capture  $H(n,\gamma)$  reaction. Therefore, using a lower minimum threshold setting in ASEDRA would have triggered a fissile SNM / WGPu flag in QuickID, yielding a correct result.
- \*\*\*\*\* F-18 attribution was turned off in QuickID, since this isotope has a 110-minute half life and was screened out by the software settings used (only days or longer half-lives were considered using QuickID).

The evaluation metric that is used to assign color codes is subjective to some extent, so explanations for why the analysis results were ascribed in this way are required for some of the unknowns. Results that were obtained by both analysis algorithms for Unknown 2 are assigned to the yellow (generally correct result) despite the fact that both algorithms reported several isotopes in addition to  $^{133}\text{Ba}$ , which was the only isotope that was actually present. What neither of the analysis teams could have known was that the rotating shielding produced artifacts that could not be associated with  $^{133}\text{Ba}$  with a static shield. Therefore, the analysis results would have prompted additional inspection despite the ambiguities, which would have been the correct response, though not necessarily for the proper reason.

Misidentification of a neutron source is another case that does not have a significant impact on the outcome because the identification of any neutron source is sufficient to prompt additional inspection. Shielded neutron sources are very difficult to distinguish based on measurements with low-resolution gamma-ray detectors. Beta emitters are another class of radioactive materials that are very difficult to distinguish, but the presence of any beta emitter would have a similar significance when an inspection is performed. Therefore, the DHSIsotopeID assessment that Unknown 6 was consistent with  $^{90}\text{Sr}$  when the actual source was  $^{89}\text{Sr}$  is also viewed as a generally correct result.

The significance of some of the isotope identification results can only be evaluated in the context of other isotopes that were present at the time the measurement was made. For example, DHSIsotopeID misidentified the contaminant  $^{232}\text{U}$  in HEU as  $^{232}\text{Th}$  for Unknowns 16 and 17, but this had no bearing on the importance of these assessments because  $^{235}\text{U}$  was identified correctly in both cases. However, the assessment was rated as incorrect when DHSIsotopeID failed to identify  $^{232}\text{U}$  in Unknown 11 even though it did identify NORM correctly in the roofing tiles. This evaluation was rendered

because by failing to identify  $^{232}\text{U}$ , the algorithm might have missed the only observable if HEU had been concealed in the roofing tiles. On the other hand, ASEDRA correctly identified the  $^{131}\text{I}$  source in Unknown 12 (U12) but it only weakly indicated NORM in kitty litter for this event (ASEDRA did not indicate  $^{226}\text{Ra}$  in U12, but did indicate a weak presence of  $^{238}\text{U}$  at low confidence; kitty litter is known to contain on the order of 5 ppm of uranium). However, this is viewed as an entirely correct result because the presence of NORM is of no consequence when other isotopes are present.

## 4. Conclusions

Given the challenges of the calibration and background data supplied for these tests, ASEDRA was able to extract many unique gamma lines/signatures of interest based on the source terms identified. In discussion of the results, it is important to differentiate results of the noise reduction and peak extraction algorithm ASEDRA, and the still “under development” nuclide identification code QuickID, which was used throughout the ASEDRA peak analysis.

As the goal of the project was to test ASEDRA, which renders peaks from a given spectrum, the spreadsheet in Appendix A is necessary to consider in the evaluation. The spreadsheet shows all peaks with energies and counts found for the ASEDRA analysis of each unknown (as well as attribution results from QuickID). As the spreadsheet transmitted in the blind test demonstrates, ASEDRA analysis in most cases indeed yielded the primary peaks associated with the unknowns present.

ASEDRA proved to be most effective at energies above 500 keV, and was in most cases reasonably effective below 500 keV. It is encouraging that principal isotope lines were detected with ASEDRA even when specific tunable settings (e.g., scattered counts scaling and aliasing of DRFs, for example) were very different. Moreover, analysis with less conservative “Settings 2” in some cases also yielded some weaker peaks that were quite revealing in the analysis, such as the  $\text{H}(n, \gamma)$  peak due to the presence of WGPu or Cf-252.

The built-in noise reduction ACHIP algorithm proved to be quite valuable in discerning low-count effects, particularly the 2.22 MeV  $\text{H}(n, \gamma)$  peaks when neutrons were present. Also, when statistics were very good, ACHIP denoising had little influence, which was by design.

Misidentifications of isotopes using the ASEDRA/QuickID analysis resulted from several factors, which are listed below:

1. Uncertainty in calibration—the lack of stable energy and FWHM detector data (essential for accurate analysis and therefore had to be estimated for the spectra)
2. Calibration offsets between spectra were often significant and varied by 25 keV or more, leading to a necessity for nuclide gamma line search windows as large as 3.75%

3. Artificial elimination of nuclides from consideration based on the Test Plan (e.g.,  $^{166m}\text{Ho}$ )
4. Lack of a specific nuclide attribution or shortfalls within QuickID
5. Inconsistencies in analyst interpretation of the data (of which U18 and U22 are good examples); clearly, due to the nature of the analysis process for these data, the results were influenced by the skill of the analyst

The shortfalls in QuickID, noted particularly in the cases of U5, U7, U8, U17, U18, and U22 (referencing Table 1 results and associated footnotes), we are confident that with an improved QuickID tool, fully correct identifications using ASEDRA would have occurred.

One item to note is the handling of shielding; while ASEDRA does provide a scaling of the Compton region due to higher scatter, the exact DRFs for different shielding materials and detector geometries have not been explicitly calculated. Therefore, in some cases, peaks shown in the Compton region may represent scatter or have inflated counts due to scatter from shielding. Still, it is important to note that in most cases, this did not prevent ASEDRA from extracting peak energies that enabled a correct identification of the spectra. However, this may be an area for future work. Refinement of QuickID is also an area for future development; at the time of testing it had just been completed and was very much under “alpha” testing development. In any case, in the interest of providing a similar way of depicting ASEDRA results compared to those generated by GADRAS, which performs nuclide identification, QuickID was assembled. QuickID will be honed in the future to more accurately include all nuclides of interest for attribution analysis in addition to the nuclides listed in ANSI 42.43, and augmented with a more robust “Figure of Merit” logic.

The purpose of this study was primarily to evaluate ASEDRA, and GADRAS was used as a mature standard against which ASEDRA was compared. Although GADRAS was somewhat more accurate on average, the performance of ASEDRA exceeded that of GADRAS for some of the unknowns. Therefore, ASEDRA proved to be a viable alternative for the analysis of sodium iodide data. The fact that GADRAS also failed to identify many of the radiation sources attests to the difficulty of analyzing the blind-test data that were used as a basis for this evaluation.

The performance of both analysis algorithms was hampered by the lack of good calibration data. Regardless of the algorithm that is used to process the data, results will be more definitive and the analysis process will be facilitated if procedures are established to enable characterization of the detector nonlinearity as well as gain and offset parameters. Periodic measurements of  $^{232}\text{Th}$ -bearing materials such as lantern mantles or welding rods would provide a necessary calibration standard and ensure well-calibrated data. Digital multichannel analyzers also tend to provide more stable energy offsets.

This page intentionally left blank.

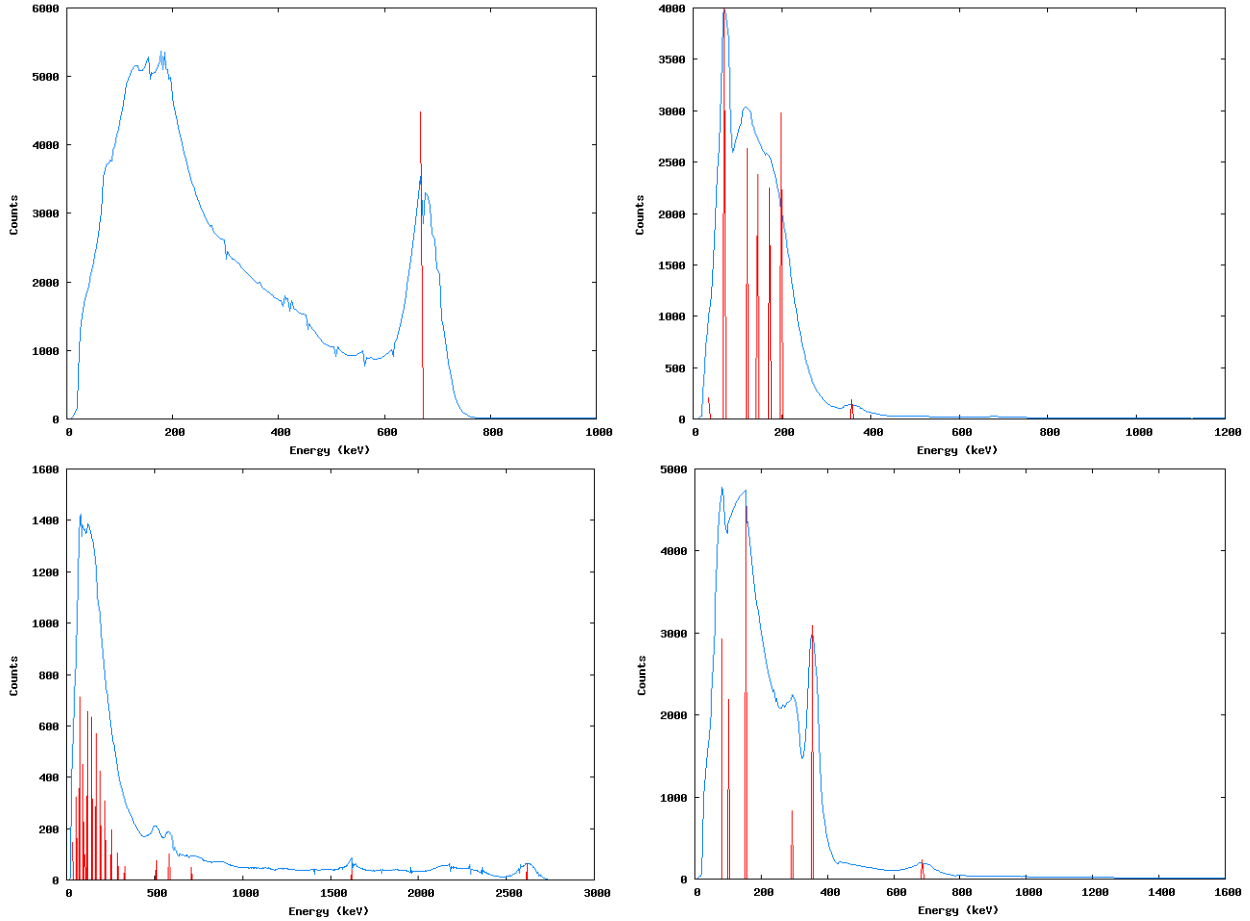
## Appendix A: Analysis Details for ASEDRA with QuickID

Analysis results are shown and discussed in greater detail for spectra U1 to U29 in the figures below, and in the included blind reported spreadsheet with detailed information on photopeaks located, where the energy of the peak rendered by ASEDRA, the nuclide identification for that peak, the counts rendered, and the % of counts attributed to that peak (norm % of counts) can be found. All spectra processed by ASEDRA are depicted in figures here employing the full denoising algorithm (ACHIP) available in ASEDRA. The QuickID software was employed as an independent package that considered nuclides with half lives of days or more. Due to calibration issues, QuickID was employed with a peak aliasing window as large as 3.75% to attribute photopeaks found by ASEDRA. The spreadsheet submitted depicts the likely nuclide identified for the sample, as well as other possible, lower-confidence nuclides identified (“Other”), and the overall recommendation for the nuclide ID based on the cumulative analysis, as already summarized in Table 1. Due to the large gain drifts in the data that degraded detector energy calibration and FWHM data vs. energy confidence, the ASEDRA results reflect a combination of two sets of settings used in ASEDRA analysis—one that incorporated data recalibration (“Settings 1”), and one less conservative without data recalibration (“Settings 2”).

Figures A-1 through 4 show the ASEDRA peaks rendered for select ASEDRA runs for unknown spectra U1-U4. As mentioned earlier in the analysis description, a full listing of all photopeaks rendered with energies, and counts, are indicated in the attached spreadsheet at the end of this appendix. Figure A-1 shows ASEDRA results for Unknown 1 (U1) was identified in ground truth as a  $^{137}\text{Cs}$  + AmBe source. Using conservative ASEDRA parameters, analysis yielded a single photopeak at 668.2 keV, leading to the identification of  $^{137}\text{Cs}$ . Using even less-conservative settings (smaller shielding multipliers in DRFs, etc.), very faint gamma lines that appeared to be consistent with WGPu were extracted by ASEDRA; for this reason the spectrum was regarded as suspicious, but no additional reporting was postulated at the time of the analysis.

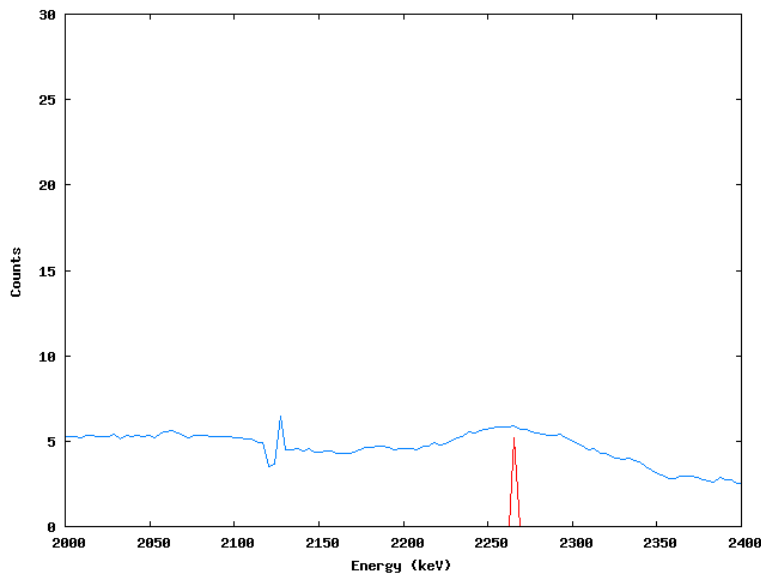
Figure A-2 shows ASEDRA analysis of Unknown 2 (U2), revealed in ground truth to be  $^{133}\text{Ba}$  behind a rotating lead shield puzzle box; ASEDRA with QuickID identified the sample as  $^{201}\text{Tl}$ ,  $^{133}\text{Ba}$ , and  $^{57}\text{Co}$  in combination. Photopeaks were rendered at 35.16, 69.34 (identified as W-Shielding), 121.7 ( $^{57}\text{Co}$ ), 145.54, 172.35( $^{201}\text{Tl}$ ), 199.19, and 357.34 ( $^{133}\text{Ba}$ ). More conservative gamma photopeak aliasing is evident in this application of ASEDRA, giving added confidence in the gamma energies detected.

Figure A-3 shows ASEDRA analysis of Unknown 3 (U3), reported in the ground truth as  $^{232}\text{U}$  behind the rotating lead shield “puzzle box”; primary ASEDRA photopeaks rendered include the  $^{232}\text{U}$  and  $^{228}\text{Th}$  daughters  $^{208}\text{Tl}$  and  $^{212}\text{Bi}$ , such as lines at 510.6 keV, 583 keV, 708, keV, 1620 keV, and 2614 keV.



**Figures A-1-4. ASEDRA peaks rendered:U1 (top left), U2 (top right), U3 (bottom left), U4 (bottom right).**

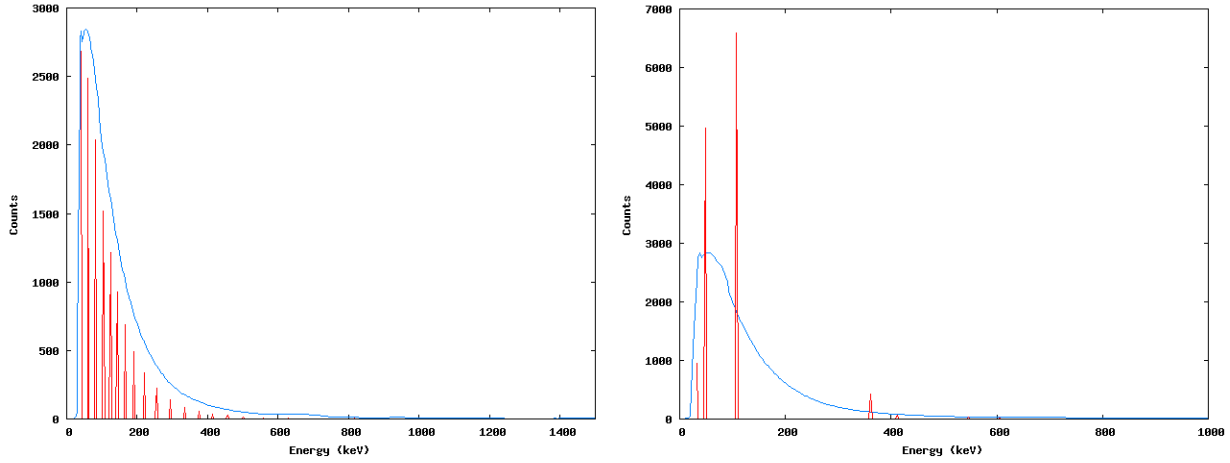
Figure A-4, Unknown 4 (U4) was reported in the ground truth as a combined  $^{133}\text{Ba}$ ,  $^{137}\text{Cs}$ , and  $^{252}\text{Cf}$ . Analysis of U4, using conservative parameters, shows primary photopeaks at 80 keV, 295 keV, 354 keV, and 685 keV, leading to the ID of  $^{133}\text{Ba}$  and  $^{137}\text{Cs}$  present in the spectrum. Also, as shown in the attached spreadsheet, blind analysis using slightly less conservative parameters and lower acceptable thresholds yields a weak photopeak at 2250 keV, indicating, in addition to the other nuclides, an attributed presence of neutrons. This  $\text{H}(n,\gamma)$  peak was extracted using lower threshold settings in ASEDRA, as shown in Figure A-4a below.



**Figure A-4a. ASEDR peak extracted at high energy from spectrum U4. Although the calibration was only passable, ASEDR was able to extract a photopeak aliased to a 2.22 MeV hydrogen H(n,  $\gamma$ ) line from the denoised spectra, indicating the presence of neutrons in the sample.**

Unknown 5 (U5) was revealed in the ground truth to be a Strontium beta emitter, and this was not attributed by QuickID. Also, ASEDR attempted to derive photopeaks from this spectrum (Figure A-5), and the results were not supportable since ASEDR is designed to synthetically render photopeaks as a result of gamma emission only, without accounting for beta emission. With more conservative settings on shielding and aliasing (Figure A-5a), and very few peaks were rendered.

Unknown 6 (U6), revealed to be  $^{152}\text{Eu}$  behind a rotating lead “puzzle box” shield in the ground truth, is a good candidate for illustration of the ASEDR and QuickID analysis. Figure A-6 shows photopeaks rendered in red, overlaid on a de-noised ASEDR post-processed spectrum. Table A-1 lists the U6 photopeaks, counts and relative percent of counts, along with the identification of photopeak energies based on QuickID processing. QuickID Results for photopeaks rendered by ASEDR for Unknown 6 show key  $^{152}\text{Eu}$  lines; the final high confidence ID of “Shielded  $^{152}\text{Eu}$ ” was chosen due to the lowered yield of the 344 keV line, and no visible line at 122 keV. It is interesting to note that ASEDR extracted a gamma line at 128 keV, in this spectrum, and this was aliased to the 122 keV  $^{152}\text{Eu}$  line.



Figures A-5 and 5a, respectively. Analysis of U5 with unconservative (left) and conservative settings (right). This was later identified as a strontium beta source; assuming it was a heavily shielded gamma source, it was attributed by ASEDRA to be  $^{235}\text{U}$ , or possibly  $^{192}\text{Ir}$ , yet data correlation was poor.

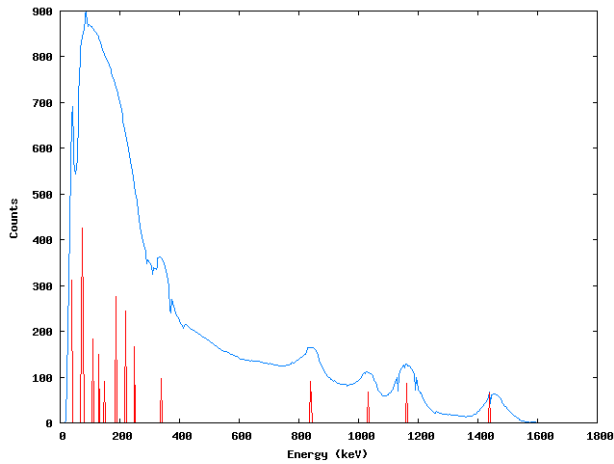


Figure A-6. ASEDRA Analysis of U6, which was revealed to be  $^{152}\text{Eu}$  behind a rotating lead “puzzle box” shield.

**Table A-1. Analysis of Unknown 6**

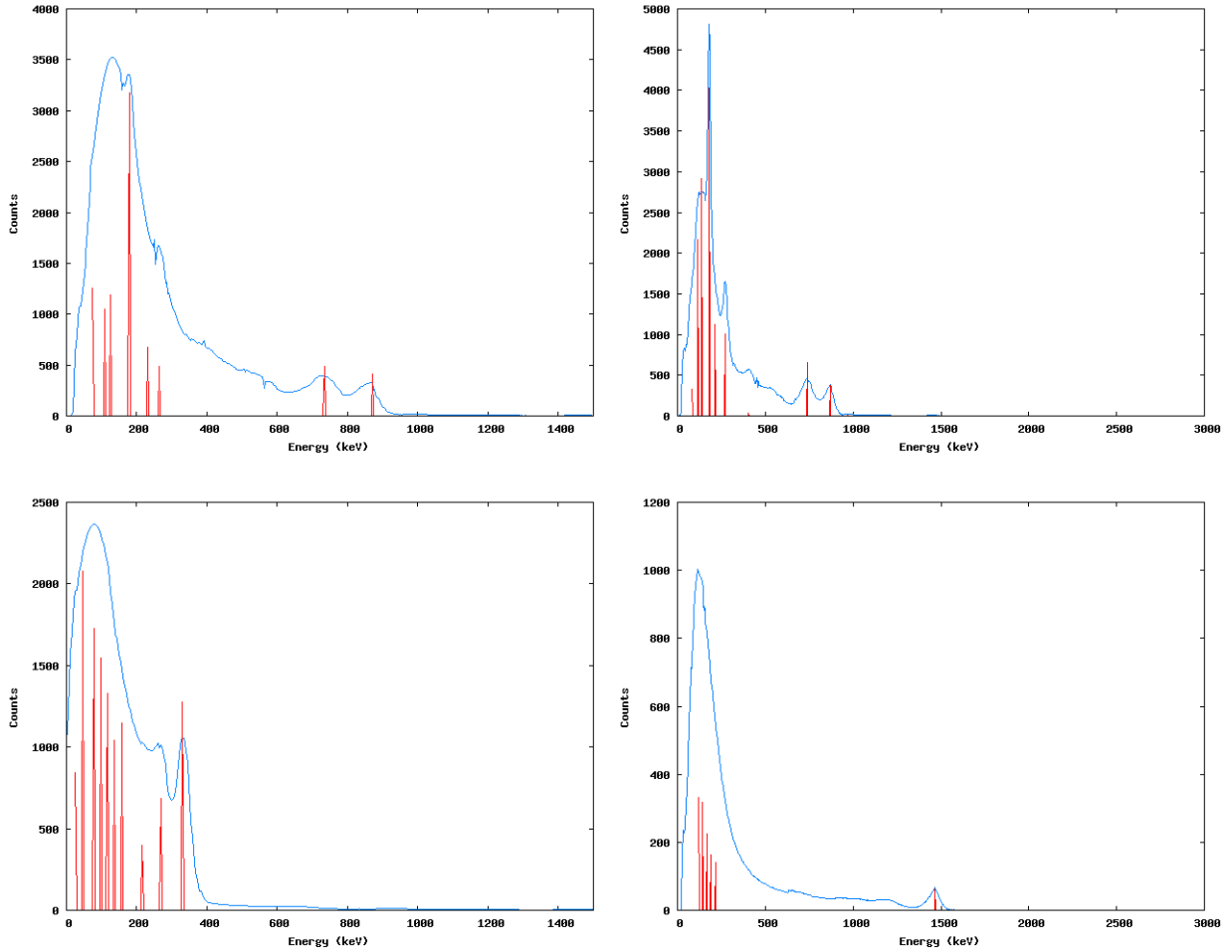
Analysis with Adjusted Calibration, Settings 1			
Likely ID: Eu-152		Other: U-235	
Isotope	keV	Counts	Norm% Cts
	43.81	2.65E+02	11.62
	80.29	4.57E+02	20.07
	110.47	2.11E+02	9.27
Eu-152?	128.09	1.54E+02	6.75
U-235	145.72	1.03E+02	4.51
U-235	189.78	2.84E+02	12.46
Eu-152/ Ba-133	222.09	2.49E+02	10.95
	257.34	1.71E+02	7.49
Eu-152	339.59	1.10E+02	4.84
Eu-152	790.19	7.08E+01	3.11
Eu-152	979.78	6.05E+01	2.66
Eu-152	1110.50	7.73E+01	3.40
Eu-152	1391.70	6.55E+01	2.87

Analysis of Unknowns 7 through 10 by ASEDRA are shown in Figures A-7-10.

In analysis of unknowns 7 and 8, identified by ground truth as  $^{166m}\text{Ho}$ , the assumption of only testing against sources listed in the ANSI standard (as noted in the Test Plan) is important to mention, as this influenced the sources eliminated from consideration in QuickID. Therefore,  $^{235}\text{U}$  was attributed since a line was detected aliased to the 186 keV line; however, this still did not fully explain the twin peaks extracted that were observed at 737 keV and 850 keV in the spectra. We note that  $^{166m}\text{Ho}$  did indeed appear in QuickID as a strong possibility with good correlation to the 737 and 850 keV lines, but was eliminated from consideration as a possibility based on the guidelines for isotopes to consider in the Test Plan, and thus  $^{166m}\text{Ho}$  was not attributed in either case for U7 or U8, and “next best” alternatives were selected.

ASEDRA analysis of Unknown 9 (U9), identified as  $^{133}\text{Ba}$  in the ground truth, yielded peaks indicating a strong  $^{133}\text{Ba}$  signature within the energy search window of 3% (at 85, 283, 342 keV), as well as peaks at 175/185 keV associated with  $^{235}\text{U}$ . Lines consistent with  $^{57}\text{Co}$  were also found with lower confidence.

U10 was identified by the ground truth as  $^{90}\text{Mo}$  and potash fertilizer (22%  $\text{K}_2\text{O}$ ) and analysis by ASEDRA shows a strong  $^{40}\text{K}$  peak (at 1466 keV) indicating  $^{40}\text{K}$ , as well as other low energy peaks indicating possible  $^{232}\text{Th}$  or Irradiated  $^{232}\text{Th}$ .



**Figures A-7-10. ASEDRA peaks rendered: U7 (top left), U8 (top right), U9 (bottom left), U10 (bottom right).**

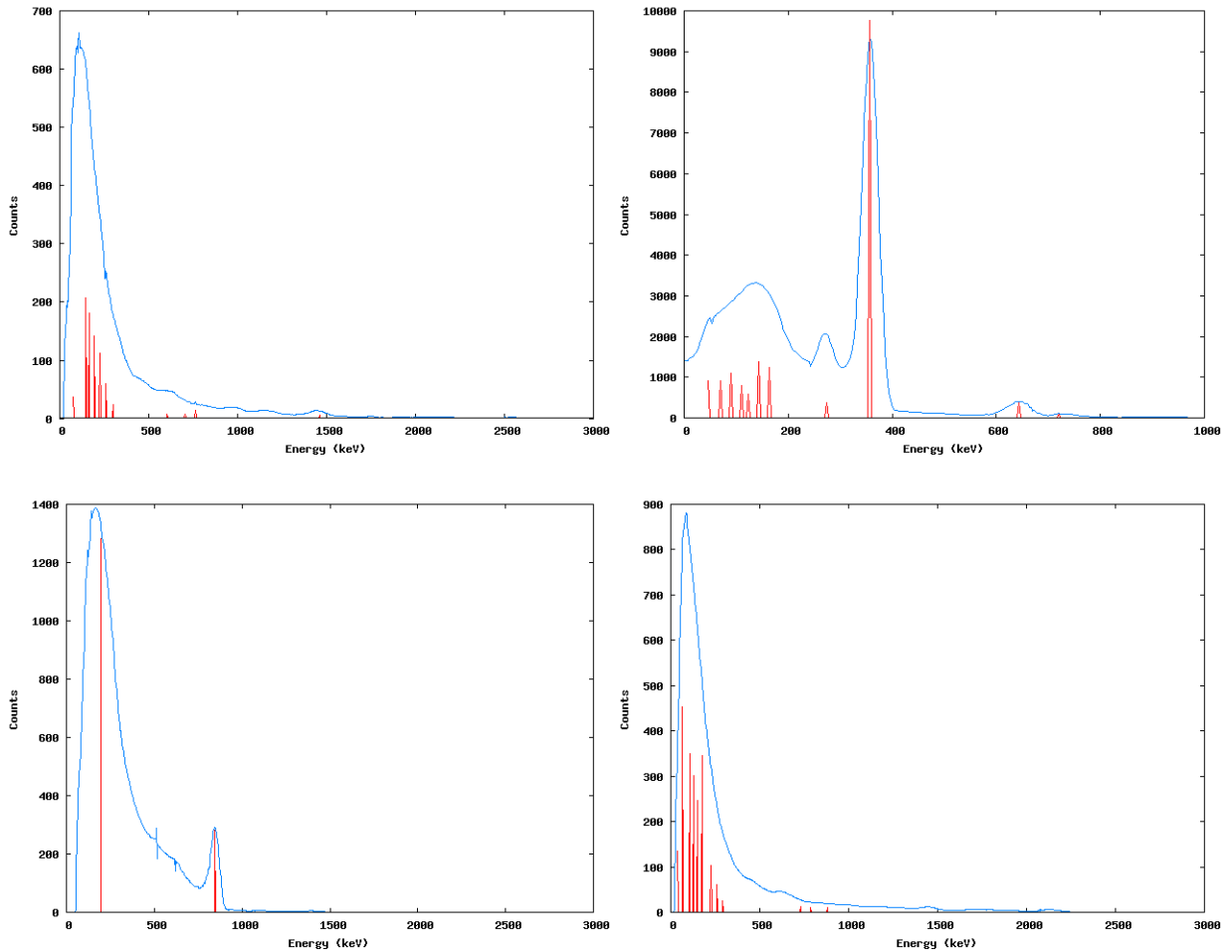
Results for unknowns U11 through U15 by ASEDRA are depicted in Figures A-11-15, respectively.

Based on the peaks rendered by ASEDRA for U11, we identified this as  $^{40}\text{K}$  (1460 keV line), with possible  $^{238}\text{U}$  or Irradiated Thorium due to other lower energy lines listed in the submitted spreadsheet.

For U12, when the calibration was adjusted, ASEDRA yielded lines at 287, 362, 637, and 711 keV, which were attributed as key lines of I-131 (284, 365, 637, 723 keV) with a 3% energy search window.  $^{133}\text{Ba}$  and  $^{133}\text{Xe}$  were weakly indicated as possibly present using "Settings 2."

Unknown 13 was identified as clean  $^{54}\text{Mn}$  (835 keV) with the adjusted calibration data due to the 845 keV line extracted. Without adjusting the calibration, a few additional lines were found, but identification was unclear.

Unknown 14 was identified as background based on peaks rendered from  $^{238}\text{U}$  and  $^{232}\text{Th}$  decay. It was later identified as  $^{252}\text{Cf}$  inside 15 cm of polyethylene; no 2.22 MeV gamma peak was extracted using a lower limit threshold of 5 counts in ASEDRA. Interestingly, after the ground truth was revealed, we went back and re-ran ASEDRA with a lower limit threshold of only 1 count, and this time a peak attributed to neutrons due to an  $\text{H}(n, \gamma)$  peak at 2188 keV at just 2.4 counts was extracted by ASEDRA, as was then another peak at 2077 keV believed to be an  $\text{H}(n, \gamma)$  peak from iron. This is shown in Figure A-14a.



**Figures A-11-14. ASEDRA peaks rendered: U11 (top left), U12 (top right), U13 (bottom left), U14 (bottom right).**

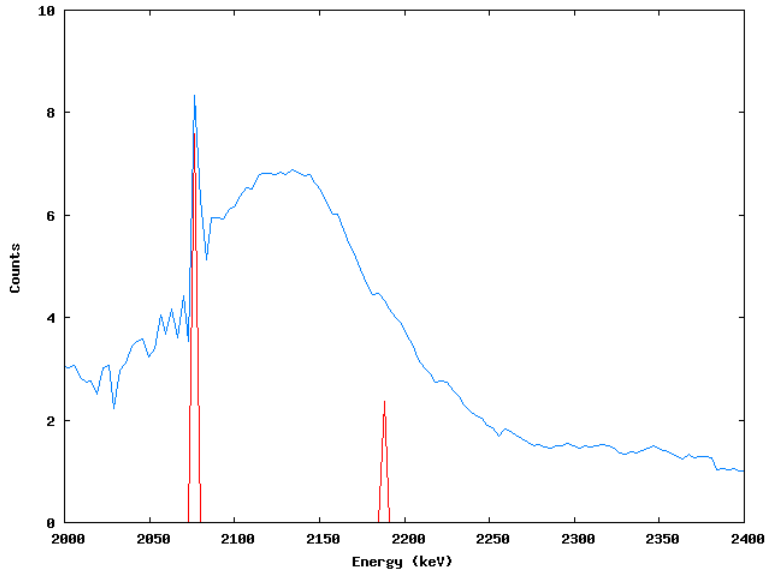


**Figure A-14a. High-energy region of U14 following post-analysis re-evaluation (denoised by ASEDRA). After it was revealed that U14 was a moderated  $^{252}\text{Cf}$  source, we re-analyzed the spectrum with ASEDRA, lowering the threshold for the number of minimum detectable counts from 5 counts to 1 count (above background). Subsequently, ASEDRA extracted a peak (on the right) at 2188 keV, which falls within the search window for the 2224 keV hydrogen  $\text{H}(n, \gamma)$  line based on the evident calibration. Also extracted was a line at 2077 keV, attributed to a 2111 keV  $\text{Fe}(n, \gamma)$  line.**

Unknown 15 was identified in the ground truth as “HEU +  $^{226}\text{Ra}$ .” ASEDRA analysis with QuickID identification attributed  $^{226}\text{Ra}$ ,  $^{67}\text{Ga}$ , and weak  $^{225}\text{U}$ , due to the peaks at 186, 609, 297, 292, 351, 609, 1259, 2215 keV, and others, as listed in the spreadsheet.

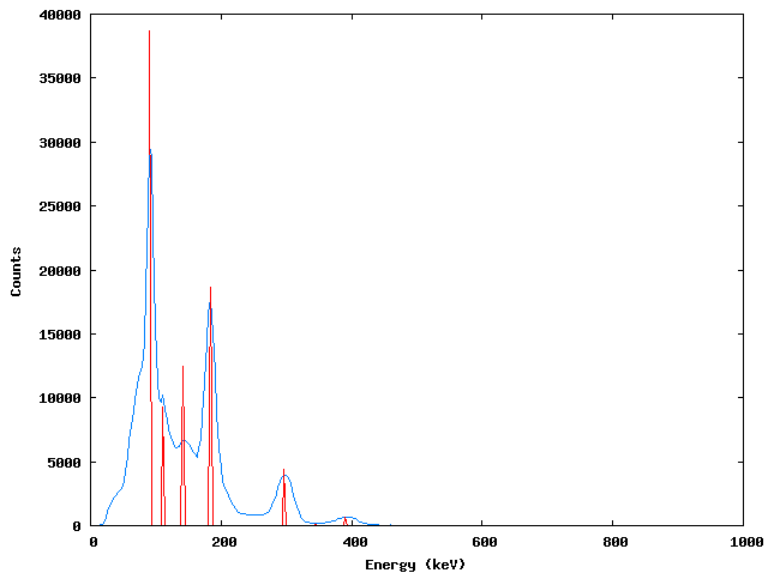
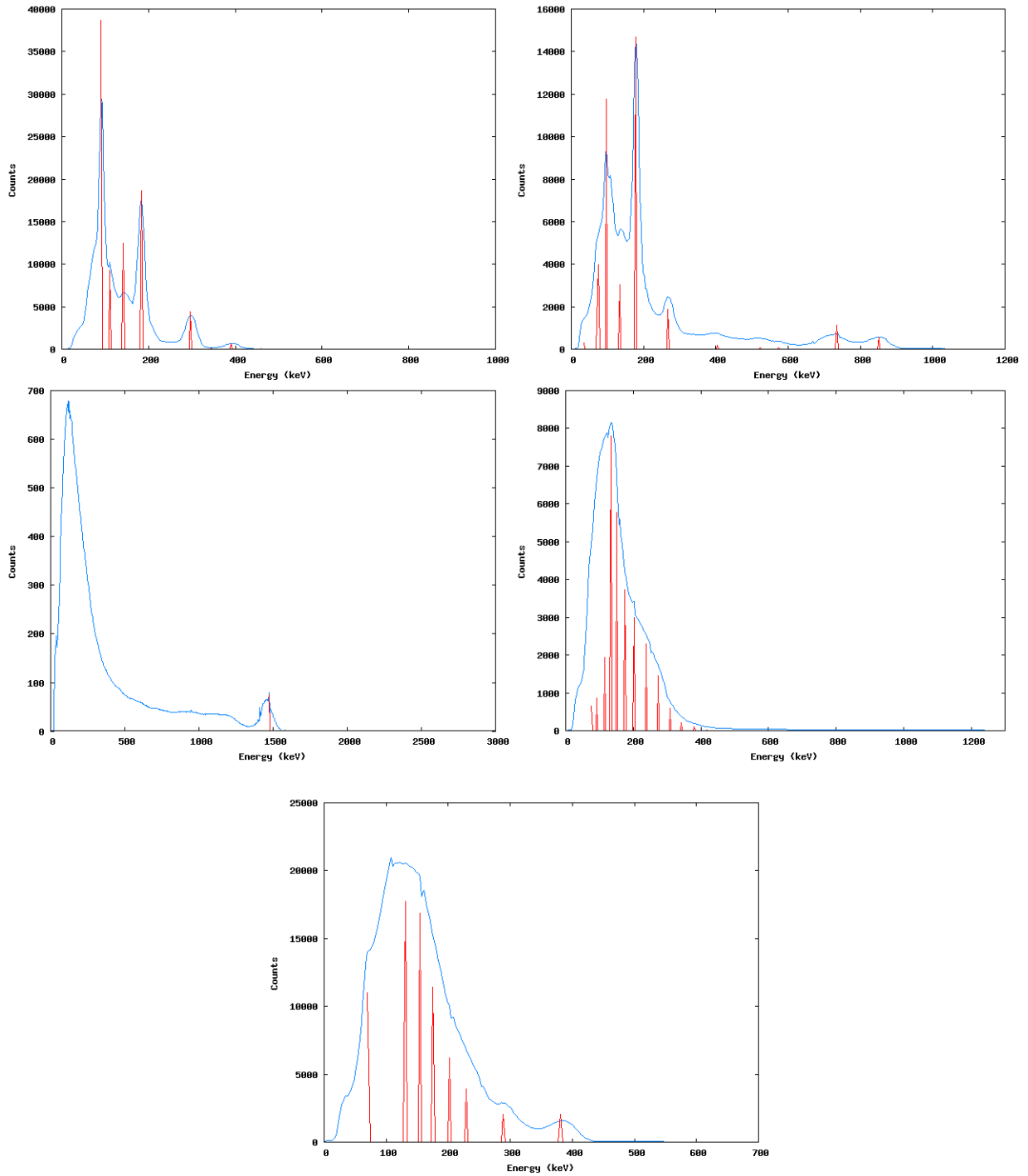


**Figure A-15. ASEDRA Analysis of Unknown U15.**

Figures A-16 through A-20 show ASEDRA analysis of Unknowns U16 – U20.



Figures A-16 – 20. ASEDRA peaks rendered: U16 (top left), U17 (top right), U18 (middle left), U19 (middle right), and U20 (bottom).

ASEDRA analysis of U16, identified in ground truth as HEU +  $^{67}\text{Ga}$ , shows photopeaks that signify  $^{67}\text{Ga}$  with an adjusted calibration (90, 184, 297, 390 keV).  $^{235}\text{U}$  was also indicated in the analysis using the less conservative “Settings 2” in ASEDRA.

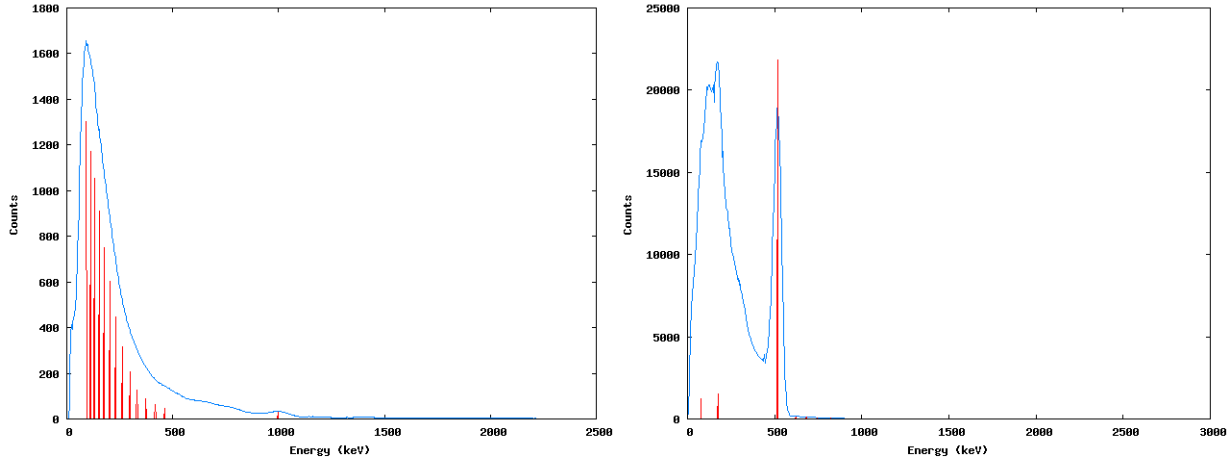
U17 was identified in ground truth as HEU +  $^{166\text{m}}\text{Ho}$ . Photopeaks from U17 showed a strong line at 178 keV aliased to the U-235 186 keV line as well as a 1015 keV line and others aliased to  $^{238}\text{U}$  (1001 keV, etc), leading to the primary ID of enriched U.  $^{166\text{m}}\text{Ho}$  was in fact attributed by ASEDRA using QuickID, but was dismissed since this nuclide was not an approved source material as noted in the Test Plan defined for this effort. As a result, the next best attribution using QuickID in this case was  $^{237}\text{Np}$ .

Unknown 18 (U18) was identified in ground truth as HEU + potash fertilizer (22%  $\text{K}_2\text{O}$ ). U18 yielded a strong peak at 1474 and was identified as  $^{40}\text{K}$ . Two significant gamma lines extracted by ASEDRA using “Settings 2” at 190 and 139 keV could have been attributed to two prominent  $^{235}\text{U}$  peaks with energies of 186 keV and 143.8 keV with the observed drift in the energy calibration, although for some reason these two lines were simply not labeled as “ $^{235}\text{U}$ ” by the analysts in reporting the blind data. This oversight would have resulted in a completely correct identification for this case had the association to the two most prominent  $^{235}\text{U}$  lines above 20 keV (the 186 and 143.8 keV lines) been made.

Unknown 19 (U19) was identified in the ground truth data as  $^{237}\text{Np}$  + terra cotta roofing tile. U19 was identified by ASEDRA as shielded WGPu (primary) with a small amount of  $^{40}\text{K}$  present, due to photopeaks rendered at 381 and 418 ( $^{239}\text{Pu}$  375 keV and 414 keV lines) and 1505 ( $^{40}\text{K}$ , 1460 keV line). However, several photopeaks were also aliased to  $^{237}\text{Np}$  using ASEDRA settings with increased shielding (as apparent from the spectra) as shown in the blind data spreadsheet (309 keV, 342 keV, aliased to the 312 keV and 340 keV  $^{233}\text{Pa}$  neptunium daughter lines). Several lines consistent with  $^{239}\text{Pu}$  were also noted, although no  $\text{H}(n, \gamma)$  neutron peaks were extracted.

U20 was identified in the ground truth data as  $^{237}\text{Np}$  behind a rotating lead “puzzle box” shield. U20 did show strong peaks at 292 and 391 keV; due to the energy calibration these were aliased more closely to the  $^{67}\text{Ga}$  300 keV and 394 keV lines than  $^{237}\text{Np}$ . An identification of shielded  $^{67}\text{Ga}$  was attributed since the lower energy  $^{67}\text{Ga}$  peaks (209 keV, 185 keV, 94 keV) were not extracted by ASEDRA.

Unknowns 21 (U21) and 22 (U22) are shown below in Figures A-21 and A-22.

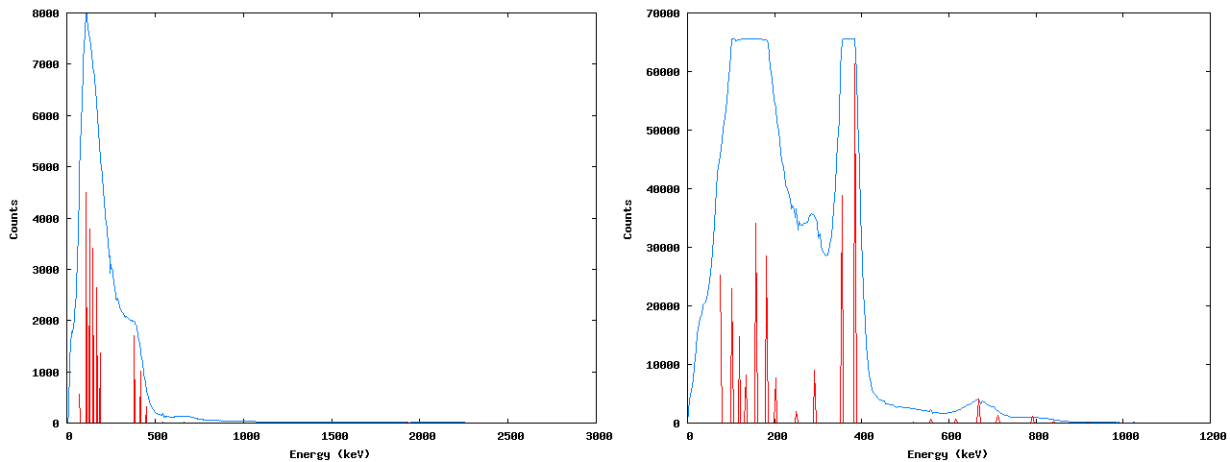


**Figures A-21 – 22. ASEDRA peaks rendered: U21 (left) and U22 (right)**

Unknown 21, identified in the ground truth data as Cf-252 + DU, was analyzed with ASEDRA, and this analysis yielded a peak at 998 keV aliased to U-238 daughter Pa-34m, as well as a peak at 178/181 keV, aliased to U-235 or Ra-226. Based on these, identifications of enriched U and U-238 were given. “Settings 2” settings netted “fair” confidence hits on U-235, Co-57, and K-40 as well.

Unknown 22 in the ground truth data as F-18. Unfortunately, F-18 attribution was turned off in QuickID, since this isotope has a 110-minute half life and was screened out by the software settings used—only half lives of days or more were considered using QuickID. Hence, U22 was identified as irradiated U with low confidence based on weak U-238 and U-233 lines seen; however, the strong peak at 516/520 keV based on the given calibrations was not explained. In any case, this identified a need to include all known medical isotopes will be made as development of QuickID progresses.

Unknowns 23 (U23) and 24 (U24) are shown below in Figures A-23 and A-24.

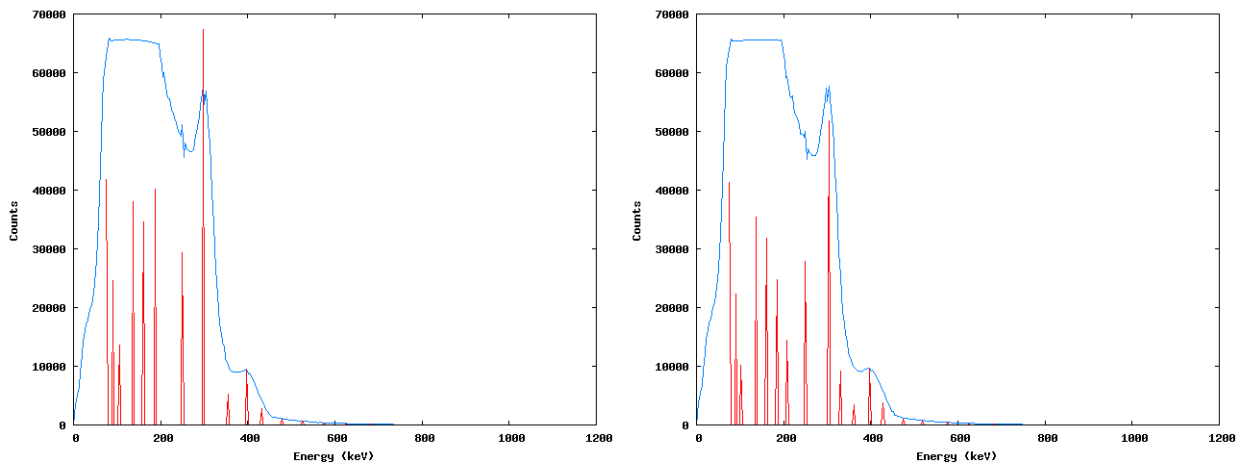


**Figures A-23 – 24. ASEDRA peaks rendered: U23 (left) and U24 (right)**

Unknown 23 (U23) was identified by the ground truth as Pu-239. Based on the ASEDRA analysis, U23 was given a primary identification as WGPu based on the photopeaks rendered at 383, 418, and 451 keV aliased to the 375, 414, and 450 keV Pu-239 peaks; the peak rendered at 662 keV was also aliased to the Pu-241 daughter (Am-241, 662 keV). ASEDRA analysis with “Settings 2” also netted a peak at 2191 keV (only 7.4 counts), attributed to a H(n,  $\gamma$ ) peak, indicating a presence of neutrons. The waver in the energy calibration also led to fair or low indications of other nuclides as well.

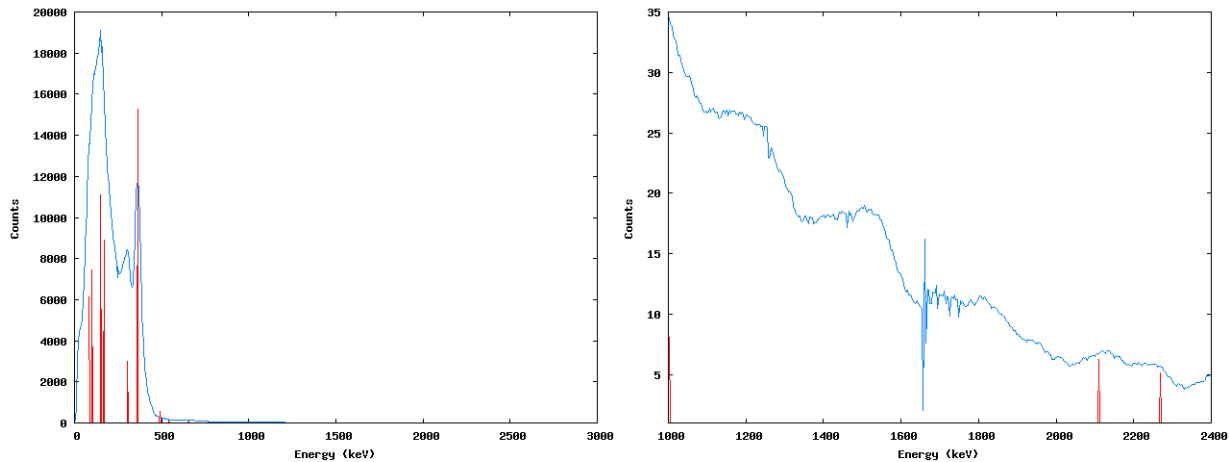
Unknown 24 (U24) ground truth results were reported as Pu-239 + I-131. ASEDRA analysis of U24 revealed the top two components as I-131 with Pu-239; ASEDRA yielded photopeaks at 286, 354, 616, and 735/712 keV, aliased to I-131 peaks, 377 keV aliased to Pu-239, and 2191 keV, aliased to the 2223 keV H(n,  $\gamma$ ) peak as shown in the “Settings 2” column using lower count thresholds. The unknown was therefore identified as I-131(primary) with Pu-239 as secondary, due to the possible Pu-239 lines and presence of neutrons. Several photopeaks (354, 377, 286 keV) were also possibly aliased to Ba-133 due to uncertainty in the calibration, so Ba-133 was also included as a secondary possible nuclide.

Unknowns 25 (U25) and 26 (U26) are shown below in Figures A-25 and A-26.



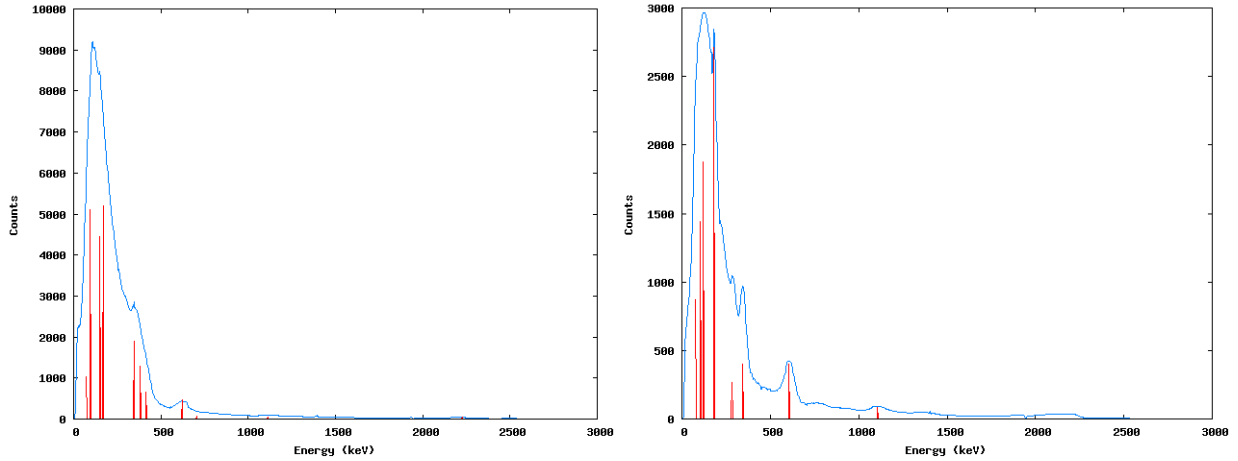
**Figures A-25 - 26. ASEDRA analysis of Unknowns 25 (U25) and 26 (U26). The figures are remarkably similar.**

Unknown 25 (U25) was identified by the ground truth as Np-237, and Unknown 26 (U26) was Np237 + Ga-67. ASEDRA Analysis of 25 and 26 yielded photopeaks at 92/90, 187, 292/298, 389/398 keV; and 89/90, 184, 298/304, 389/398 keV respectively, aliased to Ga-67 based on the uncertain energy and FWHM calibrations. The analysis with less conservative “Settings 2” also yielded a 330 keV peak which could have been aliased to Np-237 (342 keV), as could the 298/304 keV peak (312 keV Np-237 daughter). However, based on the calibration, Ga-67 fit the energies rendered more closely and was listed as the primary identification in both U25 and U26, which were quite similar. Moreover, from the similarities, it is difficult to accept that U25 had no Ga-67 in the source.



**Figures A-27a - 27b. ASEDRA Analysis of Unknown 27; Figure 27a (left), the figure shows the lower energy region; Figure 27b (right) shows the higher energy regions and 2223 H(n,  $\gamma$ ) peak. The other peak just below this is likely the 2111 keV Fe(n,y) peak—a definite indicator of SNM neutrons. Note that denoising of the spectra in ASEDRA makes attribution of (n,y) peaks possible.**

Unknown 27 (Figures A-27a,b) was reported in the ground truth to be Pu-239 + Ba-133, and was identified as WGPu with possible Ba-133 or Ga-67 present, due to lines rendered at 277 (aliased to Ba-133, 276 keV), 304/307 keV (aliased to Ba-133, Ga-67, or Pu-239), 362/367 keV (aliased to Ba-133 or Pu-239), 394 (aliased to Ga-67), 424 keV (aliased to Pu-239 414 keV line), 655/673 keV (aliased to Pu-241 daughter Am-241). Also, with the lower threshold and less conservative “Settings 2,” photopeak as 2198 keV was seen, and was aliased to the H(n,  $\gamma$ ) capture line indicating presence of neutrons. This, coupled with the 414 keV Pu-239 line seen and not aliased to Ga-67 or Ba-133, led to WGPu as the primary identification.



**Figures A-28 - 29. ASEDRA Analysis of Unknowns 28 (U28) and 29 (U29).**

Ground truth for Unknown 28 (Figure A-28) was Pu239 + Ra-226. ASEDRA Analysis of Unknown 28 (U28) yielded WGPu as the primary identification due to the lines rendered at 346, 383, 414/425, 622, 668 keV, as well as the 2226/2198 keV line aliased to H(n,y). Additional lines observed with lower thresholds at 301 and 391 keV led to the “possible” listing of Ga-67. It is also important to note that in “Settings 2”, ASEDRA did extract a 178 keV line and Bi-214 lines at energies of 636, 909, 1119, 1203, and 1769 keV (Bi-214 photopeaks 609, 934, 1120, 1238, 1765 keV), which together would indicate Ra-226 if the calibration had been adjusted. However, due to the poor energy calibration, the 178 keV peak was tentatively aliased to Ga-67, rather than the Ra-226 186 keV line; therefore, the Bi-214 lines were tentatively aliased to DU rather than Ra-226.

Unknown 29 (U29, Figure A-29) was identified by the ground truth report as HEU + Ra-226. Analysis of U29 rendered lines at 181/187, 283, 343, 605, 1106, and others which were aliased to Ra-226 daughters as detailed in the attached spreadsheet (Appendix B), leading to Ra-226 as the primary identification. A more detailed calculation of ratios of the 186 keV peak to Bi-214 peaks could indicate the additional presence of HEU. This level of analysis was not conducted in this work as efficiency calibrations and analysis of peak ratios are currently not implemented in the QuickID code, but would be an important future addition to ASEDRA and the QuickID attribution software.

**Table A-2. ASEDRA/QuickID Blind Test Analysis Results**

Unknown	Analysis with Standard Calibration, Settings 1				Analysis with Standard Calibration Settings 2			
U1	Likely ID: Cs-137		Other:		Likely ID: Cs-137		Other:	
	Isotope	keV	Counts	Norm% Cts	Isotope	keV	Counts	Norm% Cts
						599.42	8.88E+01	1.94574
	Cs-137	668.20	4.49E+03	100.00	Cs-137	668.2	4.47E+03	98.05425

Recommended ID: Cs-137

Unknown	Analysis with Standard Calibration, Settings 1				Analysis with Standard Calibration Settings 2			
U2	Likely ID: Ba-133 + Co-57, Tl-201 or W-Shield		Other:Ce-141?		Likely ID: Ba-133 + Co-57, Tl-201 or W-Shield		Other:Ce-141?	
	Isotope	keV	Counts	Norm% Cts	Isotope	keV	Counts	Norm% Cts
		35.16	2.08E+02	1.42		35.16	1.54E+02	1.07159
	Tl-201/W-shield (69.5 keV?)	69.34	4.01E+03	27.42	Ce-141? / I-125 / Yb-169	35.16	1.54E+02	1.07159
	Co-57	121.70	2.64E+03	18.01	Tl-201 / W-shielding (69.5 keV?)	69.34	3.88E+03	26.99354
	Ce-141?	145.52	2.38E+03	16.24	Co-57	121.7	2.62E+03	18.21566
	Tl-201	172.35	2.25E+03	15.34	Ce-141?	145.52	2.36E+03	16.43895
		199.19	2.98E+03	20.32	Tl-201 / Yb-169?	172.35	2.23E+03	15.52382
	Ba-133	357.34	1.83E+02	1.25	Yb-169?	199.19	2.93E+03	20.3505
					Ba-133	357.34	2.02E+02	1.40593

Recommended ID: Tl-201, Ba-133 + Co-57

Comments: Possible W-shielding?

Unknown	Analysis with Standard Calibration, Settings 1				Analysis with Standard Adjusted, Settings 1				Analysis with Adjusted Calibration Settings 2			
U3	Likely ID: U-232 or Th-228		Other: Am-241, Ra-226		Likely ID: U-232 or Th-228		Other: Am-241, U-235, Ra-226		Likely ID: Irrad Th-232 w/ Am-241		Other:	
	Isotope	keV	Counts	Norm% Cts	Isotope	keV	Counts	Norm% Cts	Isotope	keV	Counts	Norm% Cts
		35.16	1.35E+02	2.88208		35.16	1.54E+02	1.0715 g	Am-241	60.24	3.18E+02	5.89986
	Am-241	53.09	2.06E+02	4.41273	Am-241	54.59	3.25E+02	6.48	Tl-208(Th-232 Dau)	77.18	6.76E+02	12.53584
	Tl-208	74.44	8.61E+02	18.42975	Tl-208	74.35	7.11E+02	14.19	Am-241/Th-229/U-233?	97.5	6.73E+02	12.49538
		92.49	3.89E+02	8.33124	U-233?	94.59	4.50E+02	8.98		117.93	8.42E+02	15.61575
		113.43	6.01E+02	12.87631		103.34	9.87E+01	1.97	Th-232/U-233	144.19	6.73E+02	12.49427
		139.56	5.86E+02	12.5384	U-233	117.93	6.57E+02	13.11	Pa-231/U-233	167.53	6.05E+02	11.22579
		163.41	5.27E+02	11.2752	U-233 daughter	144.19	6.34E+02	12.65	Th-229(U-233 Dau)	193.78	4.43E+02	8.21787
	Ra-226/ U-235	187.26	3.87E+02	8.27984	U-233 daughter	167.53	5.71E+02	11.40		225.88	3.34E+02	6.19861
		214.09	4.51E+02	9.66124	U-235/Ra-226	190.87	4.22E+02	8.43		260.89	1.91E+02	3.54233
		276.7	1.18E+02	2.52875		220.04	3.07E+02	6.13	Pa-231 (Irr Th?)	292.98	1.02E+02	1.89326
	Tl-208?	532.18	4.97E+01	1.06377	Tl-208	255.05	1.97E+02	3.93	Pa-231/U-233?	330.91	5.67E+01	1.05145
	Ra-226	606.14	8.08E+01	1.73066		290.06	1.07E+02	2.13		371.93	2.41E+01	0.44749
		681.37	2.42E+01	0.51742	U-233	330.91	5.19E+01	1.04		410.29	2.61E+01	0.48516
	Ra-226?	751.58	5.17E+01	1.10696	Tl-208	510.60	7.62E+01	1.52		463.39	2.99E+01	0.55389
		817.4	3.78E+01	0.81047	Tl-208	583.00	1.04E+02	2.08	Co-56/Tl-208(Th-232 Dau)/Zn-65	510.6	8.30E+01	1.54005
	Ra-226?	899.46	4.14E+01	0.88706	Bi-212	708.83	4.82E+01	0.96		546.8	1.85E+01	0.34256
	Tl-208?	1654.3	4.26E+01	0.91323	Tl-208	1620.60	4.00E+01	0.80	Tl-208(Th-232 Dau)	583	9.12E+01	1.69165
		2302.9	1.79E+01	0.38363	Tl-208	2617.00	6.40E+01	1.28	Cs-137	654.42	1.35E+01	0.24976
	Tl-208	2617	6.40E+01	1.37127					Bi-212(Th-232 Dau)	708.83	4.11E+01	0.76289
									Bi-212(Th-232 Dau)	770.04	2.67E+01	0.49465
									Co-56/Tl-208 (Th-232 Dau)	834.66	1.31E+01	0.24292
									Ac-228 (Th-232 Dau)	885.67	2.03E+01	0.37748
									Co-56	1048.9	8.14E+00	0.1511
									Zn-65?	1133.9	1.00E+01	0.18586
									Co-56	1219	6.24E+00	0.11585
									Tl-208(Th-232 Dau)/Co-56	2617	6.40E+01	1.18827

Recommended ID: U-232/Irrad Th-232

Unknown	Analysis with Standard Calibration, Settings 1				Analysis with Adjusted Calibration, Settings 1b				Analysis with Settings 2			
U4	Likely ID: Ba-133 + Cs-137		Other: WGPu		Likely ID: Ba-133 + Cs-137 + WGPu		Other: WGPu		Likely ID: Pu and irradiated U, with Ba-133, I-131, or Ga-67		Other: possible Eu-152/Cs-134?	
	Isotope	keV	Counts	Norm% Cts	Isotope	keV	Counts	Norm% Cts	Isotope	keV	Counts	Norm% Cts
	Ba-133	80.00	2928.40	21.21	Ba-133?	76.36	2.44E+03	20.341	U-238 (Pb-214) / Am-243?	74.44	2.99E+03	10.78019
	*Scatter	102.47	2192.40	15.88	*Scatter	95.96	1.31E+03	10.92228	Pu-239/ U-238 (Pa-234) / Ga-67 / Pu-238?	92.49	1.71E+03	6.18
	*Scatter	154.47	4541.50	32.89	*Scatter	107.51	1.06E+03	8.8073	Pu-239 / U-238 (Pa-234)	110.67	2.69E+03	9.72241
	Ba-133/Pu-239	294.59	827.47	5.99	Ba-133/Pu-239	153.25	3.51E+03	29.23326	Pu-239/ U-238 (Pa-234) / Ce-144	130.62	2.85E+03	10.27078
	Ba-133/Pu-239	354.21	3088.10	22.37	Ga-67/Ba-133/Pu-239	296.56	3.89E+02	3.24195	U-238 (Pa-234) / Pu-238?	154.47	4.26E+03	15.36306
	Cs-137?	685.75	229.71	1.66	Ba-133/Pu-239	357.55	2.97E+03	24.73507	U-235 / Ga-67	178.32	2.50E+03	9.02648
					Ga-67?	400.24	1.19E+02	0.99085	Pu-239 / Ga-67	211.11	2.47E+03	8.91753
						516.11	1.82E+01	0.15188	U-238 (Pa-234)	246.89	2.33E+03	8.40091
						592.34	8.58E+00	0.07147	I-131 / U-238 (Pb-214) / Ga-67 / Ba-133	294.59	2.41E+03	8.70936
					Cs-137/ Pu(Am-241)	653.33	1.35E+02	1.1268	Pu-239/ I-131 / U-238 (Pb-214) / Eu-152/Ba-133	354.21	2.77E+03	9.98469
						856.89	7.46E+00	0.0621	Pu-239/ Ga-67 / Ba-133	387.6	3.22E+02	1.16143
						957.41	1.50E+01	0.12459	Pu-239	438.04	1.61E+01	0.05809
						1024.4	9.68E+00	0.0806	Cs-134	552.35	4.55E+01	0.16422
						1118.2	8.09E+00	0.06743	I-131 / Cs-134	626.32	5.55E+01	0.20032
					H(n,y)?	2250.5	5.21E+00	0.04342	Cs-137	685.75	1.40E+02	0.50519
									I-131 / U-238 (Pa-234)	734.02	5.37E+01	0.19381
									U-238 / Cs-134?	795.46	1.73E+01	0.06246
									U-238 (Pa-234)	867.15	2.63E+01	0.09476
									U-238 (Pa-234)	925.31	1.81E+01	0.06536
									U-238	1022.2	1.39E+01	0.05022
									Eu-152	1086.8	7.36E+00	0.02654
									Cs-134?	1177.3	5.52E+00	0.01993
									K-40 / Eu-152	1416.4	6.50E+00	0.02346
									n-gamma?	2265.7	5.21E+00	0.0188

Recommended ID: Ba-133 + Cs-137; Ga-67 + Pu-239

Unknown	Analysis with Standard Calibration, Settings 1				Analysis with Adjusted Calibration, Settings 1				Analysis with Adjusted Calibration Settings 2			
	Likely ID: Tentatively U-235		Other:		Likely ID: U-235		Other: Am-241		Likely ID: Ir-192 and U-235		Other: Am-241	
	Isotope	keV	Counts	Norm% Cts	Isotope	keV	Counts	Norm% Cts	Isotope	keV	Counts	Norm% Cts
		32	1.40E+03	10.38033	*look at this	41.56	2.70E+03	20.79	??	41.56	2.68E+03	20.64805
		48.45	2.63E+03	19.50691	Am-241	60.74	2.50E+03	19.21	Am-241	60.74	2.49E+03	19.11996
	Am-241?	67.02	2.34E+03	17.37502		82.03	2.04E+03	15.73	Ra-223?	82.03	2.04E+03	15.66695
		87.49	1.94E+03	14.36351		104.64	1.53E+03	11.77	Am-241	104.71	1.52E+03	11.68408
		107.91	1.41E+03	10.48277		122.92	1.22E+03	9.38	Am-241, or Co-57	123.89	1.22E+03	9.34695
		124.65	1.09E+03	8.10666	U-235?	141.19	9.29E+02	7.15	U-235, Th-230 (U-238 Dau)?	143.07	9.26E+02	7.12034
	U-235?	142.54	8.42E+02	6.24846	U-235?	162.51	6.94E+02	5.34	U-235	165.45	6.88E+02	5.29171
	U-235?	166.39	6.35E+02	4.71205	U-235	186.88	4.99E+02	3.84	U-235	191.02	4.91E+02	3.77662
	U-235?	193.22	4.36E+02	3.23546		217.33	3.48E+02	2.67	Fr-221?	219.79	3.39E+02	2.60606
		223.04	2.91E+02	2.15913		250.83	2.23E+02	1.72	Th-227, Th-230, (U-238 Dau)?	254.95	2.23E+02	1.7142
		255.83	1.89E+02	1.40562		287.38	1.45E+02	1.11	Ir-192	293.3	1.39E+02	1.06966
		291.6	1.26E+02	0.93612		326.98	9.86E+01	0.76	U-235 Dau ?	334.86	8.82E+01	0.6786
		330.36	8.60E+01	0.63862		366.57	6.91E+01	0.53	Pu-239??	376.41	5.94E+01	0.45707
		367.43	6.05E+01	0.44931					U-238 (Ra-226), Pu- 239?	414.77	3.67E+01	0.28255
									Ir-192	456.32	2.78E+01	0.2141
									?	501.07	1.66E+01	0.12795
									Ir-192 ?	558.61	9.56E+00	0.0735
									Ir-192	628.93	1.04E+01	0.08021
									U-235 (Pb-211)	817.52	5.39E+00	0.04144

Recommended ID: U-235

Unknown	Analysis with Standard Calibration, Settings 1				Analysis with Adjusted Calibration, Settings 1				Analysis with Settings 2			
U6	Likely ID: Eu-152 or U-235		Other:		Likely ID: Eu-152		Other: U-235		Likely ID: Eu-152 w Ba-133		Other: U-235	
	Isotope	keV	Counts	Norm% Cts	Isotope	keV	Counts	Norm% Cts	Isotope	keV	Counts	Norm% Cts
		38.31	3.13E+02	13.81861		43.81	2.65E+02	11.62	SNM Dau	86.38	1.95E+02	7.17061
		74.44	4.27E+02	18.8128		80.29	4.57E+02	20.07	U-235 / Eu-155 ?	104.71	9.25E+01	3.40349
		110.67	1.84E+02	8.13062		110.47	2.11E+02	9.27	Eu-152	120.61	2.26E+02	8.32774
		130.62	1.51E+02	6.65746	Eu-152?	128.09	1.54E+02	6.75	U-235	142.88	2.55E+02	9.37409
	U-235	148.5	9.09E+01	4.01097	U-235	145.72	1.03E+02	4.51	U-235	165.15	2.16E+02	7.95049
	U-235	187.26	2.77E+02	12.20519	U-235	189.78	2.84E+02	12.46	U-235	190.61	3.14E+02	11.53966
	Eu-152/ Ba-133	220.05	2.45E+02	10.79289	Eu-152/Ba-133	222.09	2.49E+02	10.95	U-238 (Pa-234)	225.6	3.77E+02	13.87453
		249.87	1.67E+02	7.37242		257.34	1.71E+02	7.49	Ba-133	263.78	2.29E+02	8.41901
	Eu-152	339.3	9.69E+01	4.2753	Eu-152	339.59	1.10E+02	4.84	Ba-133	305.14	1.48E+02	5.45589
		839.34	9.25E+01	4.07889	Eu-152	790.19	7.08E+01	3.11	Ba-133 / Eu-152	356.04	2.12E+02	7.80585
		1031.9	6.98E+01	3.0771	Eu-152	979.78	6.05E+01	2.66	Ba-133	394.22	9.99E+01	3.675
		1161.2	8.80E+01	3.8809	Eu-152	1110.50	7.73E+01	3.40	Ba-140??	441.94	5.09E+01	1.87331
	Eu-152?	1439	6.55E+01	2.88687	Eu-152	1391.70	6.55E+01	2.87	U-235 (Fr-223) / Cs-134	486.48	3.93E+01	1.44483
									Ba-140??	527.84	1.84E+01	0.67882
									Ru-106 / Rh-106 ??	632.83	3.48E+01	1.28035
									U-238 (Bi-214)	798.26	8.47E+01	3.11675
									U-238 / Eu-152	976.42	2.76E+01	1.01746
									U-238 (Bi-214) / Eu-152	1110	2.55E+01	0.93785
									U-238 (Bi-214) / Eu-152	1383.6	7.21E+01	2.65426

Recommended ID: Shielded Eu-152

Unknown	Analysis with Standard Calibration, Settings 1				Analysis with Adjusted Calibration, Settings 1				Analysis with Adjusted Calibration, Settings 2			
	Likely ID: Mn-54/56, Shielded Enriched U		Other:Co-57, Tl-208, Bi-212		Likely ID: Shielded U-235, Mn-54/56		Other: Possibly U-232 or Th-232		Likely ID: enriched U with Irrad Th-232		Other:Co-57	
	Isotope	keV	Counts	Norm% Cts	Isotope	keV	Counts	Norm% Cts	Isotope	keV	Counts	Norm% Cts
U7		74.44	1.25E+03	14.33		77.83	8.12E+02	8.68768	Likely	keV	Counts	Norm% Cts
		107.91	1.05E+03	12.04		111.43	2.06E+03	22.0122	U-233 (Th-229)	86.77	6.49E+02	4.0034
	Co-57	124.65	1.19E+03	13.57	U-235	187.64	3.78E+03	40.44524	U-233 (Th-229) / U-235 (Fr-221)??	101.66	1.10E+03	6.80002
	U-235?	178.32	3.18E+03	36.38		283.73	1.84E+03	19.73455	U-238 (U-234) / Co-57 / U-233 / Np-237?	118.06	2.27E+03	13.97322
		231.98	6.73E+02	7.70		419.58	9.24E+01	0.98869	U-235 / Th-232 / U-233 / Co-57	141.25	2.14E+03	13.18861
		264.77	4.92E+02	5.62	Bi-212	737.67	3.43E+02	3.67195	U-235 / U-233	161.13	1.85E+03	11.41211
	Bi-212?	734.02	4.90E+02	5.61	Mn-54	850.33	4.17E+02	4.4597	U-235 / U-238 (Ra-226) / U-233 (Th-229)	187.64	2.56E+03	15.79166
	Mn-54/56	870.38	4.15E+02	4.75					U-235 (Fr-221) / U-233 (Th-229)	217.46	2.08E+03	12.85305
									U-238 (Ra-226) / U-235 (Rn-219, Ra-223) / U-232	267.16	1.77E+03	10.92728
									U-235 (dau) / U-233 / U-232	326.8	4.00E+02	2.46599
									Pu-239 / U-237 ?	366.57	2.62E+02	1.61796
									U-238 (Ra-226) / U-235 (Pb-211) / Pu-239	419.58	1.66E+02	1.02457
									U-238 (Ra-226)	585.25	1.71E+01	0.10573
									Co-57 / Np-237?	684.66	1.05E+02	0.64891
									Th-232 (Bi-212)	737.67	4.01E+02	2.47451
									U-235 (Pb-211) / Co-58 / Cs-134?	803.94	1.12E+02	0.69326
									Mn-54, Co-56 ?	850.33	3.15E+02	1.94433
									Th-232 (Ac-228)	953.04	7.03E+00	0.04334
									Na-22 / Co-56?	1274.4	5.19E+00	0.03204

Recommended ID: Shielded Enriched U

Comments: Mn-54?

Unknown	Analysis with Standard Calibration, Settings 1				Analysis with Adjusted Calibration, Settings 2			
U8	Likely ID: Shielded Enriched U		Other:MN-54/56, U-232 or Th-232		Likely ID: Enriched U		Other:	
	Isotope	keV	Counts	Norm% Cts	Isotope	keV	Counts	Norm% Cts
		110.67	3.26E+02	6.10	Likely	keV	Counts	Norm% Cts
	U-235	181.30	3.57E+03	66.80	Xe-133?	82.5	8.76E+01	0.76822
	U-235(Ra-223, Rn-219)/U-238(Ra-226)	270.74	5.14E+02	9.62	U-235(Ra-233)/Am-241?	102.47	3.23E+02	2.83599
	Bi-212?	738.41	5.52E+02	10.34	Np-237	116.18	1.39E+03	12.16775
	Mn-54/56?	870.38	3.82E+02	7.14	U-235	136.58	1.55E+03	13.59162
					U-235	154.47	1.15E+03	10.117
					U-235	181.3	3.95E+03	34.59542
					U-235(Th-227)/U-235(Fr-221)	214.09	9.98E+02	8.74714
					U-235(Ra-223, Rn-219)/U-238(Ra-226)	270.74	9.27E+02	8.13174
					U-238	738.41	4.83E+02	4.23846
					U-238	795.46	1.48E+02	1.30112
					U-238 (Pa-234)	870.38	3.81E+02	3.34284
					U-238 / U-238 (Pa-234)	973.77	1.86E+01	0.1627

Recommended ID: Enriched U

Comments: Mn-54?

Unknown	Analysis with Standard Calibration, Settings 1				Analysis with Adjusted Calibration, Settings 2			
U9	Likely ID: U-235, Ba-133		Other: Co-57, Ag-111		Likely ID: U-235 w Ba-133 and Co-57		Other: Eu-155	
	Isotope	keV	Counts	Norm% Cts	Isotope	keV	Counts	Norm% Cts
	Ba-133	84.99	1.48E+03	11.57	Eu-155	43.11	7.83E+02	5.55752
		107.91	1.98E+03	15.48	Am-241 / Eu-155 ?	60.43	1.42E+03	10.10736
	Co-57?	127.63	2.11E+03	16.51	Ba-133	81.21	1.71E+03	12.1331
		151.48	1.62E+03	12.69	U-235 / Eu-155 ?	105.46	2.08E+03	14.74958
	U-235?	175.33	1.25E+03	9.77	Co-57 / Am-241	122.78	1.49E+03	10.60084
	U-235?	205.15	9.97E+02	7.81	U-235 / U-235 (Ra-223)	143.57	1.14E+03	8.10648
	Ag-111 (245)	243.90	1.02E+03	7.97	U-235	167.82	1.02E+03	7.25941
	Ba-133/Ag-111	282.66	1.21E+03	9.46	U-235	185.14	2.59E+02	1.83963
	Ba-133/Ag-111	342.29	1.11E+03	8.73	U-235	202.46	8.33E+02	5.91581
					??	226.71	6.79E+02	4.82022
					U-238 (Ra-226)	261.36	9.25E+02	6.57032
					U-238 (Pb-214) / Ba-133 ?	292.53	4.88E+02	3.46583
					U-235 Dau	330.64	1.04E+03	7.39361
					Ba-133	358.36	1.74E+02	1.23376
					Ba-133	389.53	1.53E+01	0.10859
					U-235 (Pb-211)	431.11	7.96E+00	0.05649
					??	545.43	6.18E+00	0.04388
					Co-57	694.39	5.29E+00	0.03758

**Recommended ID: U-235, Ba-133**

Comments: Possibly Co-57

Unknown	Analysis with Adjusted Calibration, Settings 1				Analysis with Adjusted Calibration, Settings 2			
U10	Likely ID: K-40		Other: Th-232 (low level)		Likely ID: K-40 with highly shielded IrradTh		Other: Eu-155	
	Isotope	keV	Counts	Norm% Cts	Isotope	keV	Counts	Norm% Cts
	Co-57	121.7	3.33E+02	26.67348	Eu-155	43.11	7.83E+02	5.55752
	Th-232	142.54	3.19E+02	25.57043	Am-241	61.25	3.83E+01	2.89847
	U-233?	166.39	2.26E+02	18.13986	U-233 (Np-237)	94.32	3.18E+02	24.01584
		190.24	1.64E+02	13.11725	U-233 (Np-237)	117.46	4.95E+02	37.42114
		217.07	1.42E+02	11.4046	Th-232	143.92	1.73E+02	13.06134
	K-40	1466.9	6.36E+01	5.09438	U-233 (Np-237)	163.76	2.36E+02	17.80645
					K-40	1466.4	6.35E+01	4.79674

**Recommended ID: K-40**

Comments: Possibly with low level of Irradiated Th

Unknown	Analysis with Adjusted Calibration, Settings 1				Analysis with Adjusted Calibration, Settings 2			
U11	Likely ID: K-40		Other: U-238		Likely ID: K-40, shielded Irrad Th		Other: U-233	
	Isotope	keV	Counts	Norm% Cts	Isotope	keV	Counts	Norm% Cts
		74.44	3.70E+01	4.63909	Irr Th?	26.23	1.52E+01	1.14478
	U-238(Pa-234m?)	145.52	2.06E+02	25.87322	U-233 (Ra-225)	39.86	7.94E+01	5.9868
		166.39	1.82E+02	22.78066	Th-232	63.69	1.88E+02	14.21864
		196.2	1.42E+02	17.83358	U-238 (Th-230)	111.37	2.32E+02	17.52737
		226.02	1.13E+02	14.10446	Co-57 / Th-232?	135.21	2.08E+02	15.71836
		258.81	5.95E+01	7.45108	U-233 (Np-237)	162.46	1.63E+02	12.28968
		300.55	2.39E+01	2.99519	U-238 (Th-230)	189.7	1.42E+02	10.68133
	Bi-214?	602.78	7.57E+00	0.94863	U-235 (Fr-221)?	220.35	1.05E+02	7.95046
		703.31	7.29E+00	0.91405	U-238 (Th-230)	251	6.60E+01	4.98181
	U-238(Pa-234m?)	764.74	1.33E+01	1.67209	U-233 / Np-237	288.47	4.12E+01	3.10701
	K-40	1460	6.29E+00	0.78795	U-233 / Np-237	322.52	3.42E+01	2.5806
					Cs-134??	588.16	2.46E+01	1.85345
					Co-57	690.33	6.65E+00	0.50185
					Zr-95??	741.41	1.30E+01	0.98349
					K-40	1473	6.29E+00	0.47437

**Recommended ID: K-40**

Unknown	Analysis with Adjusted Calibration, Settings 1				Analysis with Standard Calibration, Settings 2			
U12	Likely ID: I-131		Other:		Likely ID: I-131 with Ba-133, possibly Xe-133, BG tare?		Other:	
	Isotope	keV	Counts	Norm% Cts	Isotope	keV	Counts	Norm% Cts
		31.44	1.73E+02	1.04	Np-237 / U-238 (Pa-234)	116.7	1.40E+02	0.92268
	I-131	83.23	1.18E+03	7.14	U-238 (Pa-234)	130.03	5.09E+02	3.36096
		104.55	1.00E+03	6.05	U-238 (Th-230)	146.7	9.15E+02	6.04381
	BKG - U-238?	131.97	8.65E+02	5.21	Np-237	163.37	5.15E+02	3.39912
		159.39	2.96E+03	17.81	Xe-133m / Th-232 (Pb-212)	233.36	6.58E+02	4.34411
	I-131	287.26	7.03E+02	4.23	I-131 / Ba-133	270.03	1.73E+03	11.41294
	I-131	361.51	9.15E+03	55.15	Ba-133	306.7	6.42E+02	4.23669
	I-131	636.97	4.62E+02	2.78	I-131 / Ba-133	356.69	9.50E+03	62.73123
	I-131?	711.48	9.65E+01	0.58	low, Rh-106?	523.36	1.83E+01	0.12082
					U-238 (Pa-234)	583.36	4.24E+01	0.27973
					I-131	646.69	3.83E+02	2.52768
					I-131	733.35	7.42E+01	0.49013
					Th-232 (Ac-228) / U-238 (Pa-234)	916.68	5.91E+00	0.03899
					U-238 / Th-232 (Ac-228) / U-238 (Pa-234)	990.01	7.97E+00	0.05263
					very low, Rh-106?	1076.7	5.83E+00	0.03847

**Recommended ID: I-131**

Comments:

Unknown	Analysis with Standard Calibration, Settings 1				Analysis with Adjusted Calibration, Settings 1				Analysis with Adjusted Calibration, Settings 2			
U13	Likely ID: Mn-54		Other:		Likely ID: Mn-54		Other: Mn-56		Likely ID: Mn-54 with shielded Irrad U?		Other: U-233	
	Isotope	keV	Counts	Norm% Cts	Isotope	keV	Counts	Norm% Cts	Isotope	keV	Counts	Norm% Cts
		74.44	3.53E+02	12.73852		194.06	1.28E+03	81.96		194.06	1.28E+03	81.96
		94.98	1.52E+02	5.48136	Mn-54	844.57	2.82E+02	18.04	U-235 / U-233 (Th-229)	194.06	5.25E+02	31.0473
		127.63	5.26E+02	18.95451					U-235 (Fr-221)	225.95	8.44E+02	49.86946
		151.48	1.40E+03	50.35613					Zr-95?	704.26	1.25E+01	0.73798
	Mn-54, Mn-56	843.73	3.46E+02	12.46948					Zr-95?	755.28	2.83E+01	1.67146
									Mn-54	844.57	2.82E+02	16.6738

**Recommended ID: Shielded Mn-54**

Comments: Lower energy source possibly present

Unknown	Analysis with Standard Calibration, Settings 1				Analysis with Standard Calibration, Settings 2			
U14	Likely ID: BKG		Other: Possible Xe-133m		Likely ID: Background U-238		Other: Possible low level Xe-133	
	Isotope	keV	Counts	Norm% Cts	Isotope	keV	Counts	Norm% Cts
	Xe-133m?	38.31	1.36E+02	6.56	Xe-133m / I-129??	38.31	1.54E+02	6.94816
	U-238 (Th-230)	67.02	4.54E+02	21.96	U-238 (Th-230)	67.02	4.76E+02	21.43867
	Eu-155	105.16	3.50E+02	16.93	Eu-155??	105.16	3.61E+02	16.27263
	U-238 (Pa-234)	127.63	3.03E+02	14.65	U-238 (Pa-234)	127.63	3.14E+02	14.14968
	U-238 (Th-230)	148.50	2.47E+02	11.96	U-238 (Th-230)	148.5	2.58E+02	11.63136
	U-238 (Th-230)	175.33	3.46E+02	16.74	U-238 (Th-230)	175.33	3.64E+02	16.40067
	Xe-133m?	226.02	1.05E+02	5.07	Xe-133m?	226.02	1.14E+02	5.12231
	U-238 (Th-230)	258.81	6.30E+01	3.05	Ra-226 / U-238 (Th-230)	258.81	7.22E+01	3.25344
	U-238 (Pb-214)	291.60	2.73E+01	1.32	U-238 (Pb-214) / U-235 (Th-227)	291.6	3.71E+01	1.67383
	Th-232(Bi-212)	729.64	1.35E+01	0.65	U-235 (Th-227)	324.4	1.98E+01	0.8912
	Th-232(Bi-212)	786.68	1.10E+01	0.53		387.6	1.22E+01	0.55105
	U-238 (Pa-234)	880.08	1.19E+01	0.58	Th-232 (Bi-212) / U-238	729.64	1.39E+01	0.62809
					Th-232 (Bi-212) / U-238	786.68	1.11E+01	0.5015
					U-238 (Pa-234)	880.08	1.19E+01	0.53743

**Recommended ID: BKG**

Comments:

Unknown	Analysis with Standard Calibration, Settings 1				Analysis with Adjusted Calibration, Settings 1				Analysis with Adjusted Calibration, Settings 2			
U15	Likely ID: Ra-226?		Other:		Likely ID: Ra-226		Other:		Likely ID: Shielded Ra-226		Other: Ga-67?	
	Isotope	keV	Counts	Norm% Cts	Isotope	keV	Counts	Norm% Cts	Isotope	keV	Counts	Norm% Cts
		38.31	6.21E+02	1.99		55.41	6.83E+02	1.65536	U-238 (Pb-214) / U-235 (Th-227) / Th-232 (Pb-212)	74.44	3.86E+03	17.93531
		74.44	5.27E+03	16.85		74.44	5.95E+03	14.42715	U-235 (Ra-223) / U-238 (Pa-234) / Ga-67?	94.98	5.33E+03	24.80084
		94.98	9.71E+03	31.04		94.98	7.19E+03	17.42927	U-238 (Pa-234) / U-235	110.67	2.21E+03	10.26668
		136.58	3.40E+03	10.88		113.43	4.84E+03	11.72354	U-238 (Pa-234)	131.3	7.27E+02	3.38027
	Ra-226 (186?)	181.30	7.12E+03	22.76		140.95	7.47E+03	18.10675	U-238 (Ra-226) / U-235 / Ga-67?	186	6.46E+03	30.0616
		229.00	1.32E+03	4.22	Ra-226 (186)	186	7.80E+03	18.88914	U-238 (Pb-214) / U-235 (Th-227) / Th-232 (PB-212)	235.83	4.43E+02	2.06013
	Ra-226 daughter (Pb-214, 295)	282.66	1.11E+03	3.54	Ra-226 daughter (Pb-214, 242)	235.83	2.63E+03	6.37933	U-238 (Pb-214) / U-235 (Pa-231) / U-235 (Ra-223) / Ga-67? / Th-232 (Pb-212)	291.89	4.56E+02	2.11886
	Ra-226 dau.? (Pb-214, 352)	339.30	1.49E+03	4.77	Ra-226 daughter (Pb-214, 295)	291.89	1.46E+03	3.53906	U-235 (Bi-211) / U-238 (Pb-214) / U-235 (Ra-223)	351	9.53E+02	4.43312
	Ra-226 daughter (Bi-214, 609)	606.14	7.71E+02	2.47	Ra-226 daughter (Pb-214, 352)	351	1.64E+03	3.974	U-238 (Ra-226) / U-238 (Bi-214) / Cs-134	609	7.72E+02	3.5919
	Ra-226 daughter (Bi-214, 666/703?)	694.53	5.85E+01	0.19	Ga-67?	399.38	7.37E+01	0.1786	Co-58 / U-238 (Pb-214) / Cs-134	799.08	2.36E+01	0.10978
	Ra-226 daughter (Bi-214, 768?)	791.07	9.61E+01	0.31	Ra-226 daughter (Bi-214, 609)	609	9.10E+02	2.20521	U-235 (Pb-211)	839.1	3.95E+01	0.18378
	Ra-226 daughter (Bi-214, 1120)	1138.50	1.31E+02	0.42		729.05	6.44E+01	0.15604	U-238 (Pa-234)	889.12	2.10E+01	0.09749
	Ra-226 daughter (Bi-214, 1238?)	1254.80	6.15E+01	0.20		839.1	2.33E+02	0.56459	Cs-134 / U-238 (Bi-214)	1354.3	6.40E+01	0.2977
		1380.80	5.71E+01	0.18	Ra-226 daughter (Bi-214, 1238?)	1259.3	5.54E+01	0.13427	Th-232 (Bi-212) ??	1584.4	1.93E+01	0.08993
	Ra-226 daughter (Bi-214, 1765)	1762.40	6.54E+01	0.21		1354.3	1.40E+02	0.33808	U-238 (Bi-214)	1729.5	3.96E+01	0.18395
						1811.9	5.82E+01	0.14107	U-238 (Bi-214)	1811.9	1.97E+01	0.09159
	6.83E+02	1.65536	17		Ra-226 daughter (Bi-214, 2204)	2215.2	6.54E+01	0.15854	U-238 (Bi-214)	2215.2	5.04E+01	0.23444
									U-238 (Bi-214)	2449.5	1.35E+01	0.06265

Recommended ID: Ra-226

Unknown	Analysis with Standard Calibration, Settings 1				Analysis with Adjusted Calibration, Settings 1				Analysis with Settings 2, Standard Calibration			
U16	Likely ID: Ba-133?		Other:		Likely ID: Ga-67		Other:		Likely ID: Background uranium		Other: Co-57	
	Isotope	keV	Counts	Norm% Cts	Isotope	keV	Counts	Norm% Cts	Isotope	keV	Counts	Norm% Cts
		38.31	1.27E+03	1.79216	Ga-67	90.23	3.87E+04	45.94	U-238 (Th-230) / Sn-126?	69.34	5.51E+03	7.83688
		69.34	8.53E+03	12.0617 4		111.20	9.30E+03	11.05	U-235 / Sn-126?	89.99	2.59E+04	36.85377
		89.99	2.65E+04	37.4109		141.53	1.24E+04	14.79	U-235 / U-238 (Pa-234)	107.91	8.33E+03	11.83888
		107.91	9.77E+03	13.8185 5	Ga-67	184.00	1.86E+04	22.10	Co-57 / Pu-239?	121.7	1.84E+03	2.61755
		136.58	2.94E+03	4.15304	Ga-67	296.86	4.45E+03	5.28	Co-57 / Ce-144 / U-238 (Pa-234)	133.6	4.18E+03	5.94552
		178.32	1.72E+04	24.3666 4		345.14	5.84E+01	0.07	U-238 (Th-230)	148.5	1.55E+03	2.20173
		285.64	3.78E+03	5.34466	Ga-67	390.28	6.43E+02	0.76	U-235	178.32	1.71E+04	24.30817
	Ba-133	374.16	7.44E+02	1.05232					U-235	208.13	9.23E+02	1.31162
									Th-232 (Ra-224)	237.94	3.83E+02	0.5439
									Th-232 (Tl-208)?	285.64	3.84E+03	5.45779
									Pu-239 ?	374.16	7.22E+02	1.02548
									U-235 (Ra-223)	461.57	1.54E+01	0.02184
									Sr-89?	505.28	6.08E+00	0.00864
									U-238 (Pa-234)	562.44	1.16E+01	0.01648
									U-238 (Pa-234)	886.54	8.28E+00	0.01177

**Recommended ID: Ga-67**

Comments: Calibration was off; re-calibration is necessary

Unknown	Analysis with Standard Calibration, Settings 1				Analysis with Standard Calibration, Settings 2			
U17	Likely ID: Enriched U		Other: Np-237		Likely ID: HEU		Other: Np-237	
	Isotope	keV	Counts	Norm% Cts	Isotope	keV	Counts	Norm% Cts
		35.16	3.15E+02	0.84	U-235 / Th-232 (Pb-212)	74.44	4.27E+03	9.80779
		74.44	3.99E+03	10.58	U-238 (Pa-234) / Pu-239 / Pu-238	97.48	7.71E+03	17.71909
	Np-237	97.48	1.18E+04	31.21	U-235 / U-238 (Pa-234) / Np-237 (Pa-233)	113.43	4.99E+03	11.47546
		133.60	3.05E+03	8.08	Co-57 / Eu-154 / Pu-239	124.65	1.03E+03	2.36606
	U-235	178.32	1.47E+04	38.91	Co-57 / Ce-144	136.58	4.25E+03	9.76616
		267.75	1.87E+03	4.95	Pu-238	151.48	1.93E+03	4.4488
		404.42	2.01E+02	0.53	U-235	178.32	1.36E+04	31.36652
		522.09	8.11E+01	0.22	U-235	208.13	1.62E+03	3.73455
		572.52	9.29E+01	0.25	Th-232 (Pb-212)	234.96	4.04E+02	0.92791
	U-238	734.02	1.12E+03	2.97	U-235 (Rn-219) / Th-232 (Ac-228)	267.75	1.71E+03	3.92955
	U-238	851.00	5.58E+02	1.48	U-235 (Rn-219) / U-235 (Pb-211)	390.97	1.15E+02	0.26553
					Co-57	694.53	3.25E+02	0.74728
					Eu-154 / U-238 / Pu-238	738.41	6.99E+02	1.60751
					U-238 / Th-232 (Ac-228)	795.46	1.65E+02	0.37925
					Eu-154 / U-238 (Pa-234)	851	5.92E+02	1.36226
					Th-232 (Ac-228) / U-238 (Pa-234)	947.92	2.26E+01	0.05188
					Eu-154 / U-238	1015.8	1.33E+01	0.03069
					Eu-154	1271	5.96E+00	0.01371

Recommended ID: Enriched U

Unknown	Analysis with Adjusted Calibration, Settings 1				Analysis with Standard Calibration, Settings 2			
U18	Likely ID: K-40		Other:		Likely ID: K-40		Other:	
	Isotope	keV	Counts	Norm% Cts	Isotope	keV	Counts	Norm% Cts
	K-40	1.47E+03	7.53E+01	100.00	Th-232	139.56	7.21E+01	30.73638
						154.47	3.84E+01	16.37061
						175.33	2.63E+01	11.23864
						190.24	1.55E+01	6.62963
						1439	6.83E+00	2.9144
					K-40	1505.6	7.53E+01	32.11034

**Recommended ID: K-40**

Comments: Lower energy source may be present

Unknown	Analysis with Standard Calibration, Settings 1				Analysis with Standard Calibration, Settings 2			
U19	Likely ID: Shielded WGPu		Other: K-40		Likely ID: Shielded WGPu		Other: K-40	
	Isotope	keV	Counts	Norm% Cts	Isotope	keV	Counts	Norm% Cts
		74.44	3.25E+03	11.20906	U-235 (Bi-211) / Th-232 (Pb-212)	74.44	6.54E+02	2.29779
		133.6	7.75E+03	26.73299	Pu-239 / Np-237 (Pa-233)	92.49	8.70E+02	3.05544
		151.48	6.00E+03	20.70846	Pu-239 / Np-237 (Pa-233)	116.18	1.95E+03	6.84984
		172.35	3.75E+03	12.93977	Pu-239	133.6	7.80E+03	27.39443
		202.17	3.10E+03	10.69644	Pu-241? / Pu-238 / U-235 (Ra-223)	151.48	5.77E+03	20.28598
		234.96	2.30E+03	7.93324		175.33	3.73E+03	13.1083
		267.75	2.26E+03	7.81078		202.17	3.00E+03	10.5267
	Pu-239?	327.38	3.37E+02	1.1632	Th-232 (Pb-212)	237.94	2.30E+03	8.07757
	Pu-239	364.07	1.40E+02	0.48465	U-235 (Pa-231) / U-236 (Ra-223)	273.72	1.45E+03	5.09152

		397.69	6.63E+01	0.2287	U-235 (Pa-231) / Np-237 (Pa-233) / Th-232 (Pb-212)	309.49	5.81E+02	2.04047
		485.11	8.39E+00	0.02893	U-235 (Pa-231) / U-235 (Bi-211) / Np-237 (Pa-233)	342.29	2.17E+02	0.76113
		572.52	6.28E+00	0.02165	Pu-239	380.88	1.06E+02	0.37285
	K-40	1502.7	1.22E+01	0.04216	U-235 (Pb-211) / Pu-239	417.86	2.53E+01	0.08877
					K-40	1505.6	1.40E+01	0.0492

**Recommended ID: Shielded WGPu with trace K-40**

Comments:

Unknown	Analysis with Standard Calibration, Settings 1				Analysis with Standard Calibration, Settings 2			
	Likely ID: Shielded Ga-67, or Pu-239		Other:		Likely ID: Ga-67 with weak Ir-192		Other:	
	Isotope	keV	Counts	Norm% Cts	Isotope	keV	Counts	Norm% Cts
	Ga-67?	69.34	1.40E+04	15.07	Ir-192	69.34	1.26E+04	16.72758
	Co-57?	121.70	1.95E+04	21.03	Ce-144?	130.62	1.81E+04	24.12327
		145.52	5.08E+04	54.82		154.47	1.72E+04	22.91198
	Ga-67/Pu-239	291.60	6.28E+03	6.78	In-111?	175.33	1.17E+04	15.59091
	Ga-67/Pu-239	380.88	2.13E+03	2.30	Ga-67 / weak Ir-192	202.17	6.66E+03	8.87976
						229	3.30E+03	4.39131
					In-111?	249.87	1.24E+03	1.64997
					Ga-67, weak Ir-192	288.62	1.88E+03	2.49974
					Ir-192 / Cr-51?	318.44	3.67E+02	0.48907
					Ga-67	380.88	2.02E+03	2.69003
					Ir-192	461.57	2.41E+01	0.03218
					Sr-85?	532.18	1.07E+01	0.01419

**Recommended ID: Shielded Ga-67**

Comments:

Unknown	Analysis with Settings 1				Analysis with Settings 2			
U21	Likely ID: U-238, U-235		Other: Co-57		Likely ID: Co-57 w Shielded Enriched U		Other: Mn-54, K-40	
	Isotope	keV	Counts	Norm% Cts	Isotope	keV	Counts	Norm% Cts
	U-235?	9.21E+01	1.30E+03	18.26	??	69.34	1.28E+02	2.27187
	U-237?	112.26	1.17E+03	16.44	U-235 / U-237	97.48	1.13E+03	19.99838
	Co-57	129.53	1.06E+03	14.82	U-237?	116.18	1.00E+03	17.78088
	U-235?	152.55	9.10E+02	12.78	Co-57	133.6	8.97E+02	15.9422
	Ra-226/U-235	175.56	7.52E+02	10.56	U-235	157.45	7.56E+02	13.42654
	U-235?	202.16	6.03E+02	8.47	U-235 /Ra-226?	181.3	6.12E+02	10.86931
		229.13	4.48E+02	6.29	U-235 / U-237	208.13	1.05E+03	18.63554
		262.09	3.18E+02	4.46	Co-57	707.7	8.50E+00	0.15101
		298.05	2.05E+02	2.88	U-238	773.52	2.11E+01	0.37461
		331.31	1.29E+02	1.81	Mn-54	834.95	1.65E+01	0.29368
		373.66	8.98E+01	1.26	Rh-106??	1044.8	8.69E+00	0.15437
		417.99	6.36E+01	0.89	K-40	1419.6	5.72E+00	0.10163
		460.77	4.66E+01	0.65				
	U-238(Pa-234m)	997.12	2.96E+01	0.42				

**Recommended ID: Shielded Enriched U with Co-57**

Comments:

Unknown	Analysis with Settings 1				Analysis with Settings 2			
U22	Likely ID: Sr-85 + U, I-133, I-134/135		Other: Na-22		Likely ID: Zn-65 and Ba-140		Other: U	
	Isotope	keV	Counts	Norm% Cts	Isotope	keV	Counts	Norm% Cts
		74.86	1.23E+03	4.93	Am-243??	74.44	6.87E+03	13.62621
	U-235?	175.56	1.50E+03	6.03	U-238 (Pa-234)	113.43	3.58E+03	7.10699
	Sr-85/Na-22/I-133	516.72	2.18E+04	87.56	U-238 (Pa-234) / Ce-144	130.62	2.16E+03	4.2893
		622.14	1.31E+02	0.53	U-235?	178.32	1.42E+04	28.08172
		681.87	9.50E+01	0.38		488.47	1.48E+03	2.92795
		744.92	6.07E+01	0.24	Zn-65, Ba-140, Sr-89	528.81	2.17E+04	43.09129
		821.25	3.40E+01	0.14	Rh-106?	636.40	1.34E+02	0.26583
		880.98	2.10E+01	0.08		694.53	1.03E+02	0.20473
		953.98	1.18E+01	0.05		760.35	7.95E+01	0.15761
	U-238 Daughter (Pa-234m, 1001)/I-134	1050.2	1.59E+01	0.06		834.95	5.96E+01	0.11824
					U-238 (Pa-234)	909.15	2.89E+01	0.05728
						986.69	1.39E+01	0.02747
					Zn-65	1103.00	2.29E+01	0.04539

**Recommended ID: Irradiated U**

Comments:

Unknown	Analysis with Settings 1				Analysis with Settings 2			
U23	Likely ID: WGPu		Other: Ba-133+Cs-137		Likely ID: Ga-67 w Shielded U-238 and Excess BKG		Other: Mn-54	
	Isotope	keV	Counts	Norm% Cts	Isotope	keV	Counts	Norm% Cts
		71.98	5.72E+02	2.95462	U-238 (Pb-214) / U-233?	74.44	7.96E+02	3.42099
		109.39	4.49E+03	23.20083		116.18	4.86E+03	20.88142
		129.53	3.78E+03	19.5379		136.58	4.46E+03	19.1771
		149.67	3.41E+03	17.61142		157.45	3.97E+03	17.05142
		169.81	2.63E+03	13.59634	Ga-67	178.32	4.52E+03	19.43507
		190.17	1.38E+03	7.11366	U-238 (Pb-214)	249.87	6.81E+02	2.92723
	Pu-239/Ba-133	382.73	1.70E+03	8.78609	Ga-67 / U-238 (Pb-214)	303.53	1.66E+02	0.71415
	Pu-239	417.99	1.02E+03	5.24449	U-238 (Pb-214) / Th-232 (Ac-228)	342.29	7.56E+02	3.25232
	Pu-239	450.9	3.14E+02	1.62323	Ga-67	390.97	1.65E+03	7.0757
		546.34	2.47E+01	0.12754	U-233?	427.95	1.18E+03	5.08159
	Pu daughter (Am-241, 662)/Cs-137	661.96	2.72E+01	0.14055	Cs-137	681.37	7.01E+01	0.3014
		1934	1.23E+01	0.06333	U-238 / Th-232	734.02	5.62E+01	0.24155
					U-238 / U-238 (Pb-214) / Th-232 (Ac-228)	791.07	5.13E+01	0.22061
					Th-232 (Ac-228)	928.54	2.29E+01	0.09854
					Th-232 (Ac-228)	989.92	7.46E+00	0.03207
					U-238	1064.2	1.33E+01	0.05709
					H(n, $\gamma$ )/Mn-56?	2191.4	7.39E+00	0.03177

**Recommended ID: WGPu?**

Comments: Compromised calibration

Unknown	Analysis with Settings 1				Analysis with Settings 2			
	Likely ID: I-131 + WGPu		Other: Ba-133+Cs-137, WGPu		Likely ID: I-131 with depleted or natural U, very possibly irradiated		Other: Mn-54 or Mn-56	
U24	Isotope	keV	Counts	Norm% Cts	Isotope	keV	Counts	Norm% Cts
	Pb-214?	74.86	1.46E+04	6.54838	Ba-133 / U-238 (Pb-214) /Am-243?? / U-235?	74.44	2.53E+04	9.67631
		97.88	2.75E+04	12.35038		102.47	2.30E+04	8.79786
		112.26	1.57E+04	7.02743	Co-57	118.94	1.48E+04	5.65093
	Co-57?	126.65	7.11E+03	3.18731	Co-57 / U-238 (Pa-234) / Ce-144	133.6	8.27E+03	3.16677
		155.42	2.83E+04	12.6841	U-235	157.45	3.41E+04	13.06411
	U-235?	175.56	2.63E+04	11.80404	U-235 / Ga-67	181.3	2.86E+04	10.95185
	I-131	286.07	2.56E+03	1.14883	Ga-67 / U-235	202.17	7.64E+03	2.92529
	Pu-239?	349.46	3.20E+04	14.34104	U-238 (Pb-214)	249.87	2.02E+03	0.77379
	Pu-239/I-131	376.68	6.09E+04	27.31581	I-131 / Ga-67 / Ba-133 / U-238 (Pb-214)	291.6	8.96E+03	3.43088
		500.26	4.22E+02	0.18941	I-131 /Ba-133 / U-238 (Pb-214) / U-235 (Bi-211)	354.21	3.88E+04	14.86733
		546.34	8.38E+02	0.3758	Ga-67 / Ba-133	384.24	6.12E+04	23.44807
		599	8.78E+02	0.39371	Zn-65 / Sr-85 / Rh-106	518.73	1.68E+02	0.06446
	WGPu(Am-241)/I-131	652.01	4.48E+03	2.01063	Cs-134 / U-238 (Pa-234)	559.07	6.41E+02	0.24554
	WGPu(Am-241)/I-131	734.97	1.39E+03	0.62313	I-131 / Cs-134 / Rh-106	616.23	6.12E+02	0.23438
					Cs-137 / Co-57	668.2	4.09E+03	1.56543
					I-131 / Th-232 (Bi-212) / Pr-144?	712.08	1.30E+03	0.49647
					U-238 / Cs-134 / Th-232 (Bi-212) / U-238 (Pb-214) / Co-58	791.07	1.08E+03	0.41395
					Mn-54, Mn-56 / U-235 (Pb-211)	839.34	3.56E+02	0.1364
					U-238 (Pa-234) / Np-238 / Cd-115m?	918.85	1.12E+02	0.04305
					U-238 / Cs-134 / Np-238 / Rh-106	1025.5	6.40E+01	0.02452
					Zn-65?	1109.5	3.21E+01	0.01231
					Pr-144? / Tl-209??	1542.8	9.72E+00	0.00372
					Th-232 (Bi-212)	1661	9.59E+00	0.00367
					Mn-56? / Pr-144??	2191.4	7.60E+00	0.00291

**Recommended ID: I-131**

Comments: Pile-up, high dead time

Unknown	Analysis with Settings 1				Analysis with Settings 2			
U25	Likely ID: Shielded Ga-67		Other: Ba-133		Likely ID: Ga-67 with natural or enriched U, possibly irradiated, same as U26		Other:	
	Isotope	keV	Counts	Norm% Cts	Isotope	keV	Counts	Norm% Cts
		74.86	3.22E+04	20.17	U-238 (Pb-214)	74.44	4.18E+04	13.50648
	Ga-67?	92.12	3.68E+04	23.07	Ga-67	89.99	2.45E+04	7.93368
		158.3	1.60E+04	10.04		105.16	1.35E+04	4.37815
	Ga-67	292.06	5.92E+04	37.09	Co-57 / Ce-144?	136.58	3.81E+04	12.3199
	Ga-67/WGPu	388.78	1.33E+04	8.31	Ba-140	160.43	3.46E+04	11.16888
		467.35	1.54E+03	0.96	Ga-67 / U-235	187.26	4.02E+04	12.99125
		559.5	3.57E+02	0.22	U-238 (Pb-214)	249.87	2.94E+04	9.50683
		608.87	2.15E+02	0.13	Ba-133 / Ga-67 / U-238 (Pb-214) / Ba-140??	297.57	6.74E+04	21.77308
					Ba-133 / U-238 (Pb-214) U-235 (Bi-211)	354.21	5.29E+03	1.71147
					Ba-133 / Ga-67 / U-235 (Pb-211)	397.69	9.42E+03	3.04634
					U-235 (Pb-211) / Ba-140??	431.31	2.84E+03	0.91933
						478.38	9.43E+02	0.30482
					Ba-140??	525.45	5.89E+02	0.19048
						575.89	3.45E+02	0.1114
						626.32	2.05E+02	0.06622
					Co-57, shifted Cs-137	681.37	1.06E+02	0.03414
					Zr-95?	734.02	5.97E+01	0.01929
					U-238 (Pb-214)	791.07	3.44E+01	0.0111
					U-235 (Pb-211) / Mn-54?	854.23	1.67E+01	0.00541
					very low / Sc-46? / Cd115m?	909.15	5.34E+00	0.00173

Recommended ID: shielded Ga-67

Comments: High Dead Time/Pile-up, Same source as U-26

Unknown	Analysis with Settings 1				Analysis with Settings 2			
U26	Likely ID: Shielded Ga-67		Other: Ba-133		Likely ID: Ga-67 with natural or enriched U, possibly irradiated, same as U26		Other:	
	Isotope	keV	Counts	Norm% Cts	Isotope	keV	Counts	Norm% Cts
		71.98	3.26E+04	20.31	U-238 (Pb-214) / U-235 / U-235 (Bi-211)	74.44	4.13E+04	14.33539
	Ga-67?	89.24	3.73E+04	23.22	Ga-67 / U-238 (Pb-214) / U-235 (Pa-231)	89.99	2.23E+04	7.74005
		161.18	2.23E+04	13.90	Eu-155?	102.47	1.01E+04	3.50071
	Ga-67	298.05	5.26E+04	32.75	Co-57 / Ce-144?	136.58	3.54E+04	12.28802
	Ga-67	388.78	1.34E+04	8.34	U-235 / U-235 (Pa-231) / Ba-140??	160.43	3.17E+04	11.00252
		464.06	1.73E+03	1.07	Ga-67 / U-235 / U-238 (Ra-226)	184.28	2.47E+04	8.55671
		562.79	4.30E+02	0.27	Ga-67 / U-235	208.13	1.45E+04	5.01161
		612.19	2.30E+02	0.14	U-238 (Pb-214)	249.87	2.79E+04	9.65841
					Ga-67 / U-238 (Pb-214) / U-235 (Pa-231) / Ba-140??	303.53	5.18E+04	17.9755
					U-235 (Pa-231)	330.36	9.14E+03	3.16825
					U-235 (Bi-211) / U-238 (Pb-214)	360.71	3.50E+03	1.21417
					Ga-67 / U-235 (Pb-211)	397.69	9.58E+03	3.32212
					U-235 (Pb-211) / Ba-140??	427.95	3.77E+03	1.30877
						475.02	1.05E+03	0.36307
					Ba-140??	518.73	6.71E+02	0.23255
						575.89	4.30E+02	0.1491
					low	626.32	2.29E+02	0.07939
					Co-57, shifted Cs-137	681.37	1.28E+02	0.04426
					Zr-95?	734.02	6.85E+01	0.02374
					Co-58 / U-238 (Pb-214)	791.07	4.05E+01	0.01405
					U-235 (Pb-211)	847.77	2.00E+01	0.00694
					very low	918.85	1.34E+01	0.00466

**Recommended ID: Shielded Ga-67**

Comments: High Dead Time/Pile-up, Same source as U-25

Unknown	Analysis with Settings 1				Analysis with Settings 2			
U27	Likely ID: WGPu		Other: Ba-133+Cs-137		Likely ID: WGPu (w/ neut) and Ga-67		Other: Np-237, and Irradiated Th	
	Isotope	keV	Counts	Norm% Cts	Isotope	keV	Counts	Norm% Cts
	Ba-133?	83.49	6.16E+03	11.69	Np-237 (Pa-233)? / Pu-239? / Th-232 (Pb-212)	87.49	1.07E+03	1.40407
	Pu-239?	100.75	7.44E+03	14.13	Np-237 (Pa-233) / Pu-238?	102.47	4.98E+02	0.65073
		149.67	1.11E+04	21.04	Pu-239 / Np-237 (Pa-233)	113.43	4.39E+03	5.73435
		169.81	8.91E+03	16.92	Pu-239 / U-232?	130.62	8.99E+03	11.75281
	Pu-239/Ba-133/Ga-67	304.08	3.00E+03	5.70	Pu-238?	154.47	1.12E+04	14.59769
	Pu-239/Ba-133	361.56	1.53E+04	29.02	Ga-67	178.32	8.23E+03	10.75601
		490.39	5.60E+02	1.06	Ga-67	205.15	5.66E+03	7.40083
		543.05	1.16E+02	0.22	Th-232 (Pb-212)	243.9	5.99E+03	7.82771
	WGPu(Am-241)	655.33	1.15E+02	0.22	Ba-133 / U-232?	276.7	4.32E+03	5.65329
					Ga-67 / Ba-133 / Th-232 (Pb-212) / Np-237 (Pa-233)	306.51	7.88E+03	10.30899
					U-232? / Np-237 (Pa-233)	333.34	2.50E+03	3.26301
					Ba-133 / Pu-239	367.43	1.14E+04	14.9677
					Ga-67 / Ba-133 / Np-237 (Pa-233) / U-235 (Pb-211)	394.33	2.94E+03	3.84874
					Pu-239 / U-233 (Bi-213) / Np-237 (Pa-233) / U-235 (Pb-211)	424.59	1.09E+03	1.43153
					Cs-137 / Np-237 (Pa-233) / Te-129m?? / Au-198??	672.59	1.07E+02	0.13941
					Th-232 (Bi-212) / U-238	734.02	8.18E+01	0.10699
					Co-58 / Th-232 (Bi-212) / U-238 / Pu-238?	791.07	5.12E+01	0.06692
					Mn-54 / U-235 (Pb-211)	847.77	3.28E+01	0.04293
						931.77	1.59E+01	0.02073
					U-238	1002.8	8.12E+00	0.01062
						2110.3	6.25E+00	0.00817
					H (n-gamma)	2269.1	5.17E+00	0.00676

Recommended ID: WGPu and Ga-67

Unknown	Analysis with Settings 1				Analysis with Settings 2			
	Likely ID: Shielded WGPu		Other: Ga-67		Likely ID: Shielded WGPu with Ga-67 with DU?		Other: K-40	
U28	Isotope	keV	Counts	Norm% Cts	Isotope	keV	Counts	Norm% Cts
		71.98	1.03E+03	5.08505	U-238 (Pb-214)?	74.44	3.57E+03	11.2379
	Pu-239/Ga-67	95	5.11E+03	25.23645	Pu-240?	107.91	3.44E+03	10.85214
		149.67	4.46E+03	22.02567	Pu-239	121.7	1.84E+03	5.79228
		169.81	5.19E+03	25.66992	Pu-240 / Pu-241	154.47	6.05E+03	19.05885
	Pu-239/Ba-133	346.43	1.91E+03	9.4287	Ga-67	178.32	4.55E+03	14.35071
	Pu-239/Ga-67/Ba-133	382.73	1.28E+03	6.32023	Ga-67	205.15	2.90E+03	9.15439
	Pu-239	414.69	6.60E+02	3.26055	Xe-133m?	234.96	1.73E+03	5.45034
	Pu-239/Pu	622.14	4.58E+02	2.26405		264.77	1.12E+03	3.53954
	Pu?	705.1	6.26E+01	0.30945	Ga-67 / Ba-133	300.55	1.12E+03	3.52063
		1113.3	4.40E+01	0.21747	Ba-133	351.23	2.09E+03	6.59531
	H(n,y)	2225.9	3.69E+01	0.18245	Ga-67 / Pu-239 / Ba-133	390.97	1.52E+03	4.78441
					Pu-239	424.59	8.51E+02	2.68269
					U-238 (Bi-214)? / Pu-240?	636.4	3.38E+02	1.06489
					Cs-137	668.2	1.83E+02	0.57816
					U-238	725.25	1.19E+02	0.37652
					U-238 / Co-58	799.85	1.47E+02	0.46281
					U-238 (Bi-214)?	909.15	2.17E+01	0.0685
					U-238	967.31	1.20E+01	0.03783
					U-238 (Bi-214)?	1119.2	9.24E+00	0.02913
					U-238 (Bi-214)? / Co-60?	1203.2	2.09E+01	0.06599
					Co-60?	1293.6	1.14E+01	0.03589
					K-40	1439	3.36E+01	0.10591
						1654.3	1.46E+01	0.04592
					U-238 (Bi-214)?	1769.1	2.14E+01	0.0675
					H-1_n-g	2198.2	7.55E+00	0.02378
					U-238 (Bi-214)?	2373.8	5.71E+00	0.01799

Recommended ID: Shielded WGPu

Unknown	Analysis with Settings 1				Analysis with Settings 2			
	Likely ID: Ra-226		Other: Co-57		Likely ID:Ra-226		Other: Trace I-131, K-40	
U29	Isotope	keV	Counts	Norm% Cts	Isotope	keV	Counts	Norm% Cts
	Pb-214 X-ray	77.74	8.72E+02	10.82	U-238 (Pb-214)?	74.44	8.22E+02	5.31626
		103.63	1.44E+03	17.89	Ga-67?	92.49	1.33E+03	8.5842
	Co-57	120.89	1.87E+03	23.27	U-235?	110.67	1.65E+03	10.69953
	Ra-226(186)	181.32	2.71E+03	33.66		133.6	2.75E+03	17.79374
	Ra-226 daughter (Pb-214, 295)	283.07	2.67E+02	3.32		154.47	2.55E+03	16.47384
	Ra-226 daughter (Pb-214, 352)	343.41	4.03E+02	5.00	Ra-226 / Ga-67?	187.26	2.43E+03	15.71398
	Ra-226 daughter (Bi-214, 609)	605.58	4.01E+02	4.98		223.04	9.21E+02	5.95571
	Ra-226 daughter (Bi-214, 1106)	1106.6	8.57E+01	1.06	Ra-226	252.85	5.74E+02	3.70878
					Ga-67?	288.62	8.64E+02	5.58897
					I-131?	348.25	7.38E+02	4.77013
					Ra-226 / Ga-67?	401.05	2.12E+01	0.13699
						478.38	2.47E+01	0.15998
					511 peak	512	4.74E+01	0.30666
						572.52	8.58E+01	0.55517
					Ra-226 / I-131?	622.96	3.04E+02	1.96769
						672.59	7.82E+01	0.50562
					U-238 / I-131?	742.8	4.76E+01	0.30792
					U-238	808.62	7.48E+01	0.48389
						954.38	8.77E+00	0.05672
					U-238	1012.5	1.98E+01	0.12789
					Zn-65? / Sr-89?	1093.3	8.76E+00	0.05667
					U-238 (Bi-214)?	1157.9	4.21E+01	0.2721
					U-238 (Bi-214)?	1222.5	8.87E+00	0.05733
					K-40	1445.5	1.49E+01	0.09638
					Th-232 (Bi-212)	1654.3	1.05E+01	0.06822
					U-238 (Bi-214)?	1732	2.86E+01	0.18484
					U-238 (Bi-214)?	2090.1	7.85E+00	0.05077

Recommended ID: Ra-226

## Appendix B: Analysis Details for GADRAS/DHSIsotopeID

*This section presents the interim results that were reported for analysis of the blind test data using the DHSIsotopeID algorithm. Text presented in this section was written before the actual identities of the sources were known. Although Table B-1 presents some of the same information that is presented in Table 1, data that are contained in the additional columns in Table B-1 are referenced in this discussion.*

Table B-1 summarizes the analysis results that were obtained using analysis algorithms that are incorporated into GADRAS. As described in section 2.1, the process of obtaining the energy calibration parameters was interactive. However, Table B-1 was generated automatically using DHSIsotopeID after the energy calibration parameters were written to the data files. The most important result is the list of isotopes that are reported for each of the events, but the additional columns provide information that is discussed in this report. The columns labeled “Gamma (cps)” and “Neutron (cps)” report gamma ray and neutron count rates after subtracting background data. The column labeled “SNM” reports the likelihood that SNM is present, where 0 is the lowest probability and 3 is the maximum probability. The column labeled “Threat” gives a quantitative value associated with the threat, where 0 is the minimum and 7 is the maximum. The minimum threat that was reported for a data set that is included in this analysis is 4. This threat value corresponds to poor identifications or the possibility that the source might mask the emission of weaker SNM sources. All of the radiation sources that produced spectra for this set of blind-test data could have masked weak SNM sources, so the minimum threat level was 4. Selection of these sources was probably intentional because the test planners knew that these sources could mask emission from  $^{235}\text{U}$  or  $^{239}\text{Pu}$ . The large values of the reduced chi-square values ( $\chi_r^2$ ) for Events 2 and 19 are sufficient to declare the event as suspicious because the isotope identifications are questionable. Rows that are presented with white backgrounds are viewed as conclusions that are reasonably definitive in that the author cannot refute the results by visual inspection of the results. The isotopes that are listed on rows with pink backgrounds are viewed as questionable. Detailed discussions for results that were obtained for specific events are presented in subsections of Section 3.

**Table B-1. Summary of Analysis Results using GADRAS**

Event	Gamma (cps)	Neutron (cps)	SNM	Threat	$\chi_p^2$	Isotopes
1	2011	0.24	3	7	0.9	Cs137(H);Pu239(H)
2	580	-0.02	3	7	3	In111(H);U235(H);U237(H);Ba133(H);I131(H)
3	348	-0.01	3	7	0.7	U232(H);U235(F)
4	1324	1.15	2	6	1	Ba133(H);Cs137(H)
5	350	0	0	4	0.9	Sr90(H)
6	276	-0.01	0	4	0.8	Eu152(H)
7	978	0	0	4	0.7	Ho166m(H)
8	781	0.01	0	4	1.1	Ho166m(H)
9	481	0.03	0	4	1.7	Ba133(H)
10	172	0	3	7	1	K40(H);Pu239(H)
11	81	0.04	0	4	1.1	Th232(H);Ra226(H)
12	81	0.04	0	4	1	Th232(H);Ra226(H)
13	336	0.01	0	4	1.5	Mn54(H)
14	117	0.52	2	7	0.9	Pu239(H), Neutron
15	1518	-0.02	3	7	2.1	Ra226(H);U235(H)
16	2317	0	3	7	1.5	Ga67(H);U235(H);Th232(H)
17	1807	0.01	3	7	1.1	Ho166m(H);U235(H);Th232(H)
18	111	0.02	0	4	0.7	K40(H)
19	1368	0.01	2	6	4	In111(H);Ba133(H);Ga67(H);K40(H);U235(F)
20	4434	0.03	3	7	1.9	In111(H);Ga67(H);Lu177m(H);Cf252(H);U237(H); U235(F);U232(F)
21	334	0.28	3	6	1.1	U238(H);Pu239(F)
22	9639	0.03	0	4	1.0	F18(H)
23	1979	4.5	3	7	1.6	Pu239(H);U235(F)
24	21789	2.59	2	6	0.6	I131(H); Cf252
25	19435	0.03	3	7	1.3	Np237(H)
26	20780	0.04	3	7	0.7	Np237(H)
27	5837	4.15	3	7	0.9	Ba133 (H);Pu239(H)
28	2542	4.39	3	7	0.6	Pu239(H);Ra226(H)
29	781	0	3	7	0.8	Ra226(H);U235(H)

## Event 1

The first event provides a good example of an analysis result that cannot be refuted by an analyst even though the spectroscopic information is ambiguous. The DHSIsotopeID algorithm reported that  $^{137}\text{Cs}$  and plutonium were both present when the spectrum was performed. The spectral features are definitive with respect to the presence of  $^{137}\text{Cs}$  but spectroscopic evidence for the presence of plutonium is less definitive. The plot on the left of Fig. 1 compares the spectrum that was generated by  $^{137}\text{Cs}$  and plutonium with the measured spectrum. The figure on the right compares the fit to the data where  $^{137}\text{Cs}$  is the only radiation source. The difference is subtle, but a residual in the 300-keV to 400-keV region suggests that an additional source was present, and shielded  $^{239}\text{Pu}$  matches this spectral region better than any other radiation source. Consequently, the DHSIsotopeID algorithm concluded that  $^{137}\text{Cs}$  and  $^{239}\text{Pu}$  were both present with high confidence. The neutron count rate also appears to be somewhat elevated for this event, but it is not known whether this difference is significant because the neutron detector in the GR-135 has not been characterized and it is not known whether the measurements were performed in a sufficiently controlled way for the small difference in neutron count rates to be significant.

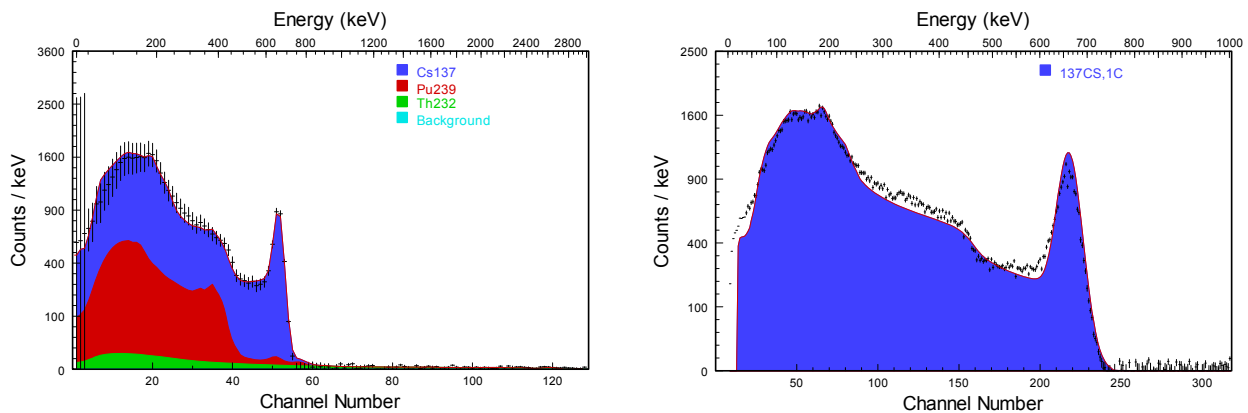


**Figure B-1.** The plot on the left compares the background-subtracted, measured spectrum for Event 1 (black  $\pm 1$ -sigma error bars) with the best fit obtained with the DHSIsotopeID algorithm. The plot on the right shows the best fit using only shielded  $^{137}\text{Cs}$ .

## Events 2, 19, and 20

The analysis results are ambiguous for the three events with pink backgrounds in Table B1. Each of these events shares characteristics that are similar to Event 2. Figure B2 shows the fit that was obtained when Event 2 was analyzed by the DHSIsotopeID algorithm. This event exhibits no distinctive spectral features, so it is difficult to evaluate the accuracy of the energy calibration parameters. The spectrum was most consistent with a computed spectrum for a combination of several isotopes. Finding  $^{237}\text{U}$  without stronger emission from  $^{239}\text{Pu}$  would be improbable, so it is unlikely that this isotope is actually present even though the DHSIsotopeID algorithm concluded that this is the case based exclusively on spectral features. The algorithm also reports the presence of both  $^{131}\text{I}$  and  $^{133}\text{Ba}$ , but ambiguity results primarily from the uncertainty in energy calibration parameters; either isotope could have imposed the observed spectral features depending on the energy calibration parameters that are applicable to this data set.

Regardless of these ambiguities, a spectroscopist cannot refute the conclusion that the spectrum is consistent with the presence of  $^{235}\text{U}$  as well as additional shielded isotopes despite the fact that the quality of the fit is poor (as evidenced by a large value of  $\chi_r^2$ ) and the assemblage of isotopes that would probably not be present at one time. Therefore, the spectrum that is associated with this event suggests high confidence that SNM is present despite the fact that the isotope assessment is ambiguous.

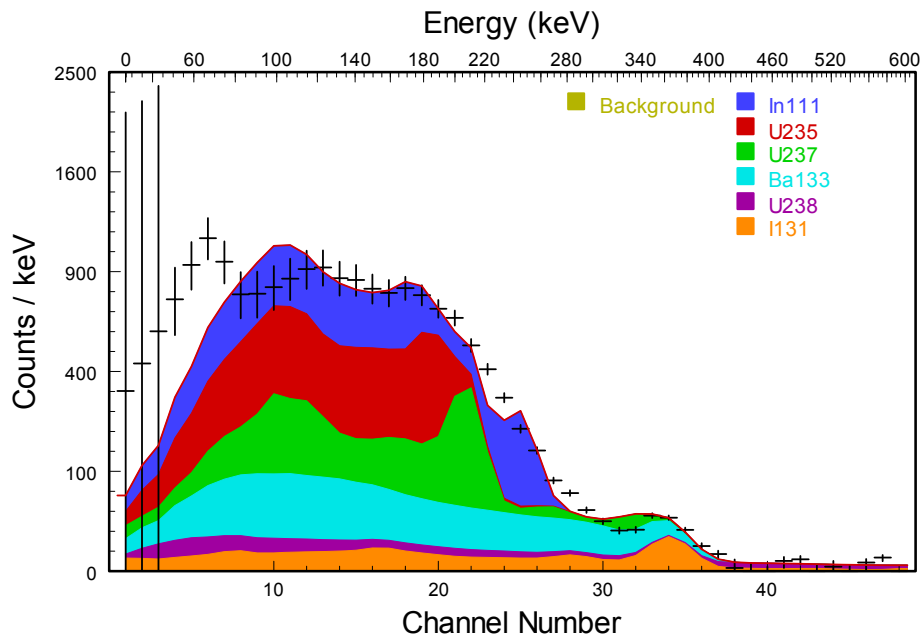


**Figure B2. Comparison of the measured spectrum for Event 2 (black  $\pm 1$ -sigma error bars) and several components associated with shielded isotopes that collectively represent the best fit to the data.**

### Event 3

Event 3 shows evidence for peaks at 511, 583, and 2614 keV plus a continuum that is irrefutably associated with either  $^{228}\text{Th}$  or  $^{232}\text{U}$ . An absence of emission in the 911-keV region indicates that the source is not associated with the NORM isotope  $^{232}\text{Th}$  unless daughter products were removed by recent chemical processing. Since  $^{228}\text{Th}$  and  $^{232}\text{U}$  exhibit almost the same set of gamma rays, the isotopes cannot normally be differentiated uniquely. Therefore, the DHSIsotopeID algorithm asserts that the spectrum is consistent with  $^{228}\text{Th}$  if little shielding is present and it asserts that the source is consistent with  $^{232}\text{U}$  if the material is shielded, as would be the case if the isotope were distributed as a trace contaminant in HEU. Spectral evidence for  $^{235}\text{U}$  is questionable, so the DHSIsotopeID algorithm concludes that  $^{235}\text{U}$  is present with only fair confidence because emission associated with shielded  $^{235}\text{U}$  improves the fit at low energy. Even though  $^{235}\text{U}$  is only reported as fair significance, this event was rated at the highest threat level, which corresponds to high confidence that SNM is present. This determination is made because the threat assessment is determined as a composite of several factors. Even though  $^{232}\text{U}$  is not a special nuclear material, it may be present as a contaminant in either HEU or  $^{233}\text{U}$ , which makes the appearance of this isotope suspicious. The threat level is elevated further because the spectrum suggests that  $^{235}\text{U}$  may also be present. Hence, the combination of these two factors yields a composite conclusion that SNM is present with high confidence.

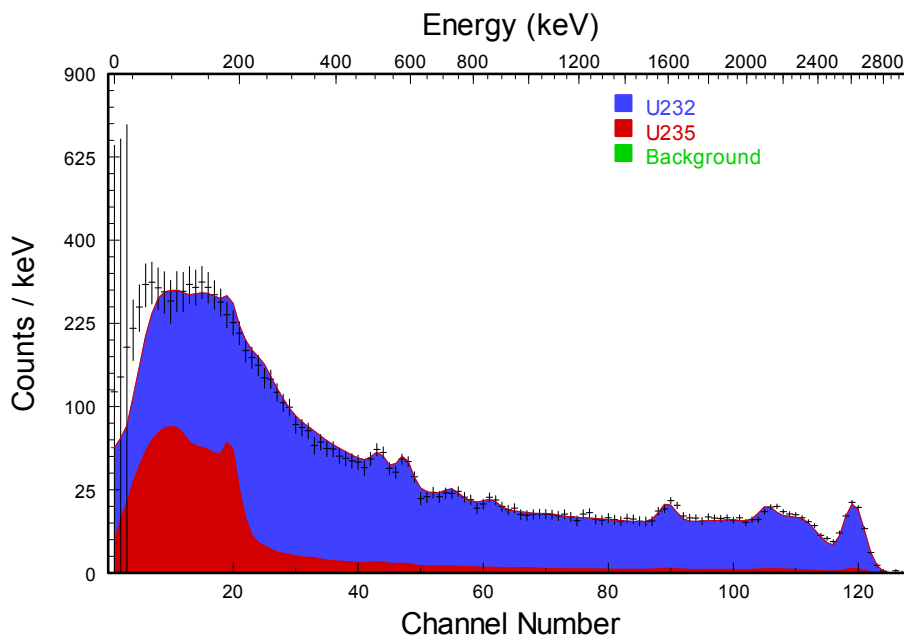


**Figure B3.** This plot gives a graphic representation of the DHSIsotopeID analysis result for Event 3.

## Event 4

The DHSIsotopeID algorithm concluded that  $^{133}\text{Ba}$  and  $^{137}\text{Cs}$  were both present with high confidence when Event 4 was recorded. Even though neither of these isotopes is particularly threatening, the gamma-ray spectrum could mask emission from either  $^{235}\text{U}$  or  $^{239}\text{Pu}$ , there is spectral evidence for the presence of a neutron source, and there was a significant increase in the neutron emission rate. Therefore, even though there is no spectroscopic evidence for SNM, this event was ranked as the second highest threat category (*Threat=6*) due to several factors that are associated with SNM. The spectral regions that are colored green in Figure B-4 represent the gamma-ray signature associated with a neutron source, which gives rise to a gamma-ray continuum plus a hydrogen capture peak at 2223 keV.

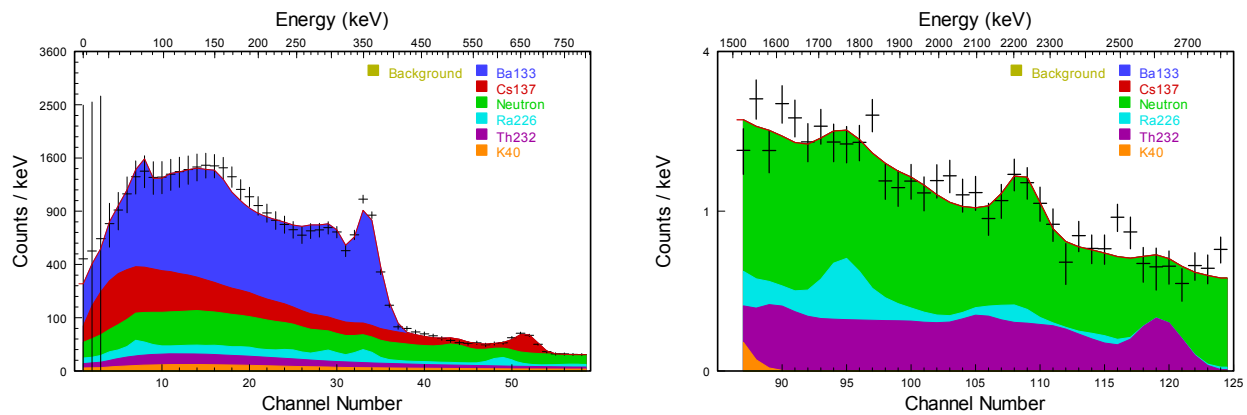


**Figure B-4.** The plot on the left side compares the measured data (black) with spectral components associated with  $^{133}\text{Ba}$  (blue) and  $^{137}\text{Cs}$  (red). Neutron emission is associated with the green continuum component that extends across the entire energy range and also gives rise to the hydrogen capture peak at 2223 keV.

## Event 5

The spectrum associated with Event 5 is the featureless continuum shown in Figure B-5. This spectrum is consistent with bremsstrahlung radiation from  $^{90}\text{Sr}$ , and DHSIsotopeID concludes that this is the radiation source with high confidence. No additional isotopes were identified.

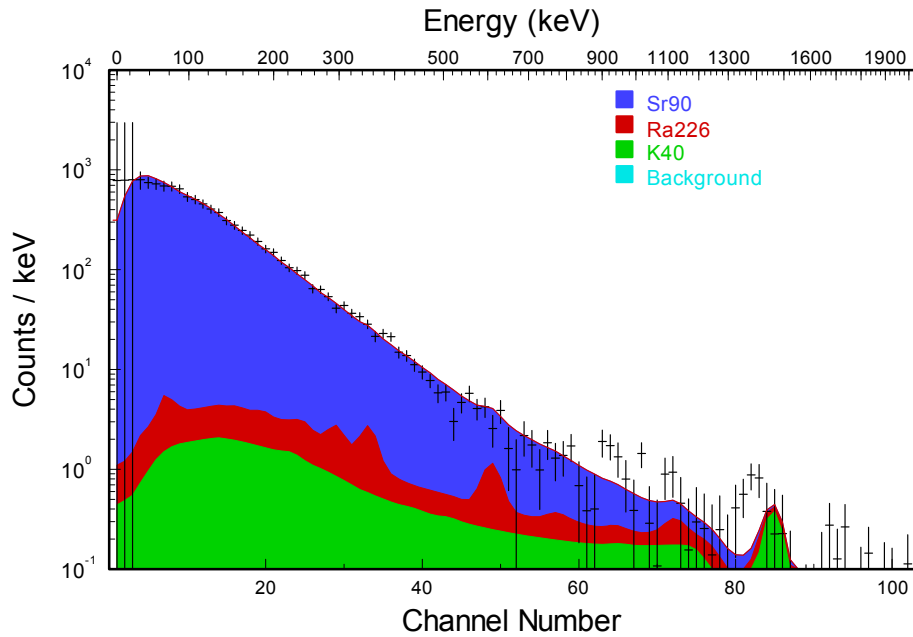


**Figure B-5.** This plot compares the spectrum that was measured for Event 5 (black) with the computed spectrum for  $^{90}\text{Sr}$  (blue).

## Events 6 through 9

Analysis of Events 6 through 9 was straightforward and the conclusions were unambiguous after determining the applicable energy calibration parameters for these events. Each of these events was ranked as threat level 4 because the sources could have masked weak uranium and/or plutonium sources. The plots shown in Fig. B6 summarize analysis results that were obtained with DHSIsotopeID. The DHSIsotopeID algorithm interpolates spectral shapes based on a pre-computed database of spectral templates, so it is not always able to match measurements based on this sparse set of shielding configurations. However, assessment using the single regression analysis tool, which is part of the GADRAS package, shows that each of these spectra can be represented adequately by a single, shielded isotope.

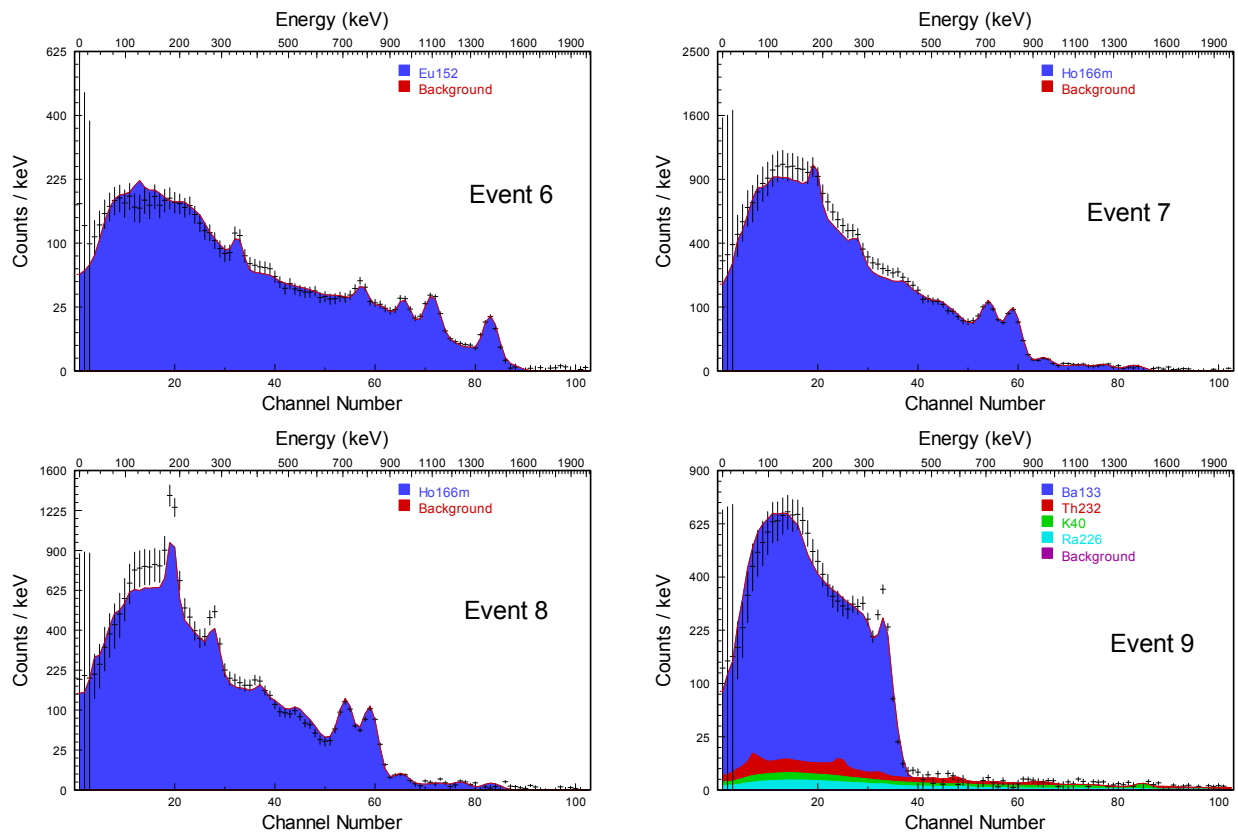


**Figure B-6.** This figure compares spectra that were measured for Events 6 through 9 with the single-isotope solutions that DHSIsotopeID concluded were consistent with the observations.

## Event 10

Event 10 exhibits spectral characteristics that clearly indicate the presence of substantially more  $^{40}\text{K}$  than was present in the associated background measurement. The DHSIsotopeID algorithm concluded that  $^{239}\text{Pu}$  was also present with high confidence, but as shown in Figure B-7, the spectrum does not exhibit any prominent features that can clearly be associated with plutonium. The neutron detector in the GR-135 did not report an excess neutron count for this event, and no evidence for the presence of a neutron source can be found in the gamma-ray spectrum. Nevertheless, the elevated count rate below 400 keV is not consistent with emission from shielded  $^{40}\text{K}$  alone, so this event would need to be treated as threatening until proven otherwise. If it turns out that  $^{239}\text{Pu}$  was not present when this event was recorded, a description of the source configuration will enable the database to be expanded so that events of this type are recognized in the future.

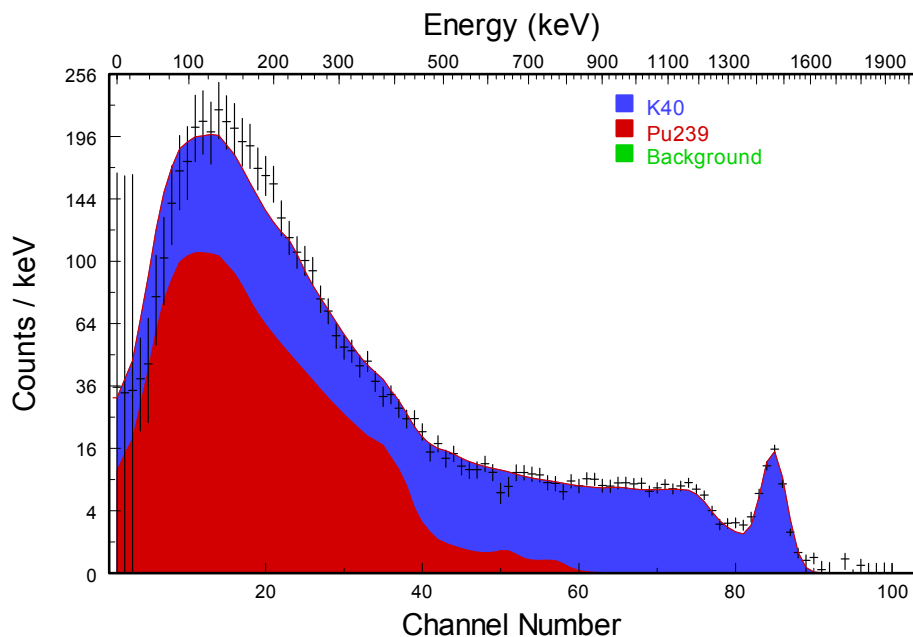


**Figure B-7.** This figure compares spectra that were measured for Event 10 with the best fit, which is obtained using a combination of shielded  $^{40}\text{K}$  and  $^{239}\text{Pu}$ .

## Events 11 and 12

Events 11 and 12 are very similar, and analysis of the gamma-ray spectra using DHSIsotopeID reveals only an excess of  $^{226}\text{Ra}$  and  $^{232}\text{Th}$  relative to the local background.

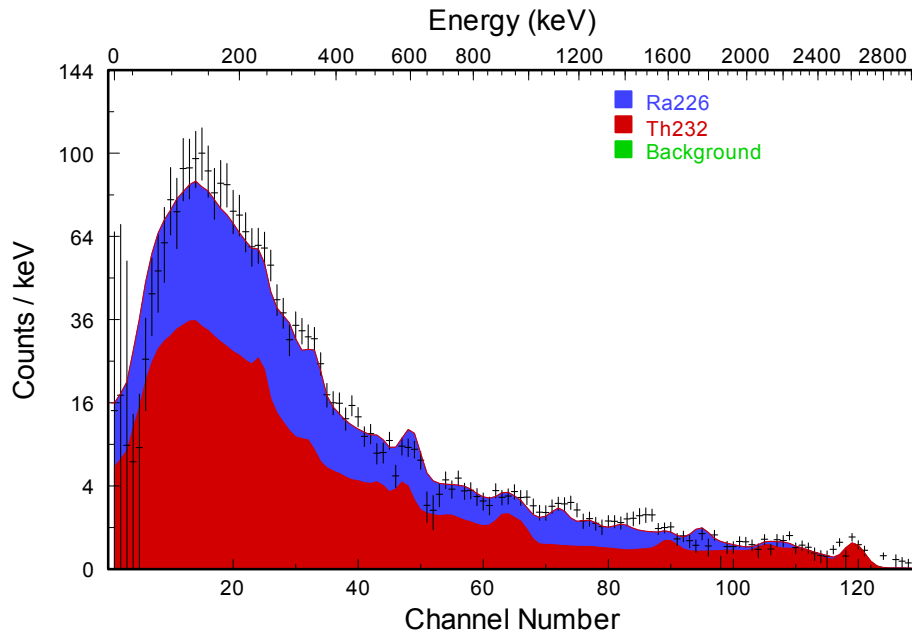


**Figure B-8.** The measured spectrum for Event 11 (black) is compared with the best fit that is obtained with a combination of  $^{226}\text{Ra}$  (blue) and  $^{232}\text{Th}$  (red).

## Event 13

Event 13 is consistent with the presence of  $^{54}\text{Mn}$ , which is a gamma ray at 835 keV. However, there is considerable uncertainty in the energy calibration parameters, and a similar spectrum could have been produced by  $^{210}\text{Po}$ , which emits a gamma ray at 803 keV. Since  $^{210}\text{Po}$  is an unusual isotope with a low gamma-ray yield, it is not likely to have been the source for Event 13.

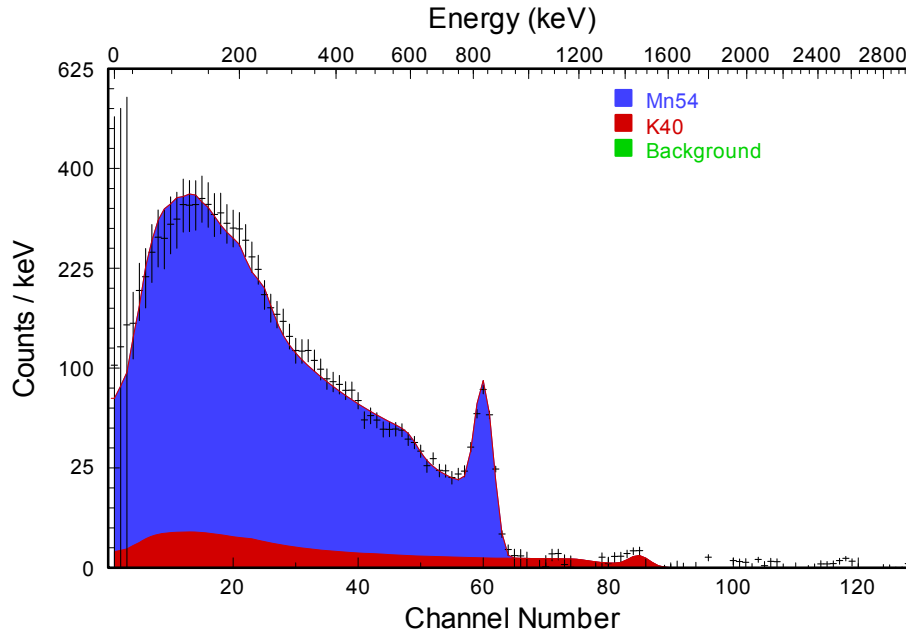
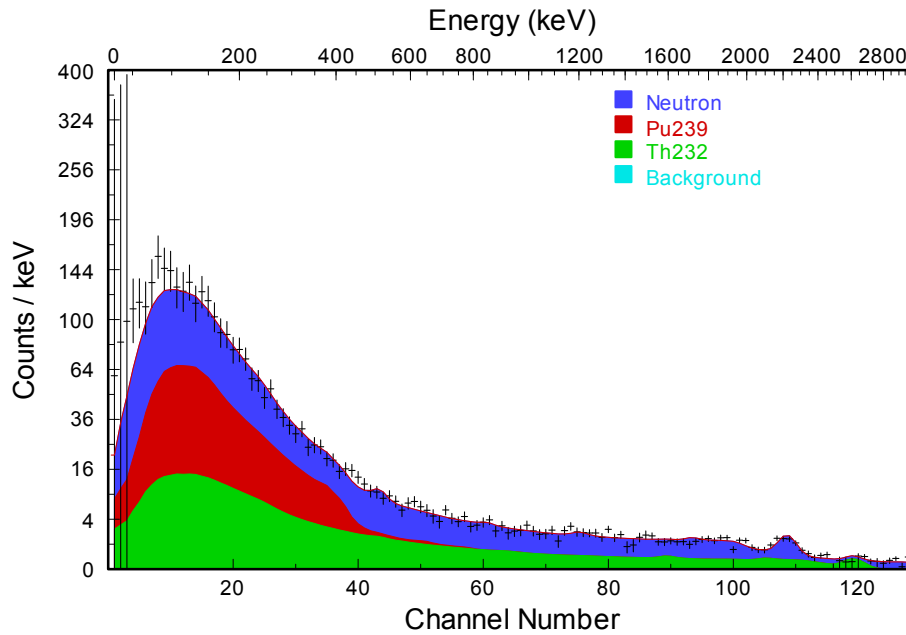


Figure B-9. The measured spectrum for Event 13 (black) is compared with the best fit that is obtained with shielded  $^{54}\text{Mn}$  (blue region).

## Event 14

The analysis result for Event 14 was that  $^{239}\text{Pu}$  and a neutron source were both present. The calibration spectrum did not show the presence of a calibration source, so there is no way to verify the offset. A small change in the offset parameter could have produced an analysis result that reported  $^{133}\text{Ba}$  or  $^{131}\text{I}$ . Nevertheless, the presence of a neutron source was determined with high confidence and this result was not impacted substantially by uncertainty in the energy offset parameter, so this event would have produced an alarm even if another isotope that emits gamma rays in the 400 keV region had been identified.



**Figure B-10.** The measured spectrum for Event 14 (black) is compared with the best fit that is obtained with a combination of  $^{239}\text{Pu}$  (red) and gamma rays associated with neutron emission (blue).

## Events 15, 16, 17, and 29

The series of four events numbered 15, 16, 17, and 29 all show evidence of emission from  $^{235}\text{U}$  in addition to other isotopes that are viewed as masking sources because they also emit radiation in the 185-keV region. Despite interference from the other isotopes,  $^{235}\text{U}$  was clearly identifiable in these spectra due to excess counts in the 185-keV regions as well as near 100 keV, where uranium x-rays were emitted. The other isotopes for events 15, 16, 17 and 29 were  $^{226}\text{Ra}$ ,  $^{67}\text{Ga}$ ,  $^{166\text{m}}\text{Ho}$  and  $^{226}\text{Ra}$ , respectively. Figure B-11 shows analysis results that were obtained using DHSIsotopeID. The isotope  $^{232}\text{Th}$  was also reported for Events 16 and 17, but this may have been an incorrect assessment, and  $^{232}\text{U}$  may have been the source of excess emission at 2614 keV.

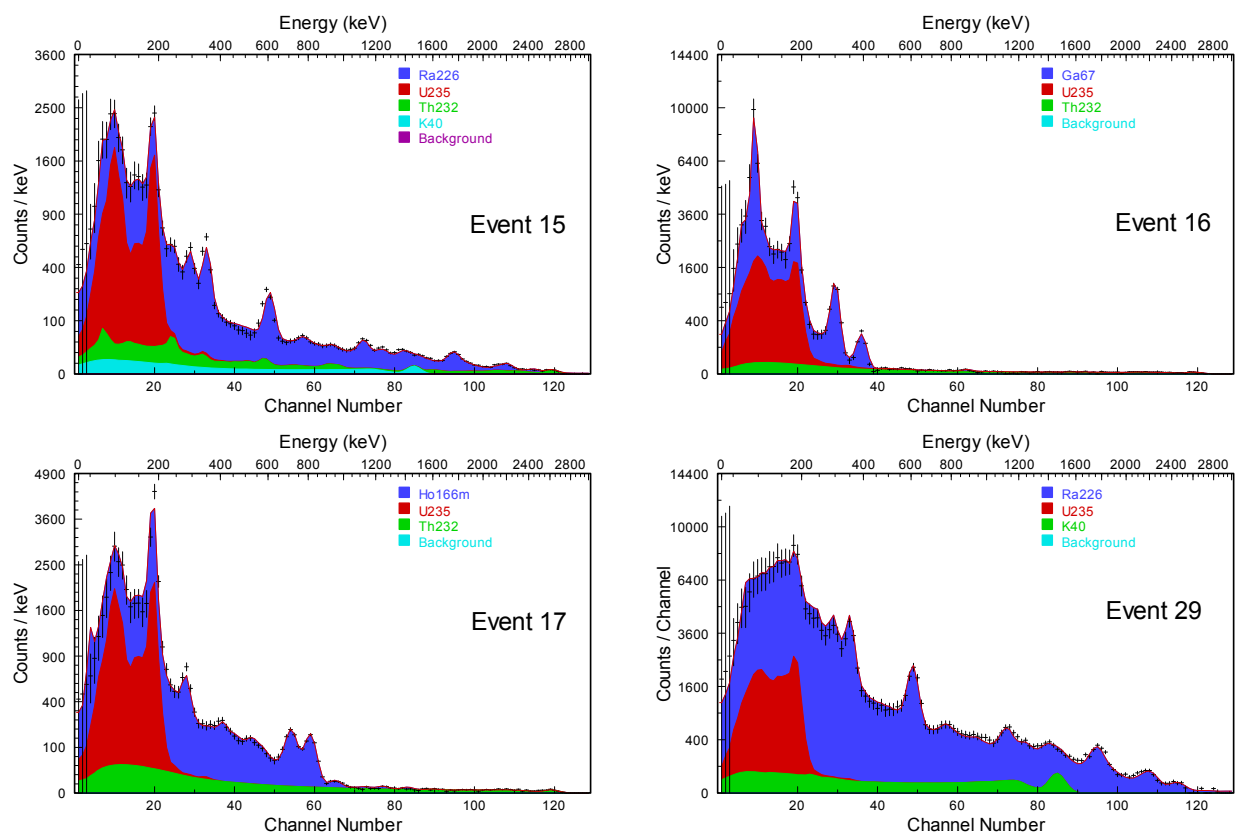


**Figure B-11.** This figure compares spectra that were measured for Events 15 through 17 and 29 with analysis results that were obtained with DHSIsotopeID. Each of these events was produced by  $^{235}\text{U}$  in combination with a “masking” source.

## Event 18

As shown in Figure B-12,  $^{40}\text{K}$  was the only isotope that was identified for Event 18.

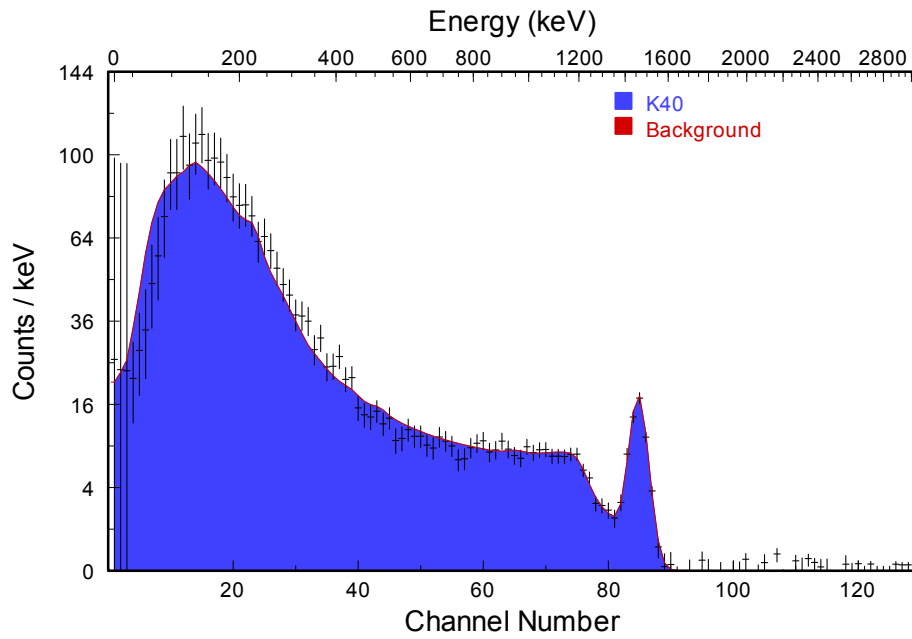
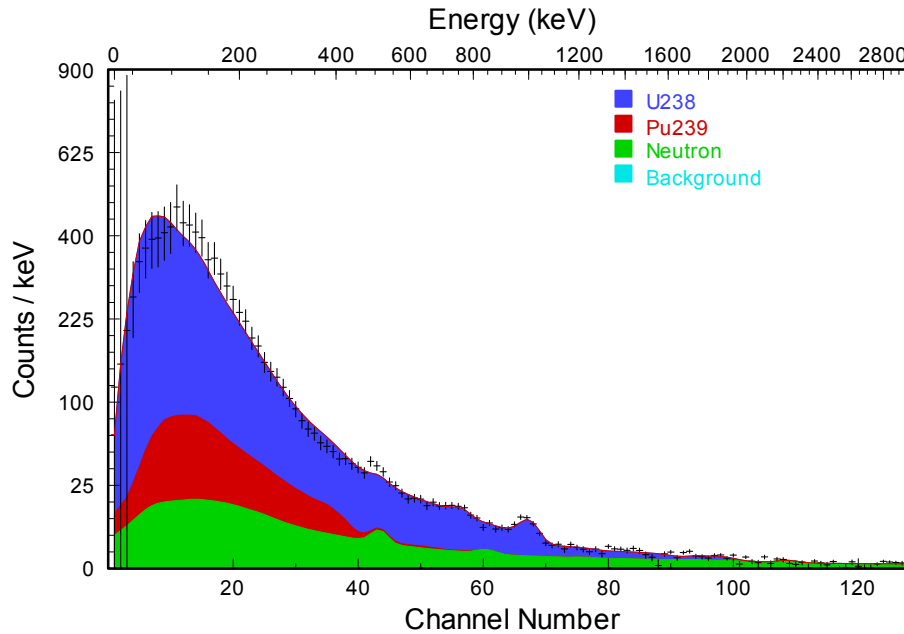


Figure B-12. The only isotope that DHSIsotopeID identified from analysis of Event 18 was  $^{40}\text{K}$ .

## Event 21

Analysis of event 21 identified  $^{238}\text{U}$  with high confidence. The result shown in Figure B-13 also indicates the presence of weak emission from  $^{239}\text{Pu}$ , but this conclusion is much less certain because of uncertainty in the energy calibration parameters. Small changes in the energy offset caused the analysis algorithm to report only  $^{238}\text{U}$ . The calibration spectrum that was associated with the event did not exhibit emission from  $^{133}\text{Ba}$ , which the database indicated should have been present.



**Figure B-13. Analysis of Event 21 revealed the presence of  $^{238}\text{U}$  with high confidence. Plutonium may also have been present, but the confidence in this conclusion is much less certain because of uncertainty in the energy calibration offset parameters.**

## Event 22

The analysis result for Event 22 indicated that  $^{18}\text{F}$  was present. However,  $^{18}\text{F}$  is a positron emitter, and this isotope cannot be distinguished from several other positron emitters, so the specific identity of the isotope cannot be confirmed. The distinguishing feature is a peak at 511 keV, which results when positrons annihilate with electrons.

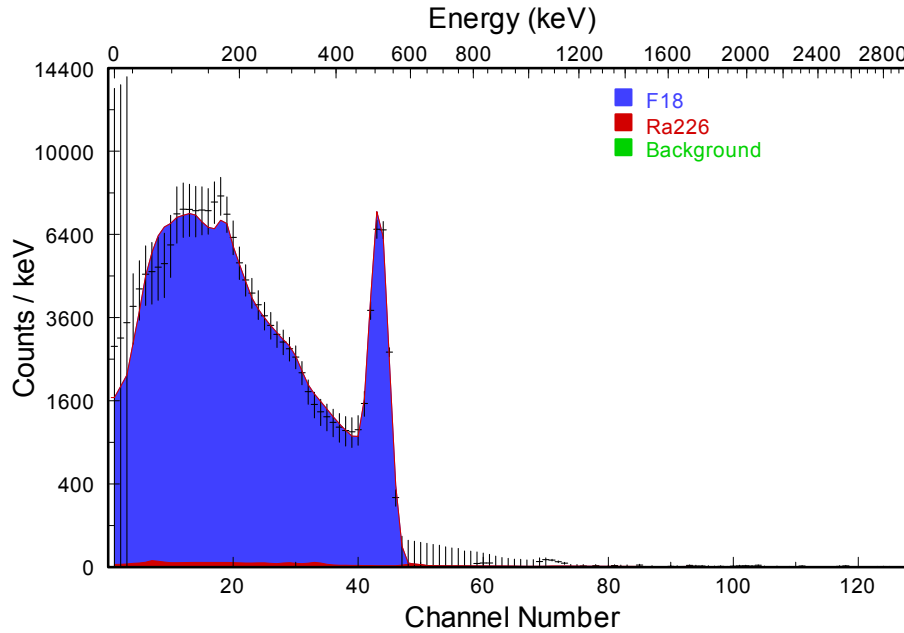


**Figure B-22.** Analysis of Event 22 revealed the presence of a positron emitter, which was identified as  $^{18}\text{F}$  because this is a common positron emitter.

## Event 23

The analysis result for Event 23 revealed the presence of  $^{239}\text{Pu}$  with high confidence and  $^{235}\text{U}$  with fair confidence. The GR-135 also reported a neutron count rate of 3.34 counts per second, which is a fairly high rate that is consistent with the presence of plutonium or another neutron-emitting material.

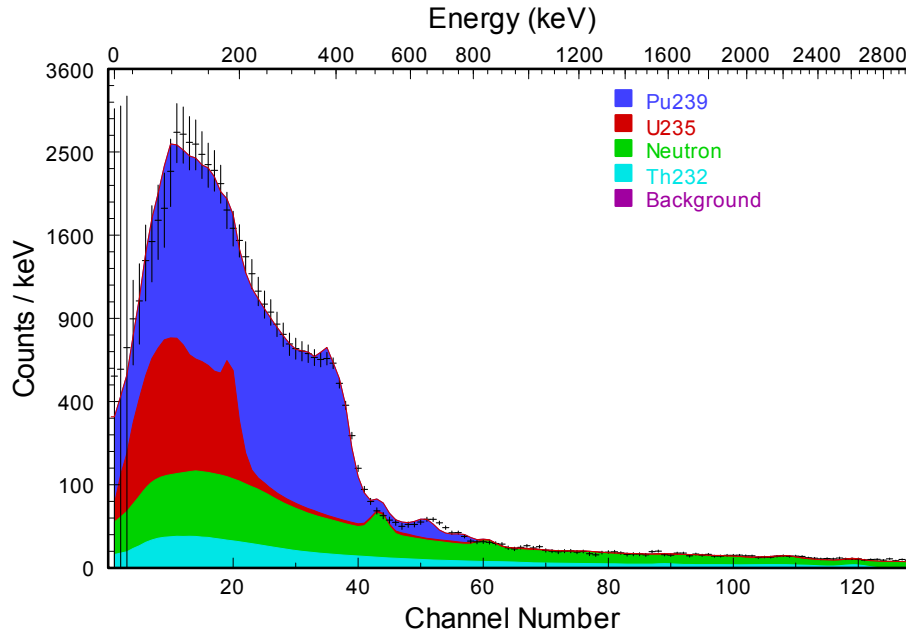


**Figure B-16. Analysis of Event 23 revealed the presence of  $^{239}\text{Pu}$  with high confidence and  $^{235}\text{U}$  with fair confidence.**

## Event 24

Analysis of Event 24 revealed the presence of  $^{131}\text{I}$  with high confidence. The DHSIsotopeID algorithm also reported that  $^{252}\text{Cf}$  was present despite the fact that the only apparent evidence for  $^{252}\text{Cf}$  was a broadening on the high-energy side of the 364-keV peak from  $^{131}\text{I}$ . Although the DHSIsotopeID algorithm only reports  $^{252}\text{Cf}$ , this feature is actually associated with the 388-keV gamma ray emitted by  $^{249}\text{Cf}$ , which is found in old  $^{252}\text{Cf}$ . Since it appeared that this feature may also have resulted from an inaccurate resolution setting, the resolution parameters were adjusted and the analysis was repeated. Regardless of the resolution settings, the analysis algorithm persisted in reporting  $^{252}\text{Cf}$ . The GR-135 also reported that the neutron count rate was 2.6 cps, which is a significant neutron count rate. Therefore, manual inspection of the data supports that conclusion that was obtained by DHSIsotopeID, which is that both  $^{131}\text{I}$  and  $^{252}\text{Cf}$  were present.

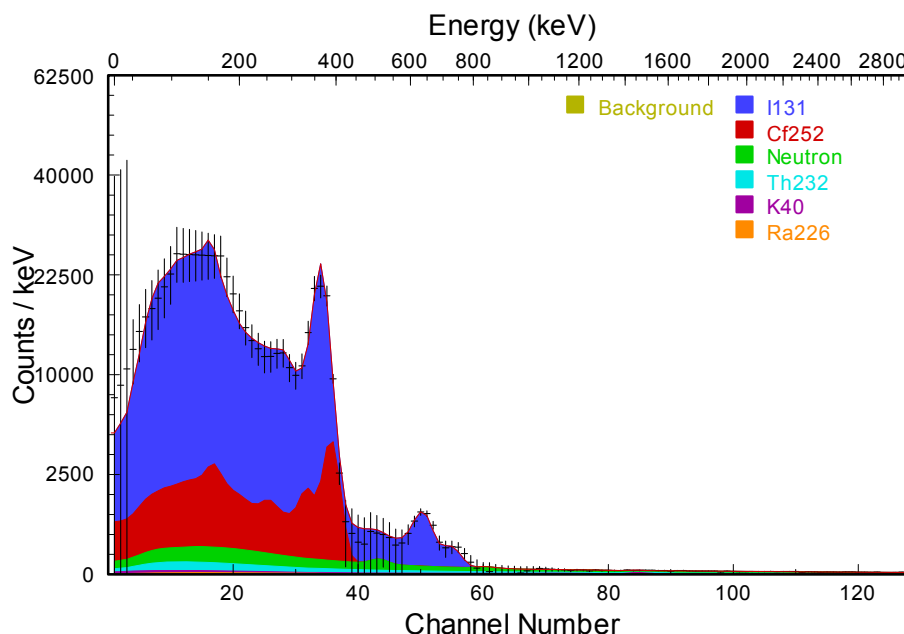


**Figure B-17.** The measured spectrum for Event 24 (black) is compared with the best fit that is obtained with a combination of  $^{131}\text{I}$  (blue) and  $^{252}\text{Cf}$  (red)

## Event 25 and 26

The analysis result is essentially the same for Events 25 and 26:  $^{237}\text{Np}$  was present. However, the quality of the data was compromised in both cases. One problem is that the counts per channel are truncated to 64k counts for a series of channels extending from about 70 to 190 keV. This problem would render it impossible to determine whether additional sources such as  $^{185}\text{U}$  are present. Another problem is that the same energy calibration spectrum is reported for both events, yet the foreground spectra clearly have different energy calibrations. Therefore, energy calibration parameters were determined in part by observing similarities between the two spectra and adjusting the parameters based on features that associated with  $^{237}\text{Np}$ . The spectra shown in Figure B-17 also display large error bars below 190 keV; the expanded uncertainties were imposed to address the problem that was noted previously regarding truncation of the counts in the low energy channels. Despite the deficiencies in the quality of data that were reported for these two events, the results showing the presence of  $^{237}\text{Np}$  appear to be definitive. The analysis results are summarized in Fig. B18.

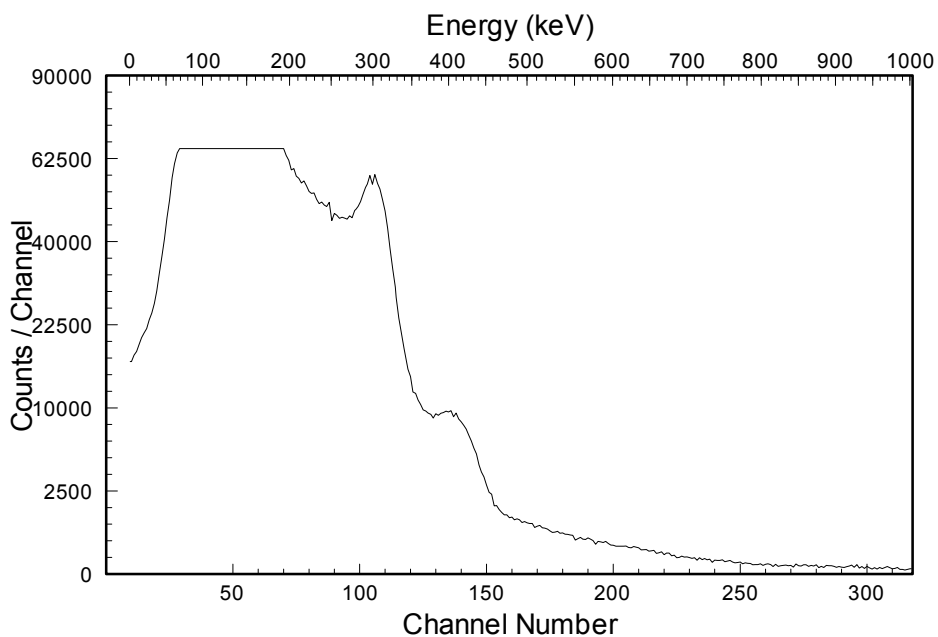


**Figure B-18. The original spectrum for Event 25 without background subtraction shows that counts in the range 70 to 190 keV were truncated to a maximum of 64k channels.**

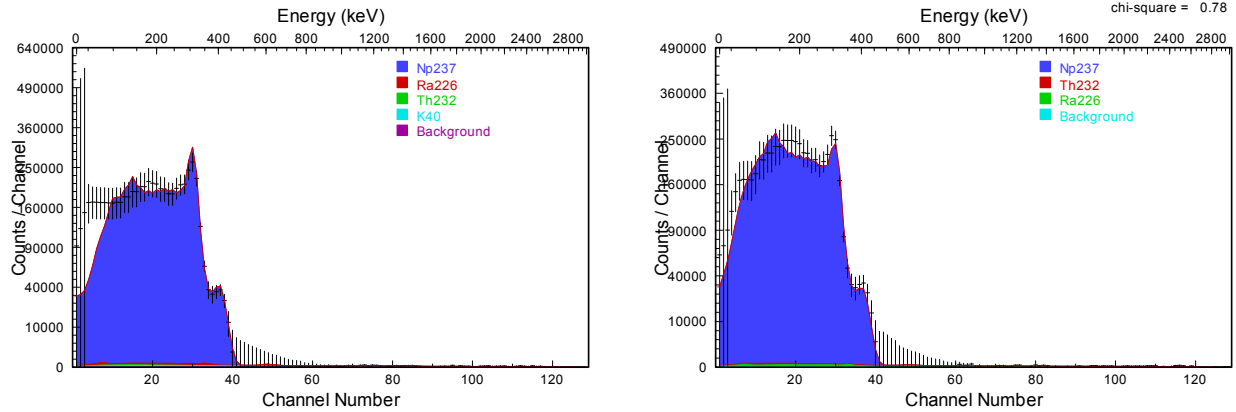


**Figure B19. Analysis of Event 25 (left) and Event 26 (right).**

### Event 27

The analysis result for Event 27 shows that  $^{133}\text{Ba}$  and  $^{239}\text{Pu}$  were both present. Even though the spectral component for  $^{133}\text{Ba}$  is more distinctive, the component associated with  $^{239}\text{Pu}$  also exhibits a substantial count rate and the presence of this isotope was also confirmed with high confidence.

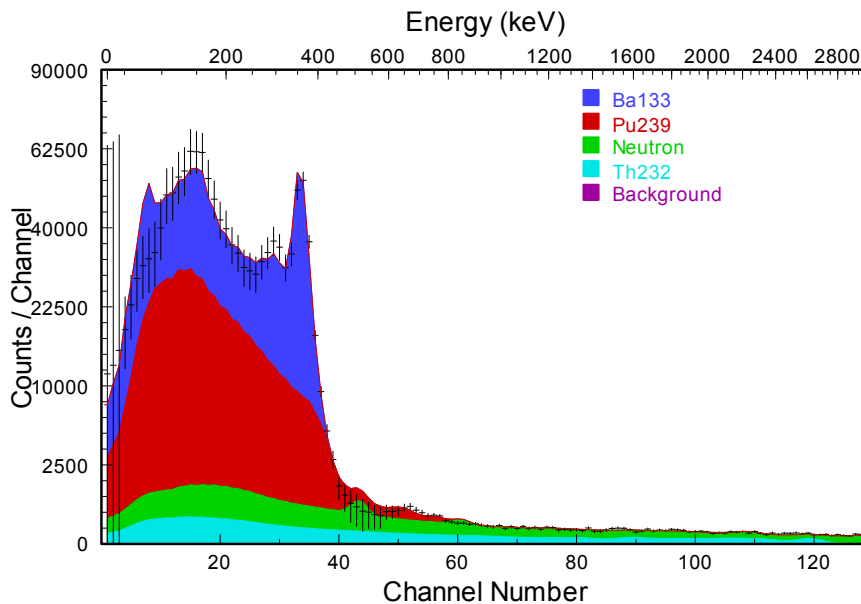


**Figure B-20. Analysis of Event 27 shows that  $^{133}\text{Ba}$  (blue) and  $^{239}\text{Pu}$  (red) were both present with high confidence.**

## Event 28

The analysis result for Events 28 shows that  $^{239}\text{Pu}$  and  $^{226}\text{Ra}$  were both present with high confidence. Features associated with  $^{226}\text{Ra}$  help pin down the energy calibration parameters.

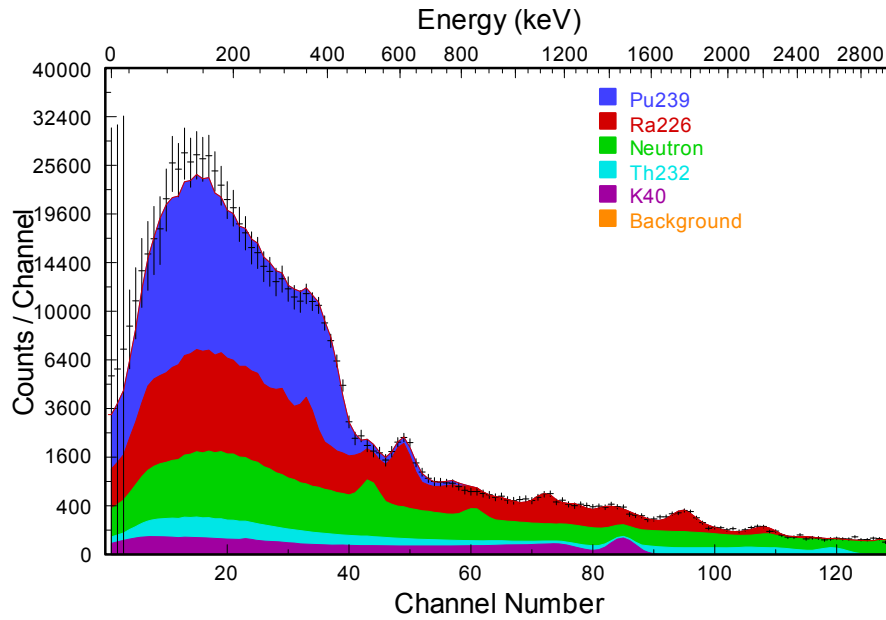


**Figure B-21.** Analysis of Event 28 shows that  $^{239}\text{Pu}$  (blue) and  $^{226}\text{Ra}$  (red) were both present with high confidence.

## References

- [1] Hofstadter, R., *Phys Rev*, 74, 100, (1948).
- [2] Moszynski, M., "Inorganic scintillation detectors in gamma-ray spectrometry", *Nuc. Instr. & Meth. in Phys. Res. A*, 505, 101-110 (2003).
- [3] E. LaVigne, G. Sjoden, J. Baciak, and R. Detwiler, "Extraordinary improvement in scintillation detectors via post-processing with ASEDRA—solution to a 50-year-old problem," *Proceedings of the Defense and Security Symposium*, International Society for Optical Engineering (SPIE), Orlando, Florida (2008).
- [4] R. Detwiler, G. Sjoden, J. Baciak, E. LaVigne, "Improved Plutonium Identification and Characterization Results with a NaI(Tl) Detector using ASEDRA," *Proceedings of the Defense and Security Symposium*, International Society for Optical Engineering (SPIE), Orlando, Florida (2008).
- [5] Dean J. Mitchell, *Variance Estimation for Analysis of Radiation Measurements*, Sandia National Laboratory report SAND2008-2302 (2008).

## **Distribution**

- 1 MS0735 Dean Mitchell, 06418 (electronic copy)
- 1 MS0899 Technical Library, 09536 (electronic copy)

### **External to Sandia:**

- 1 Dr. Rebecca Detwiler, Nuclear and Radiological Engineering Department, University of Florida (electronic copy)
- 1 Dr. Glenn E. Sjoden, Nuclear and Radiological Engineering Department, University of Florida (electronic copy)
- 1 Bob Mayo, NNSA/NA-22
- 1 John Blackadar, DHS/DNDO

This page intentionally left blank.

